University of Southampton

Faculty of Engineering and the Environment

School of Civil Engineering and the Environment

School of Ocean and Earth Sciences

An Initial Study into the Economic Feasibility of the Composite Seawall for Wave Energy Conversion (CSWEC) in North-West Sardinia

Barnaby Edward Wiegand

A dissertation submitted in partial fulfilment of the degree of

MSc in

Engineering in the Coastal Environment

by instructional course

September 2011

Table of Contents

SUMMARY

The Composite Seawall for Energy Conversion (CSWEC) is a shoreline wave energy converter of the overtopping-type that has a simple construction and uses novel technology to generate electricity. Meanwhile, recent studies into the wave resource around the Italian coast have identified north-west Sardinia as a potential location for harvesting wave power. The developers of the CSWEC have proposed to take the device to the pilot stage in that region.

There is a requirement to analyse the economic viability of wave energy converters on a regular basis in order to attract funding and to allow developers to assess and improve performance. This study provides an initial investigation into the economic feasibility of the proposed CSWEC project.

Although the wave resource in north-west Sardinia has been quantified in the offshore and nearshore zones, no value as yet has been given for wave power at the shoreline. The numerical model MIKE 21 was used to transform offshore waves up to the shoreline. The areas of Torre del Porticciolo and Porto Alabe were found to be the most promising sites with an average annual wave power each of approximately 7 kW / m.

Overtopping models were used to calculate hydraulic efficiencies and subsequent power outputs, including an empirical model based upon initial 2D model results of the CSWEC. This model returned hydraulic efficiencies of 14% to 18%. Expected output from the pilot plant ranged from 300 – 330 MWh / y, giving a cost of electricity of €0.13 / kWh. This is at the lower end of current industry estimates, suggesting the CSWEC can be competitive with other wave energy converters. Reductions in the cost of the technology alongside improvements in efficiency could result in an eventual cost of electricity of €0.08 – €0.12 / kWh.

ACKNOWLEDGEMENTS

I would like to thank my wife, family and friends for their continual support. I would like to acknowledge the use of DHI's MIKE 21 software as well as the use of the IRIDIS high-performance computer cluster at the University of Southampton. I kindly thank Dr Gerald Müller, Nick Linton, Professor Diego Vicinanza, Vincenzo Ferrante and Adrian Deledda for taking the time to answer any questions I posed to them. Lastly and not least I would like to acknowledge and thank my supervisor Dr Dimitris Stagonas for his continued support and enthusiasm during the course of the summer.

TABLE OF FIGURES

LIST OF TABLES

GLOSSARY OF TERMS

ARRAY	An arrangement of similar devices
AVAILABILITY	Time available for operation
CAPTURE	Measure of a device's ability to capture power
INSTALLED CAPACITY	Total power device can produce when operating correctly
HOTSPOTS	An area where there is a high concentration of energy
KILO-WATT HOUR	Supply of 1000 watts per hour (hence 1 MWh = 1000 kW per hour……)
NEARSHORE	Defined in this study as the zone extending from the low water line out to a depth of 20 m
POWER TAKE-OFF	System that allows the physical motion of a device to be converted into a useful form of energy
RATED POWER	See 'installed capacity'
SWELL	Wave propagating out from the wind region in which they were generated

LIST OF ACRONYMS AND ABBREVIATIONS USED

AEO	Annual Electrical Output
CAPEX	Capital Expenditure
CLASH	Crest Level Assessment of coastal Structures
COE	Cost of Electricity
CSWEC	Composite Sea Wall for Energy Capture
EREC	European Renewable Energy Council
FIT	Feed-in Tariff
GEBCO	General Bathymetric Chart of the Oceans
GW	Giga-Watt (1000 MW)
GWh	Giga-Watt hour
HPW	Hydrostatic Pressure Wheel
IEA	International Energy Agency
IWN	Italian Wave Network
kW	kilo-Watt
kWh	kilo-Watt Hour
LIMPET	Land Installed Marine Powered Energy Transformer
MW	Mega-Watt (1000 kW)
MWh	Mega-Watt Hour
MWL	Mean Water Level
NPV	Net Present Value
OPEX	Operational Expenditure
OWC	Oscillating Water Column
ROC	Renewables Obligation Certificate
SSG	Sea-Slot cone Generator
TAC	Total Annualized Cost
TAPCHAN	TAPered CHANnel
TW	Tera-Watt (1000 GW)

TWh	Tera-Watt hour
WEC	Wave Energy Converter
VMJ	Van der Meer & Jannsen

GLOSSARY OF SYMBOLS

a	=	Coefficient for slope geometry
b	=	Coefficient for slope geometry
A	=	Coefficient for overtopping
A_0	=	Coefficient for overtopping
B	=	Coefficient for overtopping
B_0	=	Coefficient for overtopping
BR	=	Borrowing rate (%)
C_g	=	Group velocity
d	=	water depth (m)
DF	=	Discount factor
DR	=	Discount rate (%)
E	=	Energy density per unit crest of wave (kW / m)
f	=	Rate of inflation (%)
F	=	Force
g	=	Gravitational acceleration (9.81 m^2s^{-1})
h_m	=	Water-depth at the structure toe (m)
$H_{1/3}$	=	Significant wave height (m)
H_{mo}	=	Spectral wave height (m)
H_s	=	Significant wave height (m)
H_{stoe}	=	Significant wave height at the structure toe / shoreline (m)
k	=	The wave number
k_d	=	Diffraction coefficient
k_r	=	Refraction coefficient
L_0	=	Deepwater wavelength (m)
L	=	Wavelength (m)
$P_{overtopping}$	=	Hydraulic power of overtopping water (kW / m)

$P_{installed}$	=	Installed power (kW)
$P_{structure}$	=	Hydraulic power of structure (kW / m)
P_{wave}	=	Wave power (kW / m)
q	=	Overtopping discharge ($m^3m^{-1}s^{-1}$)
q_{design}	=	Design flow / overtopping rate ($m^3m^{-1}s^{-1}$)
q_{max}	=	Maximum overtopping discharge ($m^3m^{-1}s^{-1}$)
Q	=	Dimensionless overtopping
R	=	Dimensionless freeboard
R_c	=	Freeboard (m)
S_{op}	=	Wave steepness
t	=	Project lifetime (years)
T_{mo}	=	Spectral wave period (s)
v	=	Velocity ($m\ s^{-1}$)
α_p	=	Angle of offshore wave approach (degrees)
α_s	=	Ramp slope (degrees)
β	=	Angle of wave attack (degrees)
β_0	=	Empirically derived coefficient for estimating wave height
β_1	=	Empirically derived coefficient for estimating wave height
β_{max}	=	Empirically derived coefficient for estimating wave height
ξ_{op}	=	Surf scaling parameter
γ	=	Breaker parameter
γ_β	=	Reduction factor for oblique waves
γ_b	=	Reduction factor for berm
γ_h	=	Reduction factor for shallow foreshore
γ_r	=	Reduction factor for roughness of slope
λ_a	=	Reduction factor for slope angle
λ_{d_r}	=	Reduction factor for draft
λ_s	=	Reduction factor for low relative freeboard

λ_m	=	Reduction factor for slope shape
π	=	Pi
θ	=	foreshore slope (degrees)
ρ	=	Seawater density (1025 kg /m^3)
ŋ	=	Hydraulic efficiency of HPW (%)
ŋ $ramp$	=	Hydraulic efficiency of ramp (%)

1 INTRODUCTION

The world's energy consumption is rising (Clement *et al.*, 2002) and yet traditional fossil fuels are a finite, non-renewable energy source that may not be able to meet future demand (Vicinanza and Frigaard, 2008). At the same time, fossil fuels continue to pollute the Earth's atmosphere which evidence suggests is contributing to climate change (*ibid*.). Wave energy has the potential to help mitigate these crises: firstly it is a pollution-free energy source; and, secondly it could eventually contribute globally an estimated 2000 TWh of electricity per year, which represents approximately 10% of the world's current annual consumption (Vicinanza and Frigaard, 2008). Although the cost of wave power is currently high compared with other energy sources (Belmont, 2010), this is expected to come down as the industry matures (e.g. Raventos *et al*., 2010). Therefore wave energy could become a *cheap* as well as abundant source of electricity.

The idea of wave energy conversion is not new, the first recorded patent occurring in 1799 (Girard & Son, France). There are currently thought to be around 1000 patents worldwide (Vicinanza and Frigaard, 2008) however very few wave energy converters (WECs) have proceeded to the prototype stage, let alone to commercial operation (Margheritini *et al*., 2009). In 2004 there was an installed global capacity of just 2 MW (Gross, 2004) and this has been augmented only slightly by recent projects such as the Mutriku wave-power plant in Spain (300 kW capacity). As such, the wave energy industry currently lags the offshore wind industry by 25 years (Calloway, 2007). One suggested reason for this is that many WECs have been "hopelessly uneconomic" (Thorpe, in Calloway, 2007) which may have deterred governments in the past from funding wave energy projects (*ibid*.), as well as wasted time and effort that could have been directed elsewhere (Margheritini *et al*., 2009). To address this problem there is a requirement to assess the economics of WECs at all stages of their development (Weber *et al*., 2010). This will help stakeholders to make informed funding and investment decisions and enable developers to make the necessary design changes needed to improve performance and economic viability prior to full operation (Stallard *et al*., 2009).

Although the predominant wave resources are in the offshore and nearshore zones, the shoreline wave resource can be attractive due to the presence of energy 'hot-spots', low capital costs and ease of maintenance (Polinder and Scuotto, 2005). The cost-effective utilization of shoreline wave energy has yet though to be fully addressed (Stagonas *et al*., 2010). The composite seawall for energy conversion (henceforth referred to as the CSWEC) is a shoreline WEC of the overtopping-type, developed by the University

of Southampton and described as a cost-effective solution for harvesting shoreline wave energy (Stagonas *et al*., 2010). Initial results from physical 2D models carried out at 1:50 and 1:23 scales have been promising with a power output of 1.5 kW / m for a (scaled-up) wave height of 1 m and a head difference of approximately 1 m (Stagonas *et al*., 2010). Consequently it has been proposed to take the development forward to pilot stage in north-west Sardinia, Italy. An initial economic analysis of the project is now required.

1.1 Aims & Objectives

This dissertation examines the economic feasibility of the proposed CSWEC project in north-west Sardinia. It is hoped it will give guidance as to which areas require focusing upon during the early stages of the project's design and development. The process outlined in Figure 1.1 will be followed, beginning with an assessment of the shoreline wave climate in north-west Sardinia. Recent studies have highlighted that this area has a relatively high wave resource for the Mediterranean and that at certain sites 'hotspots' exist in the nearshore zone (Vicinanza *et al*., 2009; Vicinanza, pers. comm.). This study will look at whether these 'hotspots' also exist at the shoreline, as well as try to identify other sites. The shoreline wave height is essential to know since overtopping formulae require the wave height at the structure toe. The numerical model MIKE 21 will be used to simulate the transformations of offshore waves as they propagate up to the shoreline. The results of this modelling should also be of interest to those currently assessing wave power potential around the Italian coast.

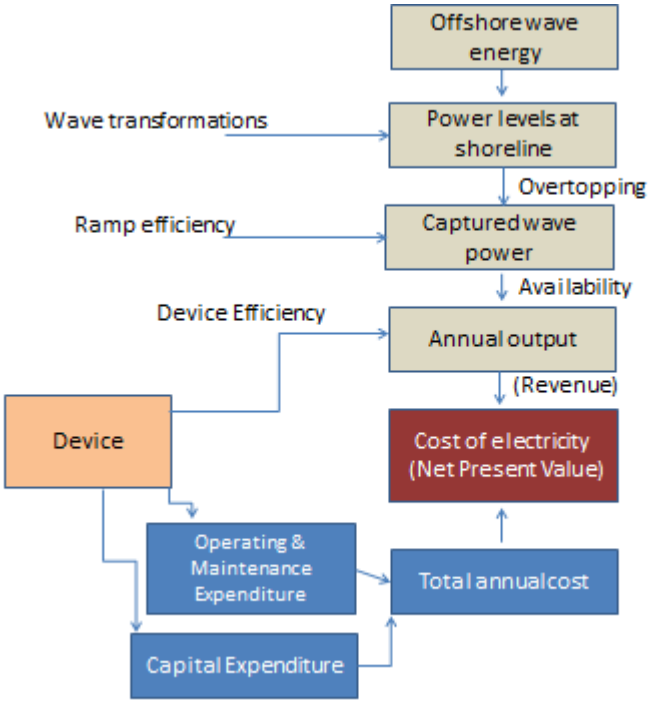

Figure 1.1 - Flow diagram for establishing the economic feasibility of the CSWEC (adapted from Thorpe, 1999)

The most promising site(s) will be chosen for further analysis, considering each of the remaining steps in the flow diagram. The final outcome will be an estimate (by way of a discounted cash-flow analysis and based on the latest available cost data) of the two

most commonly used economic indicators for renewable energy: the cost of electricity (COE); and, the net present value (NPV). It should be noted that the scope of study includes neither the environmental feasibility of the device nor its survivability, although both may be briefly mentioned.

1.1.1 Structure of dissertation

The structure of the dissertation is as follows:

1. A literature review, covering: the current state of wave energy in Italy and Sardinia; the CSWEC concept, its current development status and an overview of the proposed project; other overtopping-type and shoreline WECs; the theory of wave overtopping, introducing the models used in the study to analyse overtopping rates that determine the ramp efficiency and the hydraulic power of the structure; and, basic wave energy economics, specifically related to how the economic parameters used in this study are derived.
2. The MIKE 21 model set-up will be explained including an appraisal of the wave and bathymetric data used. The discounted cash-flow models will be introduced.
3. The results of the shoreline wave simulations will be presented and discussed.
4. The results of the remainder of the analyses will be presented for the selected sites, covering the ramp efficiency, the predicted output of the CSWEC, and the estimated economic parameters.
5. The results will be discussed in the context of the literature reviewed.
6. Conclusions and recommendations will be made regarding the project's economic feasibility and the development areas that should be prioritised going forward.

2 LITERATURE REVIEW

2.1 Wave Energy In Italy and Sardinia

There are currently no wave energy devices operating in Italy. The Mediterranean has a relatively low wave resource (30 GW) compared to Europe's Atlantic coast which is estimated to be in the region of 290 GW (Clement *et al*., 2002). Vicinanza *et al.* (2009) have indicated however that the average annual offshore wave power in north-west Sardinia is relatively high at 13.1 kW / m. The wave conditions are predominantly swell, due to the mistral winds blowing from the north-west (Vicinanza *et al*., 2009), over a fetch of approximately 350 km. These winds blow for four out of every five days (Furberg *et al*., 2002), meaning the wave resource should be both regular and reliable.

Figure 2.1 shows results from an on-going study by Vicinanza (pers. comm.) into the nearshore wave energy resource around Italian waters. At 9.05 kW / m the annual average wave power at the wave buoy is lower than previously reported, however 'hotspots' appear to exist in the nearshore at sites 1 and 6 which have average power levels above those at the offshore buoy. At the two main towns along the coast (Alghero and Bosa Marina) there is a substantial loss of energy in the nearshore zone, in the region of 40% to 60%.

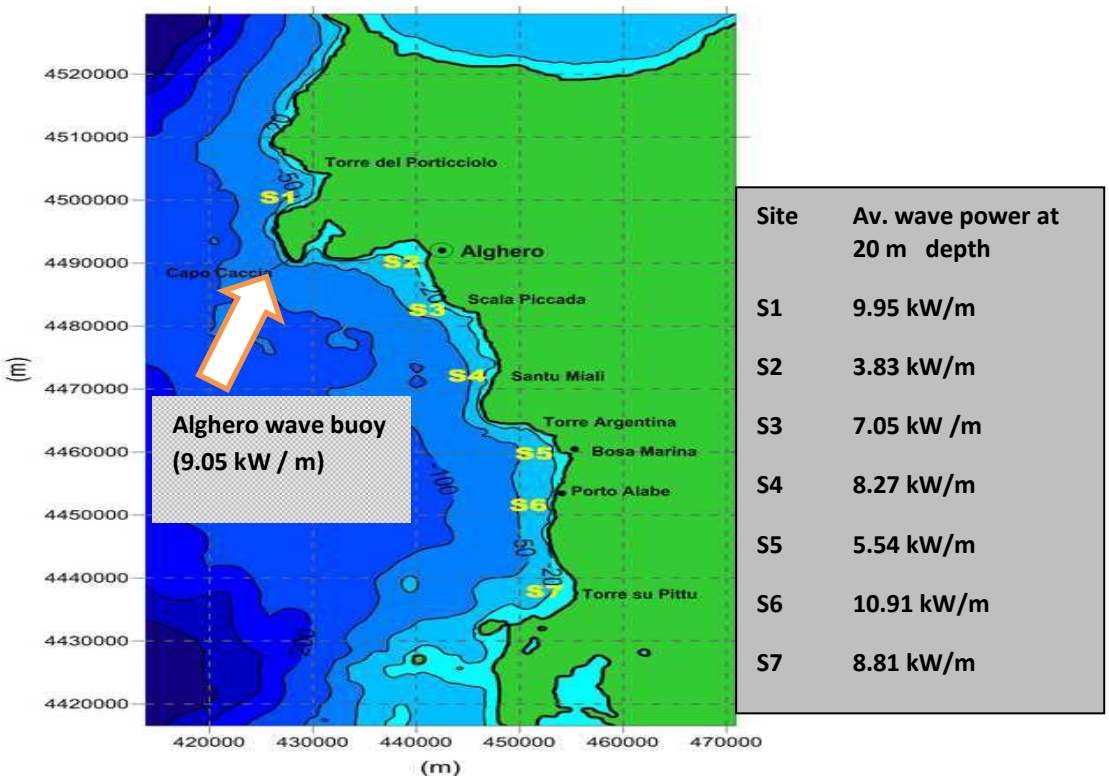

Figure 2.1 - Nearshore wave energy in north-west Sardinia (Vicinanza, pers. comm.)

(It should be noted that the sites in Figure 2.1 were chosen as being generally representative of the north-west Sardinian coast. Similarly this study does not intend to identify the exact location for the CSWEC pilot plant (which is only 70 m in length), rather suggest suitable areas in terms of wave resource).

The region also benefits from having little tide (0.3 m at most) meaning operational hours of the device are not limited to high tide, increasing availability. Although the Atlantic coast of Europe has a higher wave resource, at the shoreline this will be compromised by larger tidal ranges. Therefore the CSWEC may be better suited to the Mediterranean region.

There are socio-economic factors that make Italy and Sardinia an attractive site for the project. Italy has a high dependence on imported energy resulting in high electricity costs, particularly in Sardinia where prices are triple the EU average (Vicinanza, pers. comm.). There are concerns over energy security and in the winter of 2005-2006 Italy was severely disrupted by the Russian-Ukraine gas dispute (IEA, 2010). In the last decade there have been numerous power-blackouts due to shortfalls in supply, however a recent referendum has rejected nuclear power as a means of fulfilling demand. These factors suggest that renewable energies will play an increased role in Italy's energy portfolio. Legislation already exists to diversify energy sources within the country and there are generous feed-in tariffs (FITs) as well as subsidies to promote renewable energy. As part of the EU, Italy has an obligation for 20% of its primary power to come from renewables by 2020 (Raventos *et al*., 2010), whilst Sardinia has ambitions to meet 30% of its electricity supply with renewables by 2030 (www.refer.eu.com). Italian energy suppliers are also required by law to increase their renewable share by 0.75 % per year or face financial penalties (EREC, 2009). As part of the southern-Italian Mezzogiorno region, which suffers from high unemployment (Hospers, 2003), Sardinia would also benefit from the jobs a WEC project would bring.

2.2 The Composite Seawall for Energy Conversion (CSWEC)

The CSWEC consists of two main elements: the capturing structure; and the energy converter. Both of these are now discussed.

2.2.1 The Energy Capturing Structure

The concept of the capture structure originates from previous work done by Mori *et al*. (2008) on the use of composite seawalls to improve coastal protection. Figure 2.2a shows a permeable slit-wall in Japan which dissipates wave energy before it reaches the seawall behind it. Birks (2010) found also that overtopping rates of an existing seawall were reduced with the addition of a structure in front of the wall.

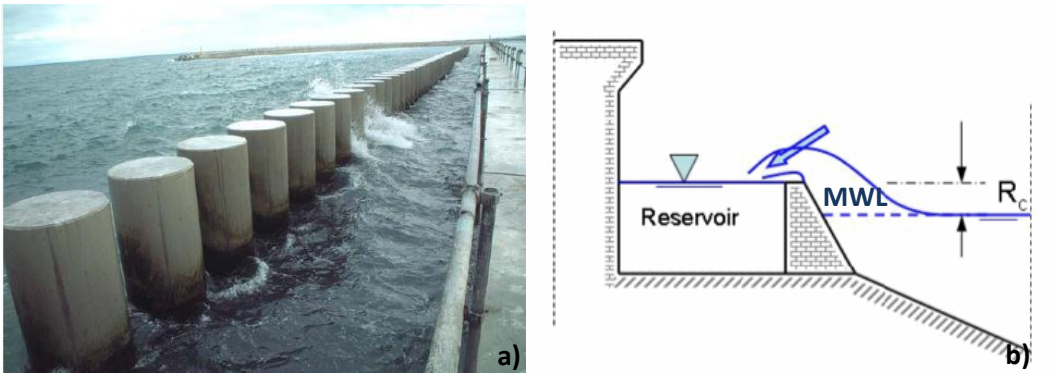

Figure 2.2 - a) slit-wall in Japan; b) CSWEC (Stagonas *et al*., 2010)

The CSWEC modifies the slit-wall to create a source of potential energy (Figure 2.2b), the protection it gives to the existing seawall now a secondary feature. An impermeable, sloped wall is used to enhance the rate of overtopping seawater that then flows into a reservoir. The level of the reservoir is at a height above the mean-water level (MWL), equal to the freeboard (R_c), creating a head-difference equal to the freeboard. The potential power of the overtopping water per meter ($P_{overtopping}$) can therefore be expressed as follows (Kofoed, 2002):

$$P_{overtopping} = \frac{qg\rho R_c}{1000} \quad \text{(kW / m)} \quad (1)$$

where: $q =$ the overtopping rate ($m^3/m/s$); $g =$ gravitational acceleration (9.81 $m\ s^{-2}$); and, $\rho =$ the density of sea-water (assumed in this study as 1025 $kg\ /\ m^3$).

For the total overtopping power of the structure for a given wave it is necessary to multiply equation (1) by the length of the structure:

$$P_{structure} = P_{overtopping} * l \qquad \text{(kW)} \qquad (2)$$

where: l = the length of the structure's capturing ramp in meters.

The efficiency ($\eta\ ramp$) of the structure per meter in capturing wave power can be expressed as:

$$\eta\ ramp\ (\%) = \frac{P_{overtopping}}{P_{wave}} \qquad (3)$$

where: P_{wave} = a given wave's power at the structure toe and can be calculated using the standard power equation:

$$P_{wave} = \frac{EC_g}{1000} \qquad \text{(kW / m)} \qquad (4)$$

where: E = energy density per meter width; and C_g = the group velocity.

The energy density is calculated as follows:

$$E = \frac{\rho g H_{s,toe}^2}{8} \qquad (5)$$

where: $H_{s,toe}$ = the wave height at the toe of the ramp.

Kofoed (2002) says some loss in the overtopping power will occur due to changes in the reservoir level. This is because the overtopping power is the potential power of the water at the height of the freeboard. There will also be losses due to spillages. These losses are ignored in this study, however with a variable wave climate there will be periods when the CSWEC's reservoir's water level is not at the height of the freeboard. A solution could be to install a pump-system to raise the water level when needed so that the required head-difference is maintained. The reservoir efficiency is therefore assumed as 100% in this study.

Figure 2.3 shows the results of 2D model experiments carried out at 1:50 and 1:23 scales. The model used a 45^o ramp, a foreshore slope of 1:10 (Birks, 2010) and regular waves from 20 mm – 50 mm with periods between 0.5 - 1.4 seconds (Stagonas *et al*., 2010), which attacked the ramp head-on. The water depth was 11.7 cm so the waves were not in shallow water. Hydraulic efficiencies ranged from 6% to 32% for freeboards of 1 m and 1.5 m. Efficiencies generally increase when the relative freeboard (H/R_c) increases. Interestingly, for a 1 m freeboard the efficiency appears to level or drop off

when $\frac{H}{R_c}$ > 1.5 (i.e. when wave heights exceed 1.5 m). It is not clear from the data whether this also occurs with a 1.5 m freeboard.

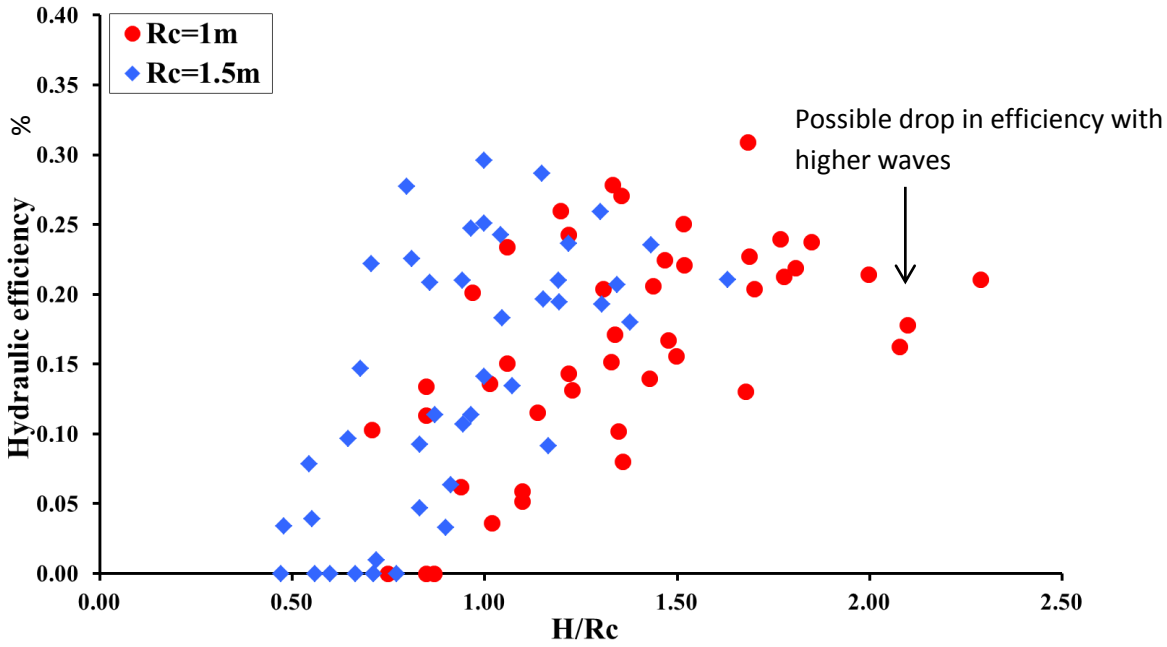

Figure 2.3 - Hydraulic efficiency of ramp - scale model tests (Stagonas *et al.*, 2010)

Figure 2.4 shows the predicted hydraulic power of a 50 m structure based on the 1:23 model results (Stagonas, pers. comm.). Although head differences are likely to be small for the CSWEC, there is potential for long capture lengths (e.g. +50m) due to the linear nature of the structure (Stagonas *et al.*, 2010). A wave height of 1.06 m gave a maximum hydraulic power of around 90 kW (1.8 kW / m). The same wave height however also produced a hydraulic power of 50 kW. Since overtopping is generally underestimated in models compared to real-life situations (Reeve *et al.*, 2008), Stagonas *et al.* (2010) concluded that a figure of 75 kW (1.5 kW / m) was most representative. This study takes a more conservative approach and uses the equations of the regression lines as one method of estimating the performance of the proposed structure. For freeboards of 1 m and 1.5 m the regression lines yield the following (approximate) linear expressions (referred to as the 1:23 models):

$$P_{50m\ structure} = \left(H_{s,toe} * 142.86\right) - 85.72 \text{ ; for } R_c = 1 \text{ m} \quad (6)$$

$$P_{50m\ structure} = \left(H_{s,toe} * 151.35\right) - 98.38 \text{ ; for } R_c = 1.5 \text{ m} \quad (7)$$

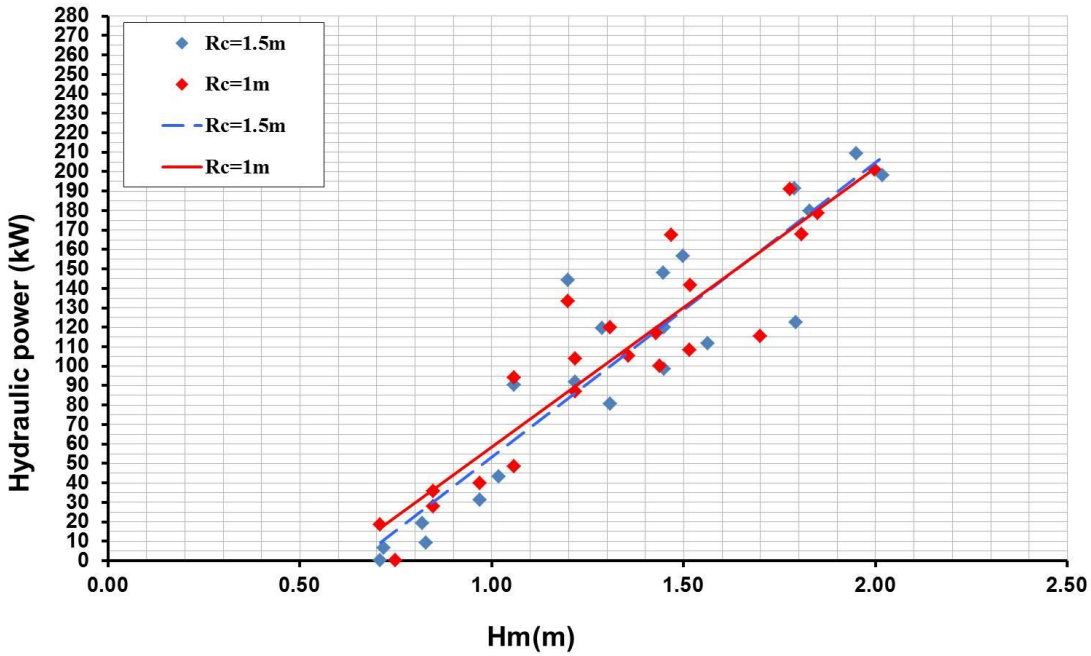

Figure 2.4 Hydraulic power of ramp (based on 1:23 model results)

2.2.2 The Hydrostatic Pressure Wheel

The Hydrostatic Pressure Wheel (HPW) is a new type of low-head energy converter originating from the University of Southampton (Senior *et al.*, 2010). (Senior *et al.*, 2008) suggest the HPW be used for power ratings of 2 – 75 kW (and possibly up to 150 kW) and for head differences of 0.5m – 2.5 m, meaning it is well suited for use as part of the CSWEC. It is a relatively simple machine, with low costs and the possibility for local manufacture (Stagonas *et al.*, 2010), which should benefit local economies and reduce lead-times on spare parts and replacements, therefore increasing the device's availability.

Figure 2.5 illustrates the HPW concept. It is essentially a wheel whose blades act as a weir, creating a head difference between the upstream (d_1) and downstream (d_2) water depths. There is a difference between the upstream (F_1) and downstream (F_2) hydrostatic forces which acts upon the wheel's blades, causing them to move at the same speed as the upstream velocity (v_1). The wheels are connected to a power take-off system in order to generate electricity.

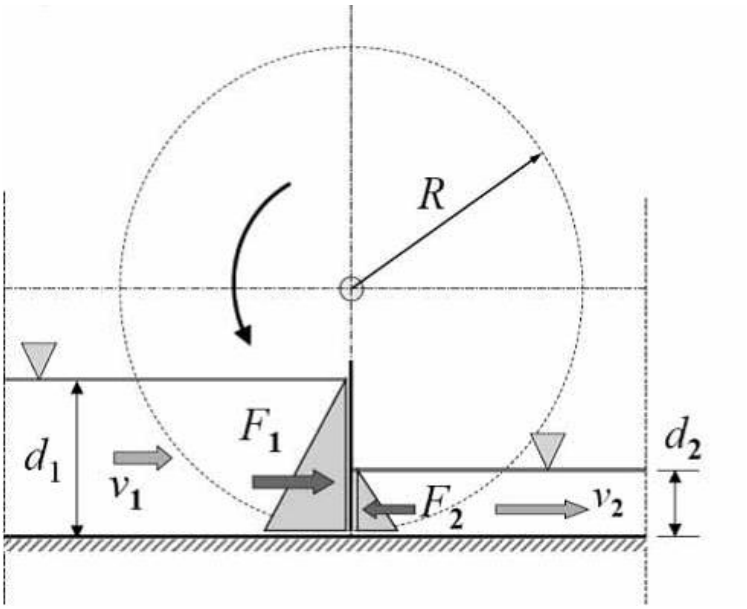

Figure 2.5 Hydrostatic Pressure Wheel (Senior *et al.*, 2010)

Figure 2.6 shows results from tests carried out at the University of Southampton with observed efficiencies similar to theoretical efficiencies (75% to 95 %).

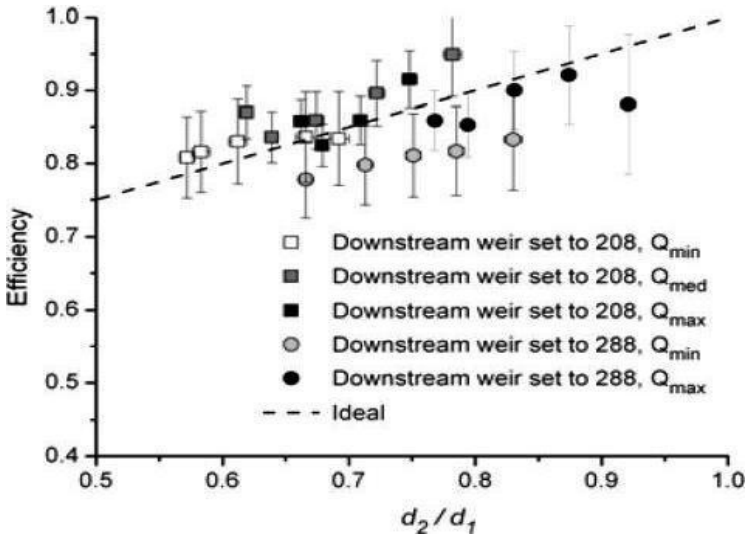

Figure 2.6 - HPW efficiency (Stagonas *et al.*, 2010)

Figure 2.7 shows the efficiency curve adopted in this study. This is a conservative approach similar to the one taken by Stagonas *et al*. (2010), with a maximum combined wheel and power take-off efficiency of 65 %. Additionally, on the advice of Müller and

Linton (pers. comm.) the efficiency drops off when flow rates are low or high. In the case of the CSWEC the flow rates correspond to the overtopping discharge (q) since this is the amount of water that must pass 'through' the wheels in order for the head-difference to be maintained. The 65 % efficiency is valid up to 65 % of the maximum flow rate, $qmax$ ($q/qmax$ = 0.65, referred to as the design flow). At flow rates higher than the design flow the wheels operate at a reduced efficiency, although power output remains constant, falling to an efficiency of 42.25% at $qmax$. At low flow rates (less than 15% of the design flow) there is also a drop in efficiency, falling to zero at 4% of the design flow (due to leakages at low flow rates).

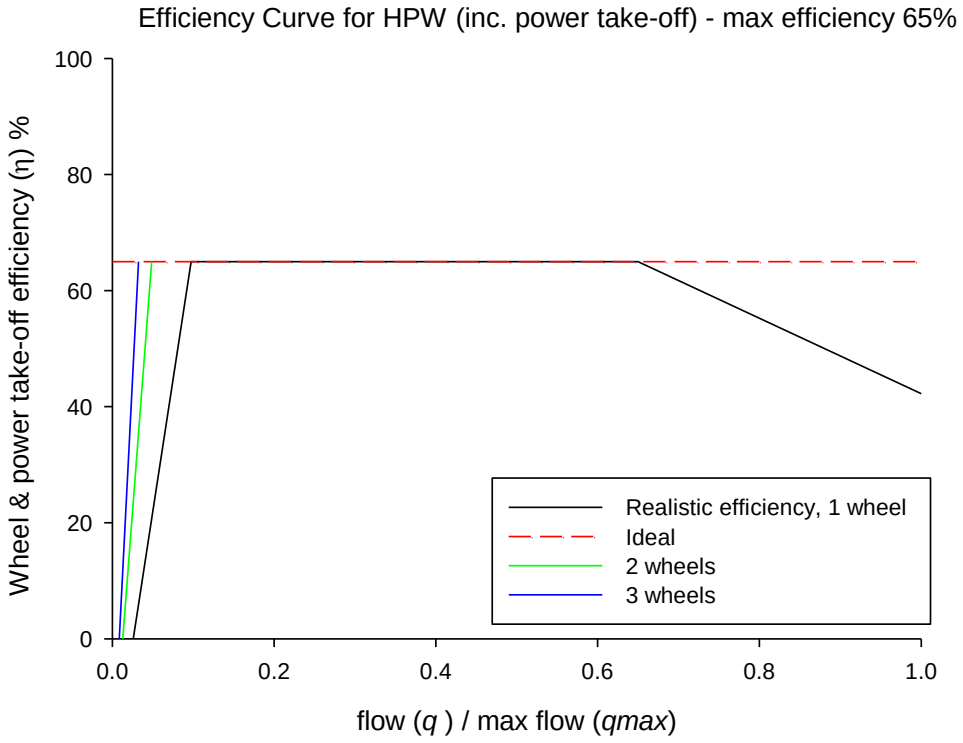

Figure 2.7 - Efficiency curve for HPW used in study

The design flow is used in this study to calculate the installed capacity of the device. Since the structure's hydraulic power is equal to the overtopping rate (q) multiplied by the length of the ramp (l) (Eq. (2)), the installed (or rated) power can be expressed as:

$$P_{installed} = \frac{q_{design}\, g \rho R_c * l}{1000} \quad \text{(kW)} \qquad (8)$$

This means there is a drop-off in efficiency when $P_{structure}$ is greater than $P_{installed}$ and when $P_{structure}$ is less than 15% of $P_{installed}$.

Figure 2.7 also shows the effect of using multiple HPWs with the same overall installed capacity, but with each unit having a lower capacity. At low flow rates a lower rated wheel is able to achieve higher efficiencies, since 15% of the lower rated wheel is less than 15% of the larger rated wheel. At high flow rates the wheels are all used together. For some of the time this means that at least one of the wheels will not be in use. This concept is known as redundancy and, whilst it may appear to be wasteful, this could benefit the availability of the structure. If one wheel fails then there will still be one or more wheel(s) that can be used. There may also be less operational wear on the wheels which reduces the need for maintenance. Smaller wheels may also take less time and money to produce and replace, again improving availability.

This study assumes the outflow system of the CSWEC is sufficiently designed to maintain a constant downstream depth. As shown in Figure 2.5, changes in the downstream depth (d_2) will lead to changes in efficiency which if frequent enough may result in reliability issues with the gearbox system (Linton, pers. comm.).

2.2.3 Proposed Installation

Figure 2.8 shows a sketch of the proposed installation. The length of the device is 70 m, consisting of the energy capturing ramp (50 m) and 20 m of rock-armouring protection. The capture length is therefore comparable with the 1:23 model results previously discussed, meaning equations (6) & (7) can be used to estimate the hydraulic power of the installation (allowing for the modifications discussed later). The structure extends out from the shoreline by 20 m (there may be an opportunity to capture power from the side ramp however this study will only consider the front ramp). The back wall was initially envisaged to be an existing, impermeable sea-wall however this may change depending on whether areas with seawalls are suitable in terms of the shoreline wave resource. For operational purposes a 1 m freeboard is assumed so that there is sufficient depth for the wheels and to minimize spillages.

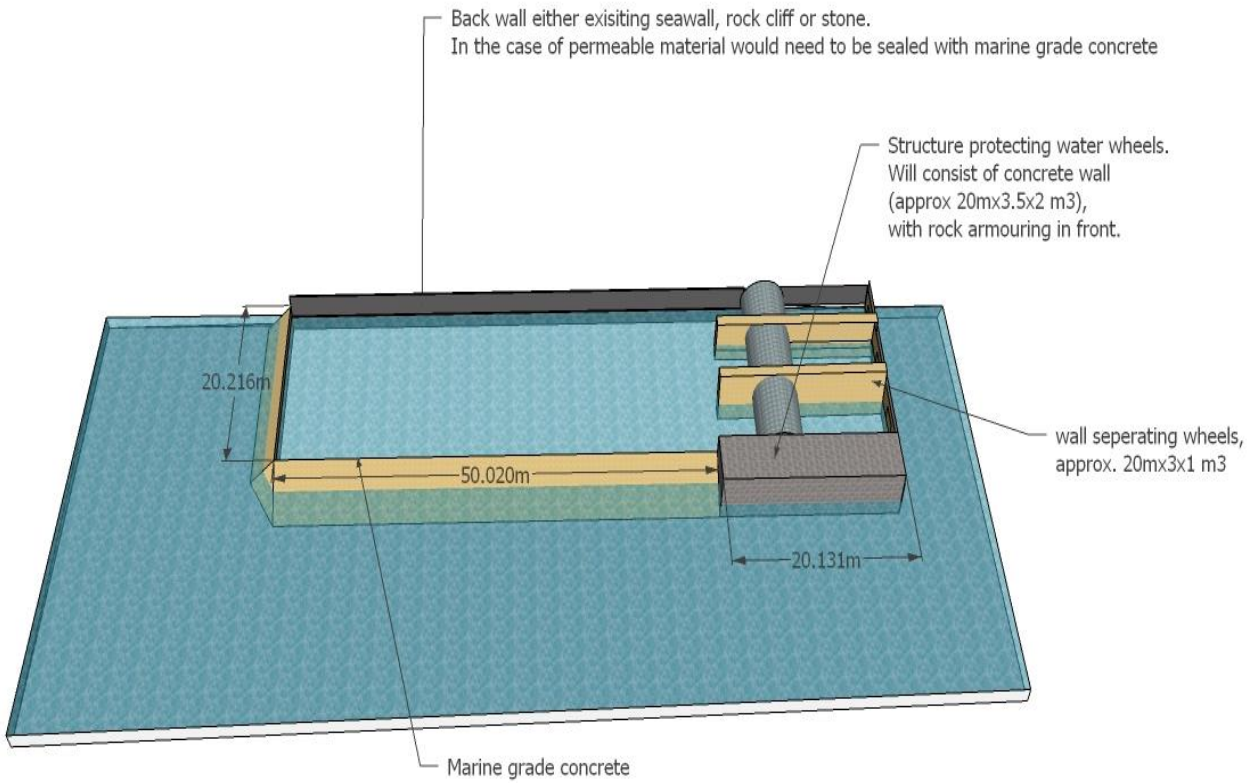

Figure 2.8 - Sketch of proposed CSWEC installation

2.3 Existing Overtopping–type and Shoreline WECs

The principle of using wave-overtopping for energy conversion is already established, if not commercially widespread. Meanwhile, of the few WECs built so far many have been at the shoreline.

The most advanced overtopping-type WEC is currently the Wave Dragon, a floating offshore device. Figure 2.9a shows the 1:45 prototype that has been operating in the Nissum Broads, Denmark since April 2003. The device uses reflectors to capture waves (increasing capture by up to 140% (Kramer and Frigaard, 2009)) and direct them towards a ramp. The waves overtop a convex-elliptic ramp and flow into a reservoir where Kaplan turbines exploit the low-head difference (Figure 2.9b). Experimental efficiencies of the ramp were estimated at 11% to 20 % by Kofoed (2002), with higher efficiencies (20% to 25 %) during operation (*ibid*.). Rated power at full-scale is estimated at 4 – 22 MW depending on site and wave climate. Wave-to-wire efficiencies are around 12 % (Kofoed *et al*., 2006).

a)

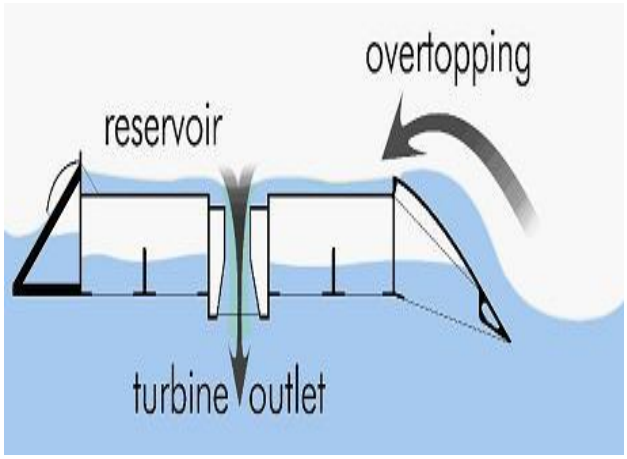

b)

Figure 2.9 - Wave Dragon: a) reflectors; b) ramp

Benefits of the Wave Dragon are that it captures waves before they enter shallower water and dissipate energy, whilst it is also not subject to the effects of the tide. On the negative side: sitting offshore it may be subject to high operating and maintenance (OPEX) costs, with reduced weather-windows for maintenance; sub-sea cabling bringing power back to the coastline is expensive, with estimates ranging from €107 – €313 / m (Beels *et al.*, 2011), and will experience power losses (Folley *et al.*, 2007); and, high environmental loadings are an issue (storms forced the prototype of its moorings in January 2005). To date no full-scale operational examples of the device exist, although there are plans for a 4 – 7 MW deployment off the Welsh coast in the near future.

Overtopping-type WECs at the shoreline include the Norwegian TAPCHAN (TAPered CHANnel) and the SSG (Sea Slot-cone Generator). The TAPCHAN (Figure 2.10) is one of earliest fully operational WECs to have been built (in the 1980s). A tapered channel causes waves to surge, pile up and overtop into a reservoir, which functions essentially as a standard low-pressure hydro-electric power station (Kofoed, 2002). The device's rating of 300 kW was slightly exceeded in operation (*ibid*.) however financial difficulties curtailed the project and as yet the project has not been resurrected.

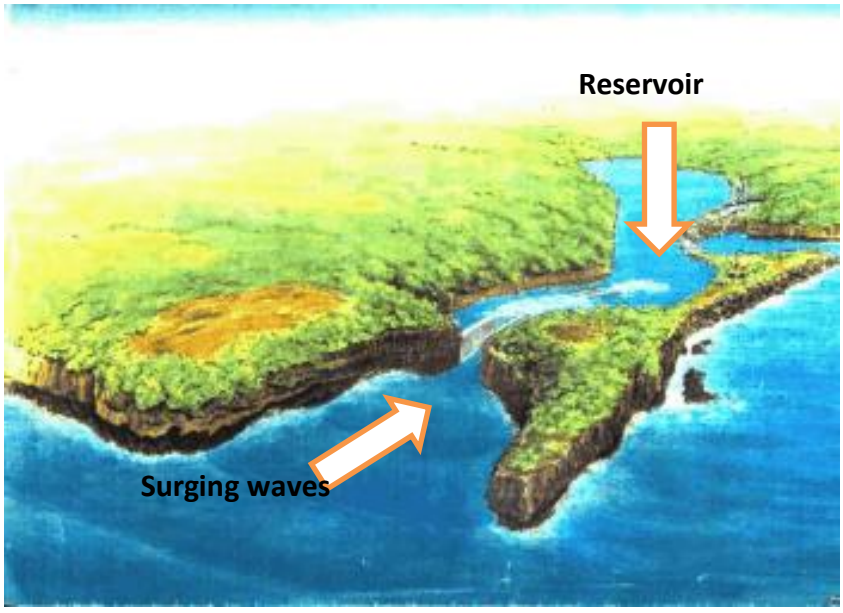

Figure 2.10 - TAPCHAN (Kofoed, 2002)

The SSG (Figure 2.11) captures and stores overtopping water in a series of three containers at different heights. The water passes through a series of Kaplan turbines on its way back to the sea, the different container heights allowing for a more efficient use of

the potential energy. Margheritini *et al*. (2009) reported hydraulic efficiencies ranging from 30% to 40% and estimated the pilot project on the island of Kvitsoy, Norway would produce 320 MWh / y from an installed capacity of 163 kW. The device is described as robust and cost effective with the additional benefit that it can be integrated into breakwaters (Margheritini *et al.,* 2009). On the other hand the device is structurally complex (Stagonas *et al*., 2010) and the Kaplan turbines are both expensive and possibly environmentally unfriendly when used in low-head situations (Senior et *al*., 2008).

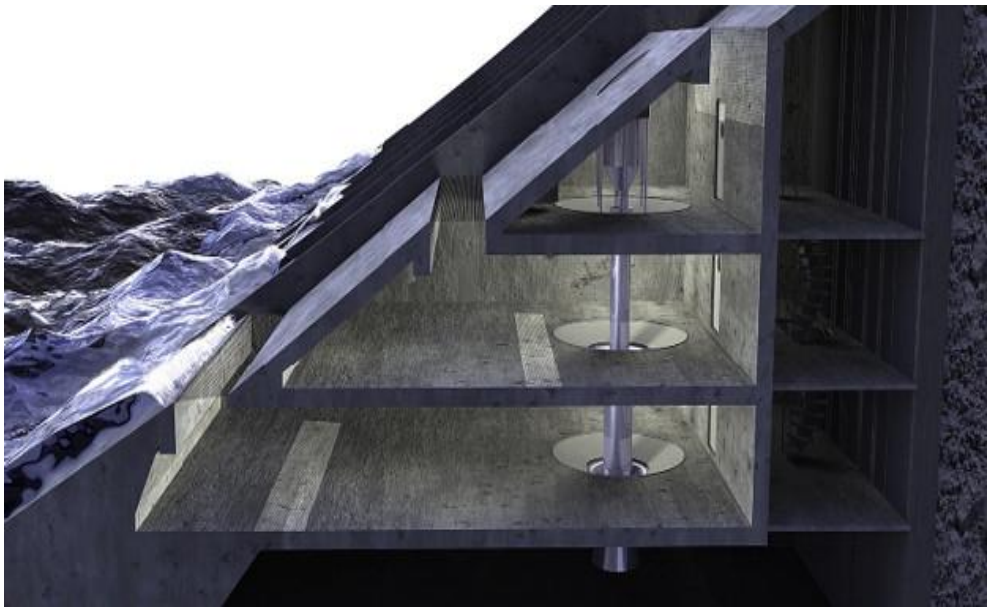

Figure 2.11 - Sea Slot-cone Generator (SSG) (Margheritini *et al*., 2009)

The most commercially advanced shoreline devices are those employing the oscillating water column (OWC) principle, such as the LIMPET which has been operating on the Isle of Islay (Scotland) since 2000, and the Mutriku breakwater wave-power plant that went operational in July 2011. Unlike overtopping WECs these devices rely on wave period as well as amplitude and have so far only been installed in relatively high energy environments (e.g. Europe's Atlantic coast). The LIMPET has been optimized for average annual shoreline intensities of 15 – 25 kW / m, making it a potentially less viable option in the Mediterranean. It has an installed capacity of 500 kW. The Mutriku plant has an installed capacity of 300 k W with the capability to supply energy to approximately 250 homes (www.wavegen.co.uk). It is a complex installation though, comprising of 16 Kaplan turbines, suggesting high capital and maintenance costs. There is also a question mark over the performance of OWC-type devices to date, with expected output at the LIMPET being less than the expected (Boake *et al*., 2002). It has been suggested (*ibid*.) that

misrepresentation of the bathymetry may be one reason for the LIMPET's under performance. A predicted foreshore slope of 1:25 was thought to extend up to the structure however it has since been found that the slope ends 60 m from the structure with a plateau extending to the shoreline, reducing the waves' energy. Therefore a detailed knowledge of the bathymetry is essential for the optimization of any shoreline WEC.

2.4 Wave Overtopping

A brief clarification of the significant wave height used for overtopping formulae in this study is required. A full explanation can be found in Appendix A1, essentially though this study uses the significant wave height at the structure toe $H_{s,toe}$. It is assumed that $H_{s,toe} = H_{mo,toe} = H_{1/3,toe}$.

2.4.1 Wave Overtopping Theory

Wave-overtopping refers to the process where waves run up a structure's face and, if the crest level of the structure is lower than the wave run-up height, overtop the structure (Kofoed, 2002). The overtopping discharge, q, is defined as the overtopping volume per second per meter width of structure ($m^3 s^{-1} m^{-1}$). Overtopping literature is mostly concerned with reducing overtopping rates than can cause damage to infrastructure, property and cars as well as injury and death to humans. Coastal protection usually requires the use of relatively large freeboards. Overtopping for generating power requires the opposite approach: the maximisation of discharge rates, for which low-crested structures are usually preferable (Tedd and Kofoed, 2009). The overtopping rates that are required for generating electricity are precisely those that engineers would otherwise seek to design against for coastal protection (Figure 2.12).

Reliable estimates of overtopping are required regardless of objectives. For WECs, over-prediction of discharge could result in prohibitively high freeboards with subsequent lower hydraulic efficiencies. Under-prediction could result in, amongst other things: freeboards being set too low with potential for increased spillages (loss of hydraulic power); and, the installation of an insufficient capacity.

For initial design purposes engineers commonly use empirical formulae and despite advances in the numerical modelling of overtopping, these formulae are currently considered the simplest and most robust ways to estimate overtopping rates (Allsop *et al.,* 2005), using simple equations based on a parameters that are easy to acquire (e.g. structure geometry). For simple slopes three formulae are widely used by engineers (Reeve *et al.,* 2008). These are: the Owen formula (1980); the Van der Meer & Janssen formula (1994); and Hedges & Reis's semi-empirical formula (1998). The Owen and Hedges & Reis formulae work best for wind waves whilst the Van der Meer & Janssen formula (henceforth written as the VMJ model) is considered better for swell waves

(Kofoed, 2002). The latter is appropriate since Vincanza *et al*. (2009) have suggested that waves above 1 m in north-west Sardinia are predominantly swell waves. Furthermore, the VMJ model has been used almost exclusively for studies of overtopping-type WECs (e.g. Kofoed, 2002; Stagonas *et al.*, 2010) and is therefore used in this study along with some more recent modifications. The Hedge's & Reis formula will not be used although its popularity amongst coastal engineers has risen recently (Reeve *et al.*, 2008).

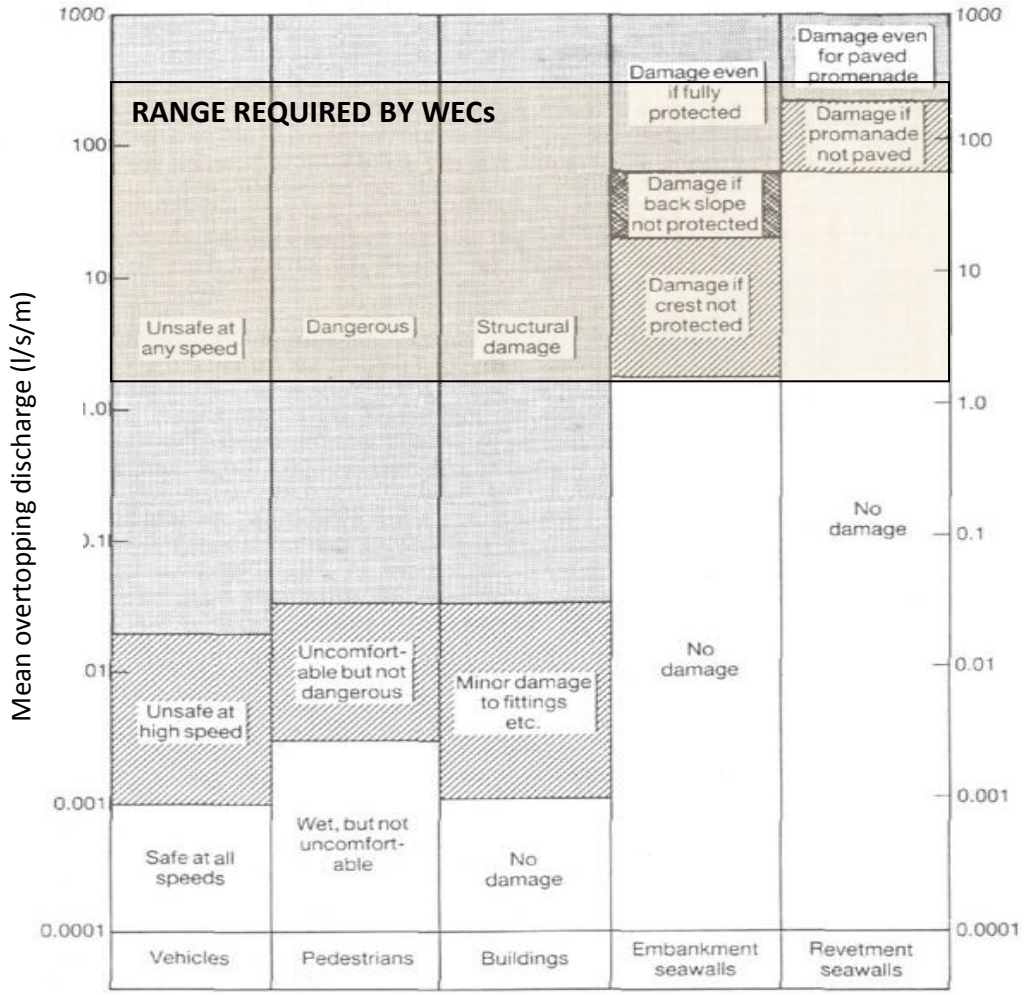

Figure 2.12 - Wave overtopping rates for WECs (Kofoed, 2002)

Owen's formula is discussed briefly since its form is the basis for much of the proceeding work on overtopping and the results upon which it was based were used by Van der Meer and Janssen (1994). The model proposes an exponential relationship between the dimensionless discharge, Q, and the dimensionless freeboard, R:

$$Q = \frac{q}{gH_sT_{mo}} = a\exp(-bR) \tag{9}$$

$$R = \frac{R_c}{T_{mo}\sqrt{(gH_{stoe})}} \quad (10)$$

where: a and b are empirically derived coefficients, dependant on the seawall geometry; R= the relative freeboard; and, T_{mo} = the mean spectral wave period.

Hedges & Reis (2008) found that Owen's formula "seriously over-predicted" overtopping rates for 1:2 slopes and for all cases where the surf-similarity parameter was greater than 2.5 (i.e. non-breaking waves), making it unsuitable for this study.

2.4.2 The Van der Meer and Janssen Model

The Van der Meer and Janssen model (1994) was derived from small and large-scale model tests on various seawalls performed in flumes at the Delft Hydraulics laboratory. The VMJ model is applicable for overtopping WECs since it is largely based upon simple, impermeable structures (Kofoed, 2002). It takes the exponential form of Owen's formula but the wave period no longer appears. Instead the surf-similarity parameter (ξ_{po}) is used to distinguish between breaking and non-breaking waves on the structure (not foreshore). ξ_{po} is also a measure of wave steepness and allows the influence of the wave period to be incorporated into overtopping expressions (Van der Meer and Janssen, 1994). Owen's coefficients *a* and *b,* are not included since the structure's slope is included when deriving the surf-similarity parameter:

$$\xi_{op} = \frac{\tan\alpha_s}{S_{op}} = \frac{\tan\alpha_s}{(\frac{H_{s,toe}}{L_0})} \quad (11)$$

where: α_s = the slope angle of the ramp; S_{op} = the deep water wave steepness; $H_{s,toe}$ = the significant wave height at the toe of the structure; and, L_0 = the deep-water wavelength.

Two equations are proposed, depending on whether ξ_{op} > 2 or < 2. For values < 2, waves are breaking and the following expression is used to calculate the average overtopping rate:

$$Q = \frac{q}{\sqrt{gH_{s,toe}^3}}\sqrt{\frac{S_{op}}{tan\alpha_s}} = 0.06\ exp(-5.2R) \quad (12)$$

When ξ_{po} > 2 (non-breaking), the alternative formula is used:

$$Q_b = \frac{q}{\sqrt{(gH_{s,toe}^3)}} = 0.2\exp(-2.6\ \frac{R_c}{H_{s,toe}}\ \frac{1}{\gamma_r\gamma_h\gamma_b\gamma_\beta}) \quad (13)$$

where: $\gamma_r, \gamma_h, \gamma_b$ & γ_β are reduction coefficients to account for slope roughness, a shallow foreshore, the presence of a berm and the angle of wave attack, respectively.

These coefficients range in value from 0.5 to 1.0, with a minimum combined value of 0.5. The best-case scenario for maximising overtopping is therefore when all coefficients equal 1. Hedges and Reis (2008) argue that a minimum combined coefficient of 0.5 may result in overestimations of overtopping. In this study however there is no berm included in the initial design (γ_b is set to 1) and the ramp material is taken to be smooth concrete (γ_r is set to 1), so it is unlikely the minimum value would be below 0.5. The coefficients γ_β and γ_h are derived are follows:

$$\gamma_\beta = 1 - 0.0033\beta \quad (14)$$

$$\gamma_h = 1 - 0.03\left(\frac{h_m}{H_{s,toe}}\right)^2 \text{ for } \frac{h_m}{H_{s,toe}} < 4;\ = 1 \text{ for } \frac{h_m}{H_{s,toe}} \geq 4 \quad (15)$$

where: β = the angle of wave approach; and, h_m = the depth of the water at the toe of the structure.

The coefficient γ_h is introduced to account for high waves on a shallow foreshore that may break before the structure, resulting in lower overtopping rates. It is important to remember that in the VMJ model ξ_{op} uses the structure's slope and not the beach slope. The use of the beach slope could indicate whether waves break before the structure and it is plausible to suggest that if the broken wave height were known then this could be used in the VMJ formula, in which case the coefficient γ_h would become obsolete. On the other hand there would then be no distinction made in the formula between say a 1 m wave that had broken and one that had not and yet broken waves may arguably behave differently when it comes to overtopping (e.g. Bruce *et al*., 2003). In any case Van der Meer and Jannsen (1994) state that Eq. (15) should only be applied for a foreshore of slope 1:100, and that for any considerable deviation above this (i.e. a greater slope) γ_h equals 1. This is somewhat ambiguous and unsatisfactory since it suggests no reduction in overtopping be made due to wave breaking on slopes greater than 1:100. This *could* result in an overestimation of overtopping. Despite this, and although wave

breaking can be established relatively simply using well known breaking parameters such as $\gamma = 0.78$ (Galvin, 1972) this study respects the conditions stipulated by Van der Meer & Jannsen (1994).

2.4.3 Kofoed's model

Kofoed (2002) revised the VMJ model after performing model tests to assess the effects that changes in ramp-slope geometry had on overtopping for the Wave Dragon. Since the device is designed to sit offshore all waves are considered non-breaking ($\xi_{op} \geq 2$). The VMJ model (Eq. (13)) becomes:

$$Q = \frac{q}{\lambda_a \lambda_{d_r} \lambda_s \lambda_m \sqrt{(g H_{stoe}^3)}} = 0.2e^{-2.6 \frac{R}{H_s toe} \frac{1}{\gamma_r, \gamma_b, \gamma_h, \gamma_\beta}} \quad (16)$$

where: $\lambda_a, \lambda_{d_r}, \lambda_s$ and λ_m are reduction coefficients accounting for the ramp slope, the draft of the ramp, the relative height of the crest and the shape of the ramp respectively.

The draft coefficient, λ_{d_r}, accounts for the fact that some of the wave passes underneath the floating structure (the ramp does not extend to the seabed). An increase in draft results in increased overtopping. In the case of the CSWEC the ramp extends to the bed and this coefficient is ignored and set to 1.

The shape-factor coefficient λ_m was derived from tests using different shaped ramps. The results showed that a double-curved convex-elliptic ramp increased the discharge, q, by 18% (assuming all other coefficients are set to 1). This is a considerable increase however there is no evidence yet to suggest this design would work on the CSWEC and this option will not be included further in this study, although it does warrant future research.

The coefficient λ_s accounts for the relative height of the freeboard and can be derived as follows:

$$\lambda_s = 0.4 \sin\left(\frac{2\pi}{3R}\right) + 0.6 \text{ for } R < 0.75; = 1 \text{ for } R \geq 0.75 \quad (17)$$

This is an important factor as it has been argued that the VMJ model could overestimate overtopping rates when the relative freeboard R is small (Oumeraci *et*

al.,1999; Kofoed, 2002; Goda, 2009a). This effect can possibly be seen from the 1:23 model results in Figure 2.3 where for a 1 m freeboard the efficiency (and therefore overtopping) appears to level off as the wave height increases (in that figure the relative freeboard expressed as $\frac{H_s}{R_c}$ rather than $\frac{R_c}{H_s}$).

The slope angle of the ramp was also investigated. Grantham (1953) suggested that maximum run-up, and hence overtopping, occurs at a slope angle of 30°. This was validated by Kofoed (2002), although earlier work by Kofoed and Nielsen (1997) suggested that overtopping rates (on the Wave Dragon) showed no significant variation between slope angles of 35° to 50°. The slope angle for the CSWEC is an important consideration since the footprint (and costs) of the ramp will change depending on slope. The reduction in overtopping due to the ramp angle is calculated as:

$$\lambda_a = cos^3(\alpha_s - 30°) \tag{18}$$

2.4.4 Goda's model

Goda (2009a) derived an alternative expression to the VMJ model from data taken from the CLASH database with the aim of deriving a unified set of formulae for inclined seawalls (and also vertical ones). A total of 1254 data were used from 24 datasets from testing facilities across the world, including freeboards ranging from zero up to heights of 2m - 3 m. The relative toe depth of the structure is included along with the influence of the foreshore slope. The resulting equation is:

$$Q = \exp\left[-\left(A + B\frac{R_c}{H_{s,toe}}\right)\right] = \frac{q}{\sqrt{(gH_{s,toe}^3)}} \tag{19}$$

where: A and B are coefficients derived as follows:

$$A = A_0 \tanh\left[(0.956 + 4.44tan\theta)\left(\frac{h_m}{H_{s,toe}} + 1.242 - 2.032tan^{0.25}\theta\right)\right]. \tag{20}$$

$$A_0 = 3.4 - 0.734cot\alpha_s + 0.239cot^2\alpha_s - 0.0162cot^3\alpha_s \tag{21}$$

$$B = B_0\tanh\left[(0.822 - 2.22tan\theta)(\frac{h_m}{H_{s,toe}} + 0.578 + 2.22tan\theta)\right] \tag{22}$$

$$B_0 = 2.3 - 0.5cot\alpha_s + 0.15cot^2\alpha_s - 0.0011cot^3 \quad (23)$$

where: $\theta =$ the slope of the foreshore in front of the structure

The inclusion of the relative depth at the toe means that the reduction factor $\gamma_h$is not required. The other reduction coefficients can be included where applicable. The reduction coefficient for oblique wave attack is modified though, resulting in a steeper rate of reduction as the wave angle increases:

$$\gamma_\beta = 1 - 0.0096(\beta) + 0.000054(\beta^2) \quad (24)$$

The structure slope angle is included in equation (19) and Goda (2009a) suggests that maximum overtopping occurs when $cot\ \alpha_s = 2$, (i.e. $\alpha_s \approx 27^o$). It is acknowledged (*ibid*.) that this figure is specific to the datasets used and that other data may yield different slope angles, although with little expected variation.

2.4.5 The Accuracy of Empirical Formulae

The accuracy of empirical formulae has been widely debated and they are generally only suitable for the conditions upon which they have been based. Douglass (1986) and Pullen *et al.* (2007) said overtopping in real-life could exceed formulae predictions by a factor of 1 to 3. Douglass (1986) based his findings though on large freeboards for coastal defence and the accuracy of formulae should increase for small relative freeboards (Kofoed, 2002). In comparisons with numerical models Reeves *et al*. (2008) found the VMJ models to be generally in agreement, underestimating by a factor of 1 to 2, and Hedges and Reis (2008) found the VMJ model agreed with the AMAZON model when ξ_{op} > 2. Underestimations could be due to several factors, including: scale-effects in the laboratory tests upon which most empirical formulae are based (De Rouck *et al*., 2003); and, wind. Besley (1999) says that for discharges larger than 10^{-1} m^3 s^{-1} m^{-1} wind plays an important role. There are also processes that could negatively affect overtopping but which are poorly understood such as the effect that run-down may have on incoming waves.

For the CSWEC, the 1:23 model (Eqs. (6) & (7)) predicts higher hydraulic powers (and overtopping rates) than the VMJ model (Stagonas *et al*., 2010). For a 1 m wave with a 1 m freeboard equation (6) predicts a hydraulic power of 60 kW for a 50 m capture

length. The VMJ model gives a hydraulic power of approximately 20 kW, lower by a factor of 3. At the time of writing it was not known whether studies have been carried out that verify the Kofoed and Goda models, other than by the authors themselves. Since they include additional parameters that should in theory reduce overtopping rates then it is likely that they will underestimate overtopping compared to the 1:23 model.

2.5 The Economics of Wave Energy Devices

2.5.1 The Cost of Electricity

The cost of electricity (COE) is the primary criterion by which most renewable energy projects are judged (Dalton *et al.*, 2010a) and is calculated by dividing the total annualized cost (TAC) of a WEC over its project life by the annual electrical output (AEO). The COE excludes any revenue received through the market price and FITs or renewable obligation certificates (ROCs), and can be expressed as:

$$\mathrm{COE} = \frac{\mathrm{TAC}}{\mathrm{AEO}} \tag{25}$$

The TAC is adjusted to present-day values through the use of a discount factor (DF), applied to the costs incurred in each year. This is because money in the future has less value than its present day value (e.g. €1 in 2030 will be worth less than €1 in 2011). The discount factor is expressed as:

$$DF = \frac{1}{(1+DR)^n} \tag{26}$$

where: $n =$ the year number, (so that costs in the later years of a project will be more heavily discounted than those in the early years); and, $DR =$ the discount rate.

The discount rate (DR) is calculated as follows (Dalton *et al*., 2010a):

$$DR = \frac{BR+f}{1-f} \tag{27}$$

where: $BR =$ the borrowing rate on the loan given to fund the project; and, $f =$ the rate of inflation.

It is widely stated that proven, mature technology will have access to cheaper borrowing rates (8%) than unproven, immature technology (15%)(Carbon Trust, 2006; Davey *et al*., 2009). The higher borrowing rate for unproven technology indicates that investors require a higher return on an investment carrying more risk (since the output of an unproven technology is less predictable than that of a proven one). Therefore the CSWEC is likely to use a borrowing rate of 15%, at least for the pilot stage.

Benchmark figures for the COE are summarized in Table 2.1. Estimates vary due to the heterogeneous nature of the technology and immaturity of the industry. Thorpe

(1999) said a figure of €0.05 / kWh was achievable a decade ago, based upon estimations made at the prototype stages of the LIMPET (shoreline) and OSPREY (nearshore). This now looks optimistic, at least in the near future. Raventos *et al*. (2010) have estimated a range of €0.10 - 0.40 / kWh across Europe by 2020, falling to €0.05 – 0.20 / kWh by 2030. Specific to the UK, a market leader in wave energy, Allan *et al*. (2011) quote a narrower range of £0.11 - 0.22 / kWh. The SSG is estimated to have a COE of €0.12 / kWh (Margheritini *et al*., 2009), and although this estimation has been made before the pilot project has been built, it conforms to the idea that shoreline WECs could have a low COE due to reduced construction and maintenance costs.

Table 2.1 – Summary of COE estimates

Study	Scale of study	COE (€ / kWh)	Comments
Thorpe (1999)	LIMPET & OSPREY	€0.05	Based upon prototype stage
Calloway (2007)	General	€0.18 – 0.61	From the Carbon Trust
Raventos *et al.,* (2010)	Europe	€0.10 – 0.40 (€0.05 – 0.20)	Approx. costs in 2020 ("" in 2030)
Allan *et al*. (2011)	UK	£0.11 – 0.22	Central estimate of £0.18
Dalton *et al*. (2010a)	Pelamis	€0.15 – 1.60	Depends on the site and number of WECs deployed
Margheritini *et al.* (2009)	SSG	€0.12	Estimated prior to pilot stage

Wave energy is relatively expensive when compared to other energy sources. Allan *et al.* (2011) quote figures for amongst other things: offshore wind (£0.06 - 0.08 / kWh); nuclear power (£0.04 / kWh); and, the most efficient combined-cycle gas turbines (£0.04 / kWh). Externalities are not included in these costs. This is beyond the scope of this study, however a comparison of different energy types should include factors such as environmental impact and greenhouse gas emissions, which should favour wave energy and increase its competitiveness (Raventos *et al*., 2010). On the other hand the intermittent supply to the grid that arises from any renewable scheme is a negative externality (Gross, 2004), although wave energy should benefit from lessons learnt in the wind industry (Polinder and Scuotto, 2005) and is in any case more reliable than both wind and solar power. Furthermore despite its current high COE, wave energy can be important to islands (such as Sardinia) where energy costs are traditionally higher, and it may even be that wave energy is already competitive in these areas (Margheritini *et al*., 2009).

2.5.2 Net Present Value (NPV)

The NPV is the sum of all costs incurred and revenues accrued over the project's lifetime discounted back to present day values and can be calculated as:

$$NPV = \sum_1^t TNC * DF \quad (28)$$

where: $TNC =$ the total net cash flow (revenue minus costs) for each year of the project; and, $t =$ the project lifetime in years.

The NPV is important since generally only a project returning a positive NPV will be considered economically attractive to investors, the return in this instance being higher than the minimum expected return (Allan *et al.*, 2011). (An attractive COE alone is an insufficient measure by which to assess the economic feasibility of a WEC since a low COE can still result in a negative NPV (Dalton *et al*., 2010a)). Different types of investors have different expectations though (Davey *et al*., 2009) and policymakers for example may look to support promising technology even if the NPV is initially negative. In any case, at a preliminary design stage, the identification of a negative NPV ought to act as a spur for design improvements, particularly to increase the efficiency and reduce the costs of a fully operational (possibly multi-device) installation (Weber *et al*., 2010).

2.4.3 Costs

The costs of a WEC project are broken down into: Capital Expenditure (CAPEX); and, Operational & Maintenance Expenditure (OPEX). Both CAPEX and OPEX for an installed WEC will be highly dependent on the device and site, due to the heterogeneous and immature nature of the technology and the various environments in which they are installed. This can be contrasted to offshore wind power, where the technology is homogeneous and mature, allowing for greater accuracy in cost estimations.

A good estimation of CAPEX is needed, since with the exception of decommissioning the CAPEX or 'overnight costs' are loaded towards the front end of a project, meaning these costs are discounted at a lower rate than the revenue stream occurring later in the project and therefore have a large bearing on the project's financial success. The true CAPEX of any particular installed WEC will only be known once a detailed design of the installation is carried out however there are models that can give some initial indication of costs.

Figure 2.13 shows a cost-model for a WEC produced by the Carbon Trust (2006), breaking CAPEX into different cost centres (e.g. device, installation and transmission). This is a simple parametric cost model, allowing an overall estimation to be made based upon knowledge of certain cost centres. Since the model is based upon various technologies (Carbon Trust, 2006), any estimation made upon one cost centre is likely to be less accurate than one made based upon knowledge of a number of cost centres.

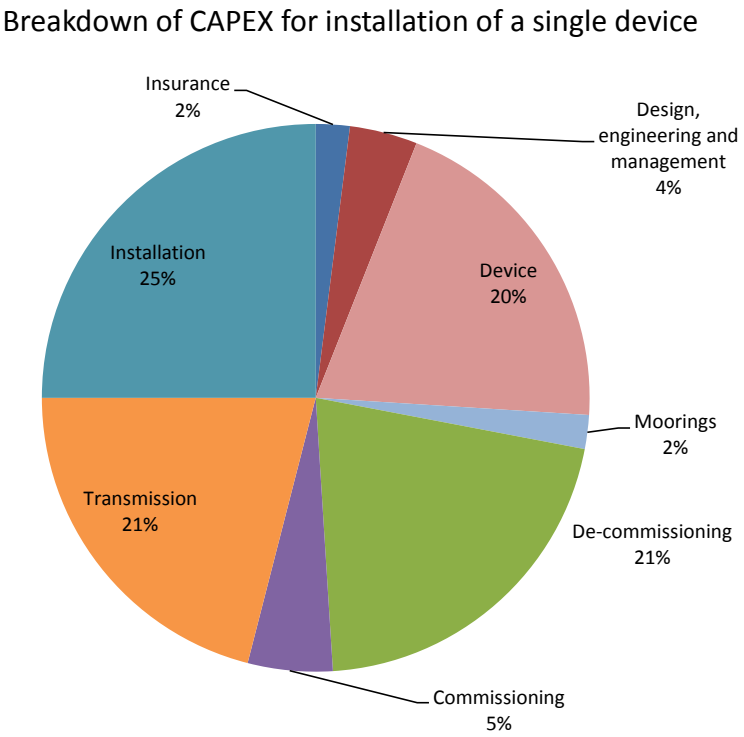

Figure 2.13 - CAPEX for a single WEC installation (Carbon Trust, 2006)

The inclusion of decommissioning in the model shows that the costs incurred over a whole project lifetime need to be considered. In reality the decommissioning costs are likely to be heavily discounted and will have a marginal effect on a project's financial viability. The device could also be left *in situ* at the end of the project and costs can sometimes be recouped through scrap (Davey *et al*., 2009). Design improvements, optimisation and learning outcomes may alter the weightings of each cost centre (Carbon Trust, 2006), so that in the course of the project design the cost model will require updating to reflect these changes.

Figure 2.14 shows the change in weighting of cost centres if an array of devices is installed. The installation, transmission and decommissioning costs go down as a percentage of total CAPEX, the devices making up the highest percentage of costs. Costs

per unit of technology are expected to decrease significantly when moving from pilot stage to larger scale production (Carbon Trust, 2006). A report by Ernst & Young (2010) suggests a reduction in costs per unit of technology of 30%. For offshore wind, costs per unit are estimated to come down by 15% to 30% when production is doubled (Gross, 2004).

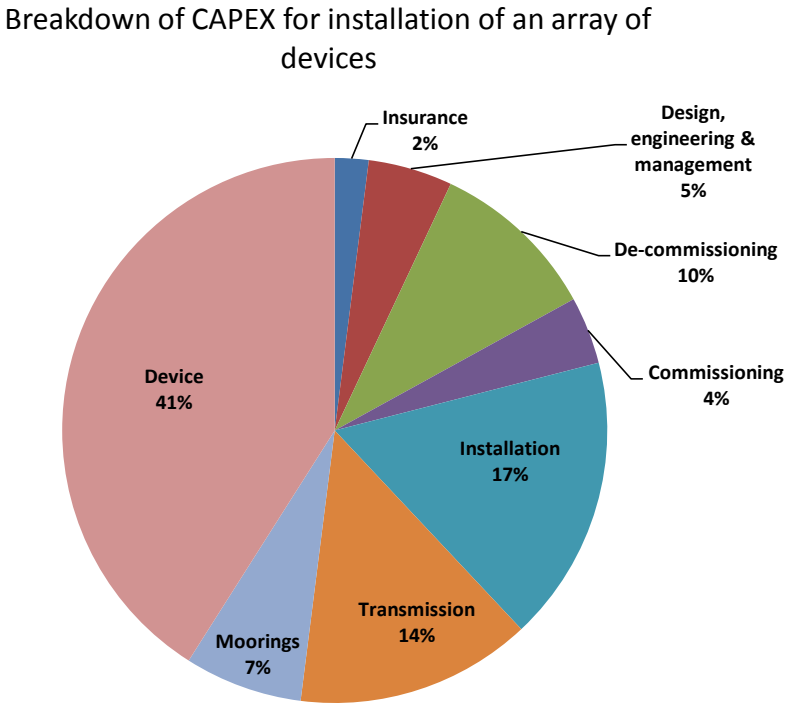

Figure 2.14 - CAPEX for array of devices (Carbon Trust, 2006)

OPEX can be estimated using similar models to those used to estimate CAPEX. Given the lack of operational and commercial activity upon which to draw information, it may however be difficult to obtain accurate figures for different cost centres, possibly until well into the operational phase. Another method is to estimate OPEX (per annum) as a percentage of initial CAPEX (CAPEX minus decommissioning costs) (Raventos *et al*., 2010).

Table 2.2 shows typical OPEX estimates. For the CSWEC the operational and maintenance has been estimated at around 5% per year of total CAPEX (Müller, pers. comm.). Thorpe (1999) reported lower figures than this: 2% for the LIMPET; and, 3% for OSPREY. Dalton *et al*. (2010b) report values ranging from 1.5% to 5%. Meanwhile a value of 4%, based upon typical values for offshore wind, was quoted by Raventos *et al*. (2010).

Although the range of these values does not appear great, OPEX is important as it continues to affect the cash flow of a scheme throughout its lifetime. It is acknowledged that shoreline WECs should in theory be easier and cheaper to maintain due to increased ease of access (Stagonas *et al*., 2010) and therefore the eventual OPEX of the CSWEC should be in the lower region of these estimates.

Table 2.2 - Summary of OPEX estimates

Study	Scale	% of CAPEX	Comment
Müller (pers. comm.)	CSWEC	5	Pre-prototype estimation
Dalton *et al*. (2010b)	General	1.5 – 5	Various technologies
Raventos *et al*. (2010)	Europe	4	Based on offshore wind
Thorpe (1999)	LIMPET & OSPREY	2 – 3	Based on prototypes

2.4.4 Project Costs

Cost data supplied by Müller (pers. comm.) are shown in Table 2.3. Ramp costs were based upon an original proposed installation in front of the seawalls at Alghero, where a rock plateau of depth 1 m exists. The estimate was €2-3000 / m with a low confidence attached. Recently data have been supplied for the ramp and walls by Ferrante (pers. comm.) based upon the sketch in Figure 2.8 (sitting in 2.5 m of water with a height of approximately 3 m). For a total length of wall of 110 m this produced a cost of €330000 (€3000 / m). The two estimations for ramp / wall costs are therefore close and in this study a cost of €3000 per m will be used regardless of the water depth and structure height and can be regarded with some degree of confidence. The HPWs cost between €4000-6000 per installed kW. Transmission costs are estimated to be low since sub-sea cables are not needed and Sardinia is well populated along the coast with an existing electricity network.

For the current project the cost models in Figures 2.15 and 2.16 are used. Moorings are not required, and since the cost of the HPWs, ramp/walls, transmission and outflow are all known they are included as one cost centre.

Table 2.3 - Project costs

Unit	Size / Length	Costs
HPWs	0 - 50 kW	€6000 / kW + €20000 installation
	50 – 100 kW	€5000 / kW + €20000 installation
	+ 100 kW	€4000 / kW + €20000 installation
Ramp/wall	110 m	€3000 / m
Outflow		€50-100000
Transmission		€20000

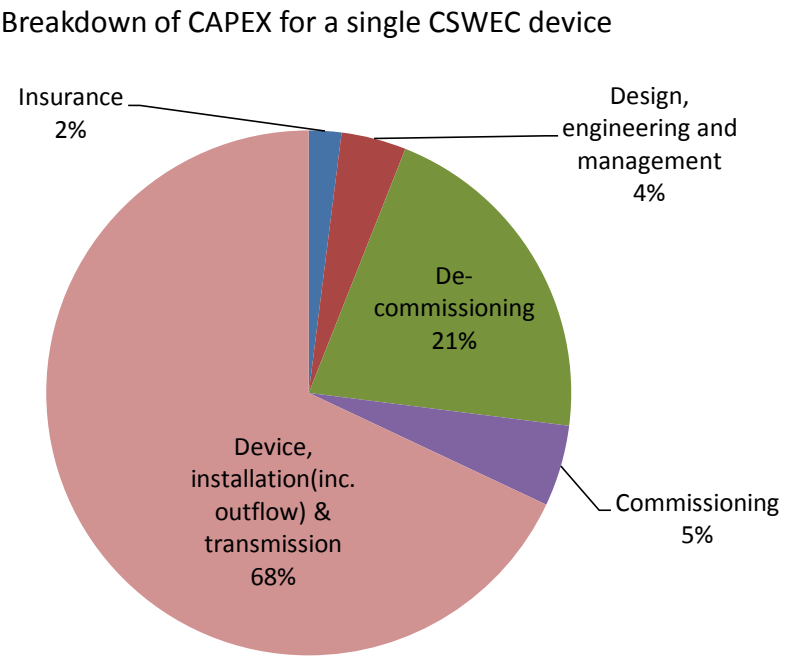

Figure 2.15 - CAPEX for a single CSWEC installation (adapted from Carbon Trust, 2006)

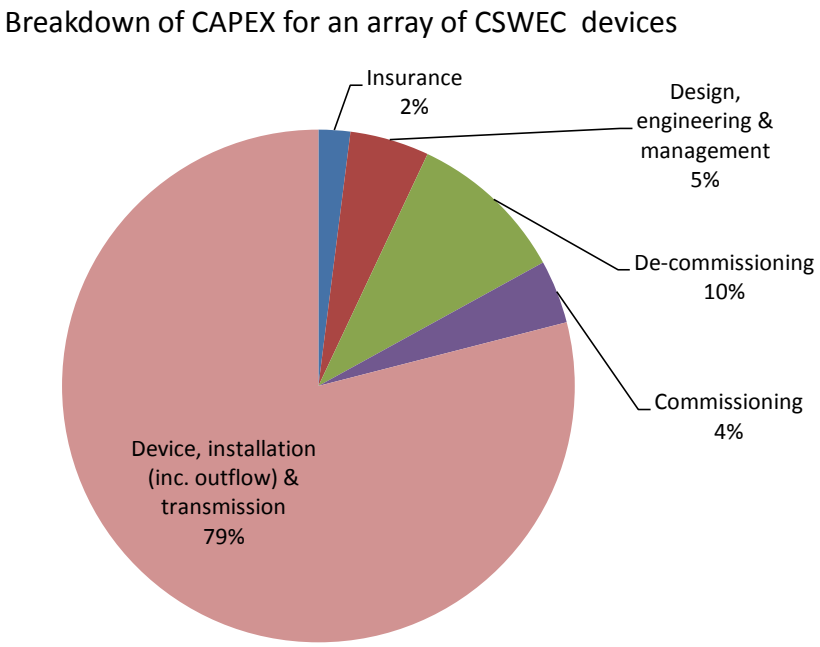

Figure 2.16 - CAPEX for an array of CSWECs (adapted from Carbon Trust, 2006)

2.4.5 Revenue

The revenue is the monetary value of a WEC's output and refers to the wholesale market-price of electricity and feed-in tariff (FIT) received for every kWh of electricity produced (Davey *et al*., 2009). Electricity is currently priced around €0.21 / kWh in Italy (source: epp.eurostat.ec.europa.eu) and the wholesale price is approximately one half of this at €0.10 / kWh (Vicinanza *et al*, 2009). The FIT is the guaranteed price of electricity that the generator receives for every kWh of electricity it produces. Currently Italy offers a fixed (index-linked) FIT of €0.34 / kWh for the first 15 years of a project after which the revenue is determined solely by the market rate of electricity (EREC, 2009). This compares beneficially to other EU countries. In Ireland the FIT is €0.22 / kWh and in Portugal €0.27 / kWh (Dalton *et al*., 2010a). Renewable obligation certificates (ROCs) are also available to projects with an installed power above 1MW (after which FITs are no longer available). These offer financial incentives for energy companies to supply more electricity from renewables. They *are* available to smaller schemes however their market value fluctuates and so the FIT may be more attractive to projects up to 1MW. The value of ROCs is currently around €100 / MWh (EREC, 2009). For wave energy the Italian government offers 1.8ROCs / MWh (€0.18 / kWh), guaranteed for the first 15 years of the project

(EREC, 2009). The revenue per kWh is therefore proportionately less for larger installations.

Other financial instruments are also available. The Italian government gives subsidies towards the CAPEX of renewable energy schemes. No value could be found for wave energy, so the subsidy is assumed to be the same one offered to wind and solar, which is 30% of the initial CAPEX (EREC, 2009). There is also various funding available from the European Union for wave energy projects and devices such as Wave Dragon, PELAMIS and the SSG have all benefited from this.

3 METHODOLOGY

3.1 Wave Resource Assessment – MIKE 21 NSW

Numerical models play an important part in marine resource characterisation at a regional scale (Vengopal *et al*., 2009), allowing for assessments to be made that would otherwise require large amounts of direct measurements, which take up time and money. In this study the numerical model MIKE 21 NSW was used to transform waves from offshore to the shoreline. MIKE 21 NSW is a third generation spectral 2-D wind-wave numerical model that describes the propagation, growth and decay of short-period and short-crested waves (applicable to this study since waves had relatively short periods in the range of 4 - 9s). The model includes the following processes: shoaling; refraction; and, energy dissipation though bottom friction. It can therefore show how wave energetics change as waves move into shallower water. The model is used widely commercially and has been validated in numerous instances. For the model to work accurately though, there is a requirement for data of reliable quality.

3.1.1 Offshore wave data

Wave data were taken from the Alghero wave buoy, part of the Italian Wave Network (IWN), available online at www.idromare.it. The Alghero wave buoy (coordinates: 40°33'11.99"N; 08°07'00.01"E) has a relatively long history of recordings, running from July 1989 to April 2008. The buoy recorded data for 30 minutes every 3 hours, returning values every 3 hours for the significant wave height (H_s) and the spectral mean period (T_{mo}). From 2000 the buoys recorded continuously but still returned one value every 3 hours. The exception to this was when wave heights exceeded 5 m, in which cases data was returned every 30 minutes.

Although wave data from the buoy have been previously analysed by Vicinanza *et al*. (2009), that study gave wave height data in relatively large bin-sizes (1 m). The data were re-analysed in order to obtain more defined bin-sizes. Values returned every 30 minutes were stripped out so only data returned every 3 hours was used in the analysis (8 records per day). This may have missed extreme wave heights but since WECs should be more concerned with maximising power from average/moderate wave heights (Cruz, 2008) this is not considered a problem.

Missing data is shown in Appendix A2. There was a low percentage of missing data from 1990-2000 & 2007 (1% to 8%), but a high percentage of missing data from 2001-2006 (21% to 55%). Data from 2001-2006 were therefore treated as unreliable and not used further. 1989 & 2008 were also discarded since they only recorded for parts of the year. This resulted in 12 years of data. Ideally more data would be needed but the use of these years only is considered better than including possible misrepresentative data. Missing data within the years 1990-2000 & 2007 were also discarded and since it was observed that the missing data in those years appeared to occur at all times of the year it is not expected that this will significantly affect the calculated frequency of occurrence.

Table 3.1 summarizes the wave conditions at the wave buoy. (A detailed list is in Appendix A3). The predominant wave directions were estimated using the wave rose in Appendix A4. Using data from Vicinanza *et al*. (2009) it was estimated that approximately 72% of waves came from the north-west quadrant (mean direction 307.5^{o}) and 28% from the south-west quadrant (mean direction 250^{o}). There is a high tendency (91%) for the largest waves (+ 2.5 m) to come from the north-west quadrant.

Table 3.1 - Summary of wave conditions at the Alghero wave buoy

Wave height (H_s), m	**Wave Period (T), s**	**Frequency of occurrence (%)**	**% of bin-size coming from north-west or south-west**	
			307.5^{o}	**250^{o}**
0 - 0.7	3.9 – 4.4	40	72	28
0.7 – 1.4	4.7 – 5.5	27	65	35
1.4 – 1.8	5.6 – 6.0	10	70	30
1.8 – 2.5	6.2 – 6.9	10	70	30
+ 2.5	6.9 – 9.2	13	91	9
TOTAL		100	72	28

The annual average offshore wave power (9.04 kW / m) was calculated using the following equation to calculate deep water wave power for each wave height (Vicinanza *et al*., 2009), and then multiplying each wave power value by its frequency of occurrence and summing the results:

$$P_{wave\ deep} = \left(\frac{\rho g^2 T_{m0} H_s^2}{64\pi}\right)/1000 \qquad (29)$$

This figure corresponds with the on-going study by Vicinanza (pers. comm.) which reports a figure of 9.05 kW / m. There is a high degree of seasonal variation with a maximum mean power of 16 kW / m in February and November and a minimum of less than 3 kW / m in August (Appendix A5).

3.1.2 Bathymetric Data

Bathymetric data were taken from the General Bathymetric Chart of The Oceans (GEBCO) using the GEBCO-08 grid, which was used in the study by Vicinanza (pers. comm.). The data was extracted under a Mercator projection (accurate for area, distance and angles over small geographic areas) and transformed into a raster dataset using ArcGIS. A high-resolution image was exported and uploaded into MIKE ZERO (Appendix A6) and used as a background image with which to create the bathymetry.

The study area was projected in MIKE using the Universal Transverse Mercator 32 (UTM32), the Mercator projection commonly used for Italy. Vector contour lines are not available for the GEBCO-08 grid and were drawn in using the MIKE ZERO bathymetry editor tool using the background image as a guide. Since this image was in raster format a degree of pixilation occurred. In other words there was no clear line to follow. This may have resulted in some error however since the study is essentially at a regional scale the effect of any error is likely to be comparatively small and is ignored for the rest of the study. The GEBCO data are accurate up to approximately a depth of 20 m. The bathymetry nearer the shoreline could however not be established during this study. Images were available online (www.sidimare.it.net) but attempts to geo-reference them in ArcGIS resulted in high errors. Instead the shoreline depth was assumed to be -2.5 m for the whole region, based on observations of a nautical map (available online at www.nauticalchartsonline.com), and from discussions with the project team.

Figure 3.1 shows the grid set-ups for the predominant wave directions. The x-axis is orientated in the direction of the waves, important since the model performs its calculations along the x-axis. For a wave direction of 307.5^{o} the grid was rotated +37.5^{o} and for a wave direction of 250^{o} the grid was rotated -20^{o}. Small grid-spaces were chosen ($\Delta x, \Delta y$ = 50m) to allow for a high degree of accuracy near the shoreline. The grids were sized as follows: 1600(x) x 1300(y) points for a wave direction of 307.5^{o}; and 1225(x) x 1800(y) points for a wave direction of 250^{o}. The grids had the respective origins: 007^{o}35’11”E, 40^{o}22’19”N; and 007^{o}56’53”E, 39^{o}50’07”N.

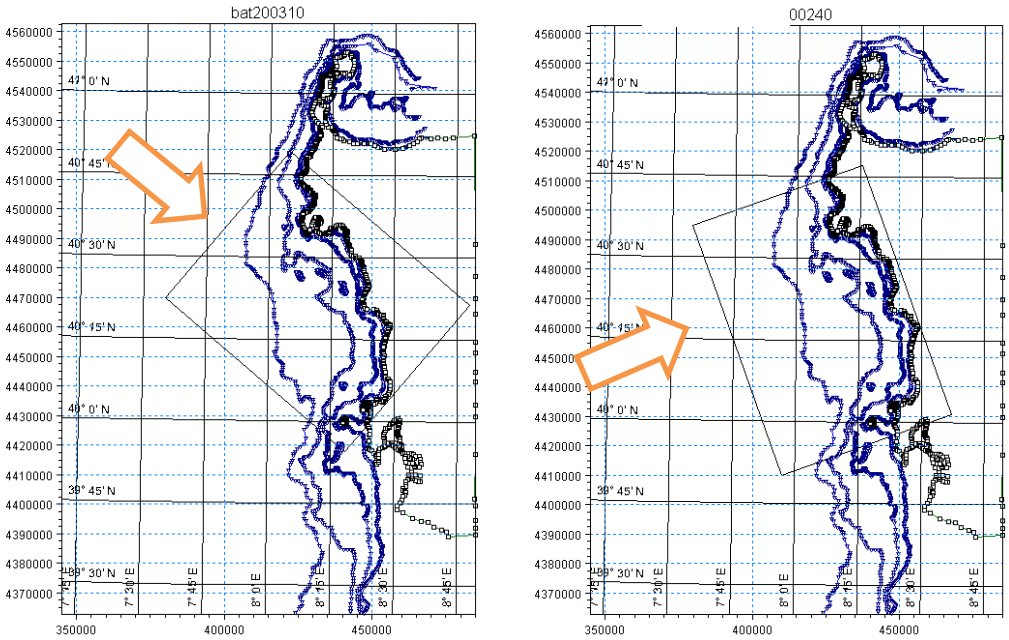

Figure 3.1 - Grid set-ups: left) 307.5°; right) 250°

Figure 3.2 shows the interpolated bathymetry for the grid set-up for waves coming from 307.5°.

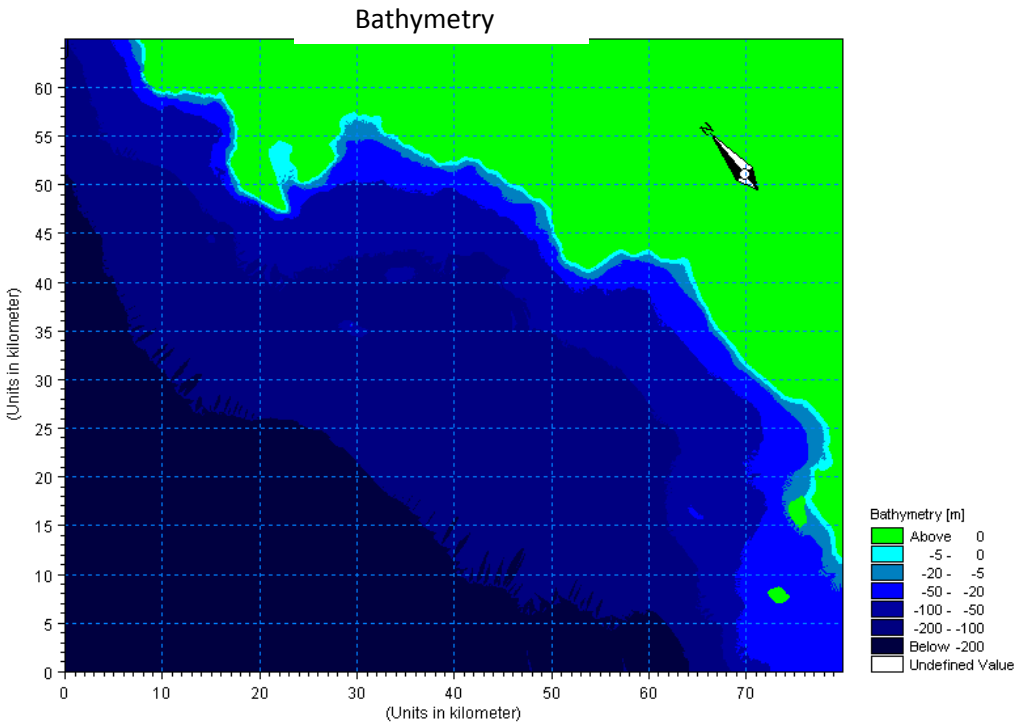

Figure 3.2 - Bathymetry for waves approaching from the north-west

A bathymetry was created for each grid using the triangular gap-filling method. This method takes the longest computationally (3-4 hours) but results in exactly the same bathymetry. Other interpolation methods included in MIKE 21 are quicker computationally but bathymetries differ between grids that are orientated differently. The bathymetries were checked against the raster dataset in ArcGIS and appeared to be consistent with that data. The interpolated grid for the south-westerly waves is in Appendix (7).

3.1.3 Errors in Bathymetry

The assumption of a uniform depth of 2.5 m along the coastline was considered acceptable at a regional scale however for the study of specific areas it is acknowledged that this may be misrepresentative. A sensitivity analysis was carried using different depths (-2 m and -3 m) to assess likely changes in wave conditions and is discussed later. Furthermore constant slopes were assumed (through interpolation) between the -20 m contour and the -2.5 m contour. The importance of the foreshore slope for shoreline wave energy devices has already been discussed (Boake *et al*., 2002), whilst Goda (2009a) includes it in his overtopping formula. In the Mediterranean it is common, at least on rocky shores, for there to be a steep slope near to the shore therefore in some instances the foreshore slopes in the bathymetry may be too gentle and could underestimate wave power. On the other hand, situations could arise where the assumed foreshore slopes were too steep. It is essential therefore that a thorough bathymetric survey is done on any final chosen site.

Figure 3.3 shows the how shoreline wave heights were calculated. An additional problem with the bathymetry was that the interpolation method did not recognise the -2.5 m contour line unless it was positioned approximately 250 m off the coastline. This creates a plateau (with constant depth of 2.5 m) in front of the shoreline which could again negatively affect wave heights and power, as seen with the LIMPET (Boake *et al*., 2002). To compensate for this an average of the wave heights was taken at each site across the width of the plateau and along the coastline (typically 1-3 km). MIKE 21 can create a selection area from which the average wave height can be statistically calculated. This is shown in Figure 3.3 as the shaded area at the shoreline. In this instance this

corresponds to the selection area at site 6. Details of all selection areas are shown in Appendix A8.

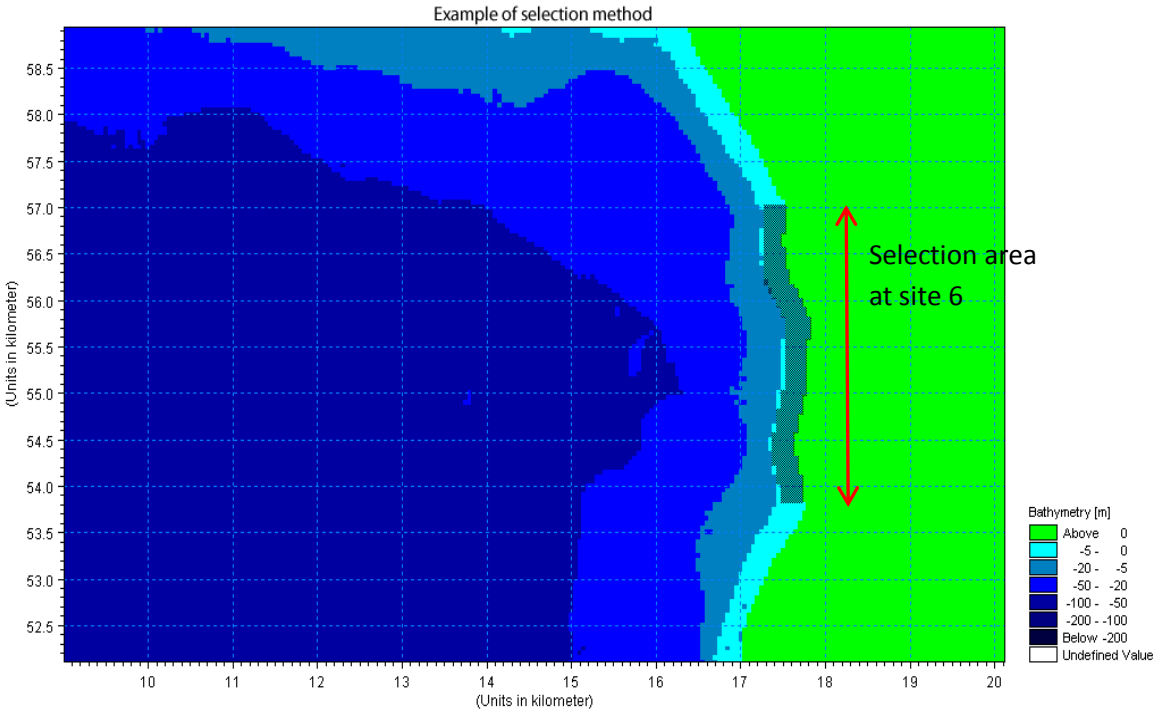

Figure 3.3 -Example of selection area used to calculate wave heights

3.1.4 Model Calibration

The model was calibrated two ways. Firstly against wave heights at the Alghero wave buoy. There was a near-perfect correlation with the buoy measurements (root-mean-squared error ≈ 0). This was expected since the buoy was close to the grid boundaries and in deep water. Secondly, the model was calibrated against shoreline wave heights estimated using empirical formulae (Goda, 2000; Goda, 2009b), which included simple methods for predicting reductions in wave heights as a result of refraction and diffraction. The full methodology is explained in Appendix A9. Whilst these methods have been validated against data from the CLASH dataset (Goda, 2009b) it would be preferable to calibrate against direct measurements taken from near the shoreline, however these options were not available in this study.

The resulting model set-up is outlined in Table 3.2. The directional spreading-index value of 4 is between those recommended for wind waves, n = 2, and long-period swell, n = 10 (Vengopal *et al.*, 2010), appropriate since waves in the region are swell (Vicinanza *et*

al., 2009) but not long-period. The nikuradse roughness-parameter was used as a calibrating coefficient. Symmetrical lateral boundaries were used and the non-breaking wave option chosen (since overtopping equations make adjustments for depth-limited waves).

Table 3.2 - MIKE 21 set-up

Offshore wave height (H_s), m	**Wave direction = 307.5°**		**Wave direction = 250°**	
	Directional spreading index (n)	**Nikuradse roughness parameter (k)**	**Directional spreading index (n)**	**Nikuradse roughness parameter (k)**
1	4	0	4	0
1.5	4	.001	4	0.005
2	4	.007	4	0.04
2.5	4	.006	4	0.15
3	4	.11	4	0.25
3.5	4	.18	4	0.35
4	4	.22	4	0.45
4.5	4	.29	4	0.60
5	4	.33	4	0.65
6	4	.41	4	0.83

3.2 Discounted Cash-flow models

Two models are used for the cash-flow analysis that will return the COE and NPV for a single installation and an array.

Figure 3.4 shows the model for the pilot stage and the following conditions are assumed:

- The borrowing rate *BR* used in equation (22) is 15% as recommended for unproven technology;
- The inflation rate *f* used in equation (22) is 3%, as used by Raventos *et al*. (2010) and which is close to the Italian inflation rate at the time of writing;
- A planning stage of 3 years, based on advice from Deledda (pers. comm.) that permits take at least 2 years to obtain;
- A construction period of two years (years 3-5);
- Operational period of 25 years (years 6-30);
- Two years decommissioning (years 31-32);
- FIT of €0.34 / kWh available for first 15 years of operation;
- Wholesale price of €0.10 / kWh available throughout operation;
- A full refit of one wheel occurs in year 15;
- OPEX costs are 5% of initial CAPEX (CAPEX minus decommissioning)
- Subsidies when applied are considered as a non-repayable loan given at the beginning of project and are taken off CAPEX at the first opportunity.
- The Total Annualised Cost (TAC) is calculated as the sum of the discounted cost for the whole project life time, divided by the number operational years (25 years).

Figure 3.5 shows the model used for array of devices. The same assumptions are made, except that planning stage is reduced to one year based on likelihood that permits will already be in place, bringing the whole project forward by 2 years, and that:

- The borrowing rate *BR* used in equation(22) is 8%
- OPEX costs are 3% of initial CAPEX, based on the approximate middle value of the estimates summarized in Table 2.2.

Figure 3.4 - Discounted cash-flow model for single installation

	YEAR	CAPEX			OPEX	TOTAL COSTS	TOTAL COSTS * Discount Rate	REVENUE			TOTAL REVENUE	TOTAL REVENUE - TOTAL COSTS	(TOTAL REVENUE - TOTAL COSTS) x Discount rate
		Project design & Commissioning	Construction & Installation	Decomissioning		=CAPEX + OPEX		Annual Output (kWh)	Market price euros/kWh 0.1	FIT euros/ kWh 0.34	=An. Output x (Market Price + FIT)		
Inflation Rate = 3% Borrowing rate = 15% Discount rate = (BR +f) / (1-f)													
Poject Management (Yrs 1-5)	1												
Commissioning	2												
	3												
Construction & Installation	4												
	5												
	6												
	7												
	8												
	9												
	10												
	11												
	12												
	13												
	14												
REFIT	15												
	16												
	17												
	18												
	19												
FEED-IN TARIFF ends	20												
	21												
	22												
	23												
	24												
	25												
	26												
	27												
	28												
	29												
	30												
Decommisioning	31												
	32												
	TOTAL						(SUM/25)/Annual Output = COE						SUM = NPV

	YEAR	CAPEX			OPEX	TOTAL COSTS	TOTAL COSTS * Discount Rate	REVENUE			TOTAL REVENUE	TOTAL REVENUE - TOTAL COSTS	(TOTAL REVENUE - TOTAL COSTS) x Discount rate
		Project design & Commissioning	Construction & Installation	Decomissioning		=CAPEX + OPEX		Annual Output (kWh)	Market price euros/kWh	FIT euros/ kWh	=An. Output x (Market Price + FIT)		
Inflation Rate = 3%										0.34			
Borrowing rate = 8%													
Discount rate = (BR +f) / (1-f)									0.1				
Poject Management, commissioning (Yrs 1-3)	1												
Construction & Installation (Yrs 2-3)	2												
	3												
	4												
	5												
	6												
	7												
	8												
	9												
	10												
	11												
REFIT	12												
	13												
	14												
	15												
	16												
	17												
FEED-IN TARIFF ends	18												
	19												
	20												
	21												
	22												
	23												
	24												
	25												
	26												
	27												
	28												
Decommisioning	29												
Decommisioning	30												
	TOTAL						(SUM/25)/Annual Output = COE						SUM = NPV

Figure 3.5 - Discounted cash-flow model for an array of devices

4 RESULTS

4.1 Wave simulations

4.1.1 Results of wave simulations

For a regional overview waves were initially simulated from 1 m to 3 m at half-meter intervals, and then at 4 m, 5 m and 6 m. Offshore waves of 0.8 m were also run, representing the likely lower boundary of useful offshore wave heights. The results are summarized in Table 4.1. Shoreline orientations were estimated using Google Earth. Transformations of offshore waves with height of 1.5 m are depicted in this section since these waves fall within the range of 1 m – 2 m that are representative of the more moderate and frequent waves that a WEC needs to utilize most efficiently (Cruz, 2008). Other offshore wave heights are referred to in the text.

Figure 4.1 shows a regional view of wave transformations approaching from the north-west (307.5°).

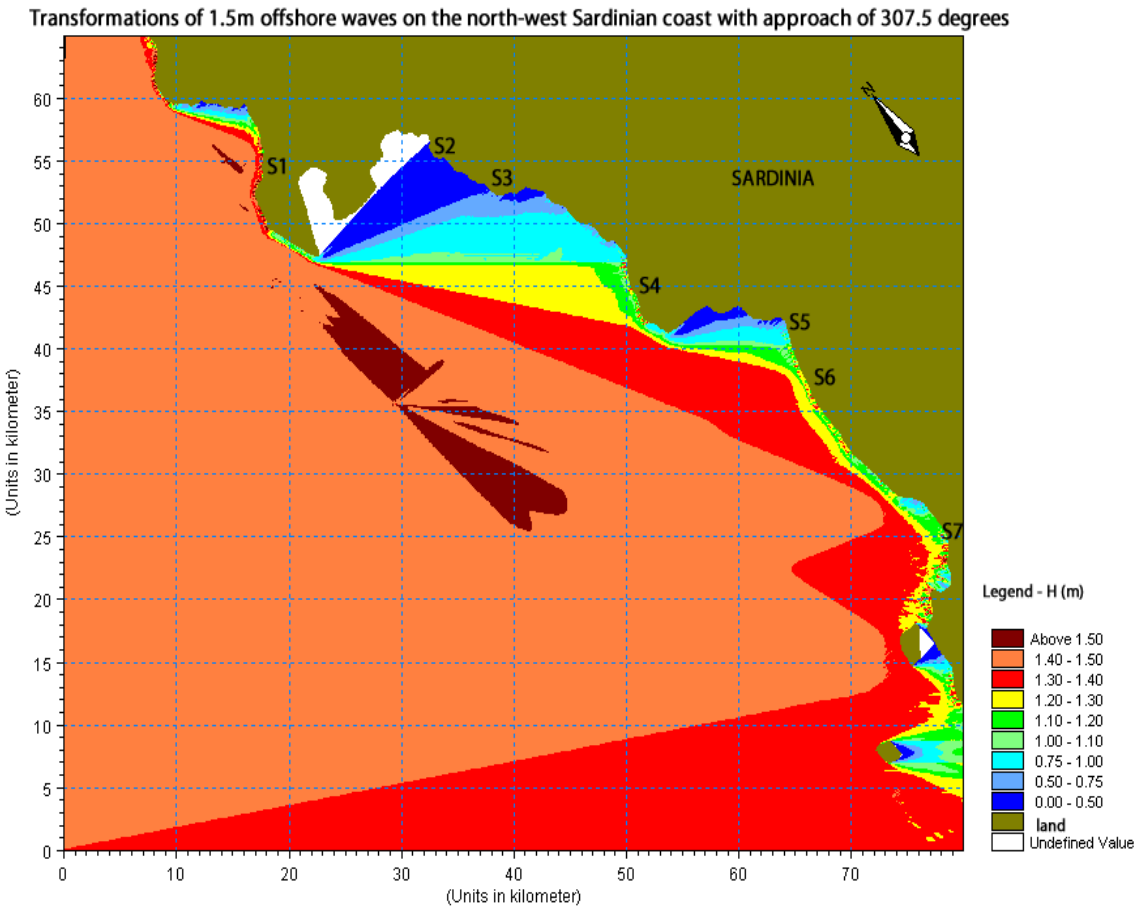

Figure 4.1 - Wave transformations for 1.5 m waves approaching from the north-west

Table 4.1 Summary of shoreline wave conditions at sites 1 to 7

OFFSHORE WAVES WITH NORTH-WEST APPROACH (307.5^o)								
Offshore wave-height (m)	**Period (s)**	**S1 Hs** (m)	**S2**	**S3**	**S4**	**S5**	**S6**	**S7**
0.8	**4.8**	0.74 m	0.04	0.26	0.62	0.46	0.67	0.69
1	**5.0**	0.93	0.05	0.32	0.79	0.38	0.84	0.86
1.5	**5.7**	1.4	0.06	0.45	1.19	0.81	1.25	1.24
2	**6.2**	1.81	0.07	0.56	1.53	0.99	1.61	1.51
2.5	**6.9**	1.98	0.07	0.57	1.64	0.90	1.72	1.36
3	**7.5**	2.14	0.08	0.58	1.73	0.87	1.83	1.29
4	**8.0**	2.43	0.11	0.59	1.91	0.80	2.02	1.14
5	**8.5**	2.61	0.13	0.61	2.00	0.74	2.11	0.99
6	**9.2**	2.84	0.14	0.64	2.16	0.74	2.26	0.94
Shoreline wave direction		305^o	270^o	270^o	295^o	270^o	285^o	270^o
Shoreline orientation		295^o	250^o	250^o	290^o	260^o	290^o	310^o
Angle of wave attack		10^o	20^o	20^o	5^o	10^o	5^o	40^o

OFFSHORE WAVES WITH SOUTH-WEST APPROACH (250^o)								
Offshore wave-height (m)	**Period (s)**	**S1 Hs (m)**	**S2**	**S3**	**S4**	**S5**	**S6**	**S7**
0.8	4.8	0.52 m	0.73	0.75	0.72	0.69	0.73	0.6
1	5.0	0.65	0.94	0.96	0.92	0.87	0.93	0.75
1.5	5.7	0.93	1.32	1.4	1.33	1.15	1.33	1
2	6.2	1.15	1.5	1.68	1.59	1.16	1.57	1.02
2.5	6.9	1.23	1.39	1.74	1.62	0.87	1.58	0.78
3	7.5	1.32	1.31	1.75	1.64	0.70	1.59	0.65
4	8.0	1.5	1.23	1.92	1.75	0.60	1.67	0.60
5	8.5	1.66	1.19	2.00	1.67	0.60	1.71	0.62
6	9.2	1.81	1.18	2.12	1.76	0.59	1.77	0.63
Shoreline wave direction		283^o	250^o	240^o	260^o	270^o	270^o	270^o
Shoreline orientation		295^o	250^o	250^o	290^o	260^o	290^o	310^o
Angle of wave attack		10^o	0^o	10^o	30^o	10^o	20^o	40^o

Figure 4.2 shows sites 1 and 2. At site 1 (Torre del Porticciolo), waves reach the shoreline with an average height of 1.4 m and with a direction of approximately 306° (no deviation from the offshore direction). This results in an angle of wave attack of 12°. At site 2 there is a 'shadowing' effect caused by the Cappo Caccia headland. For all offshore waves from the north-west, wave heights at site 2 never exceeded 0.14 m. The western side of the Cappo Caccia appears very energetic, with wave heights similar to or higher than those at site 1.

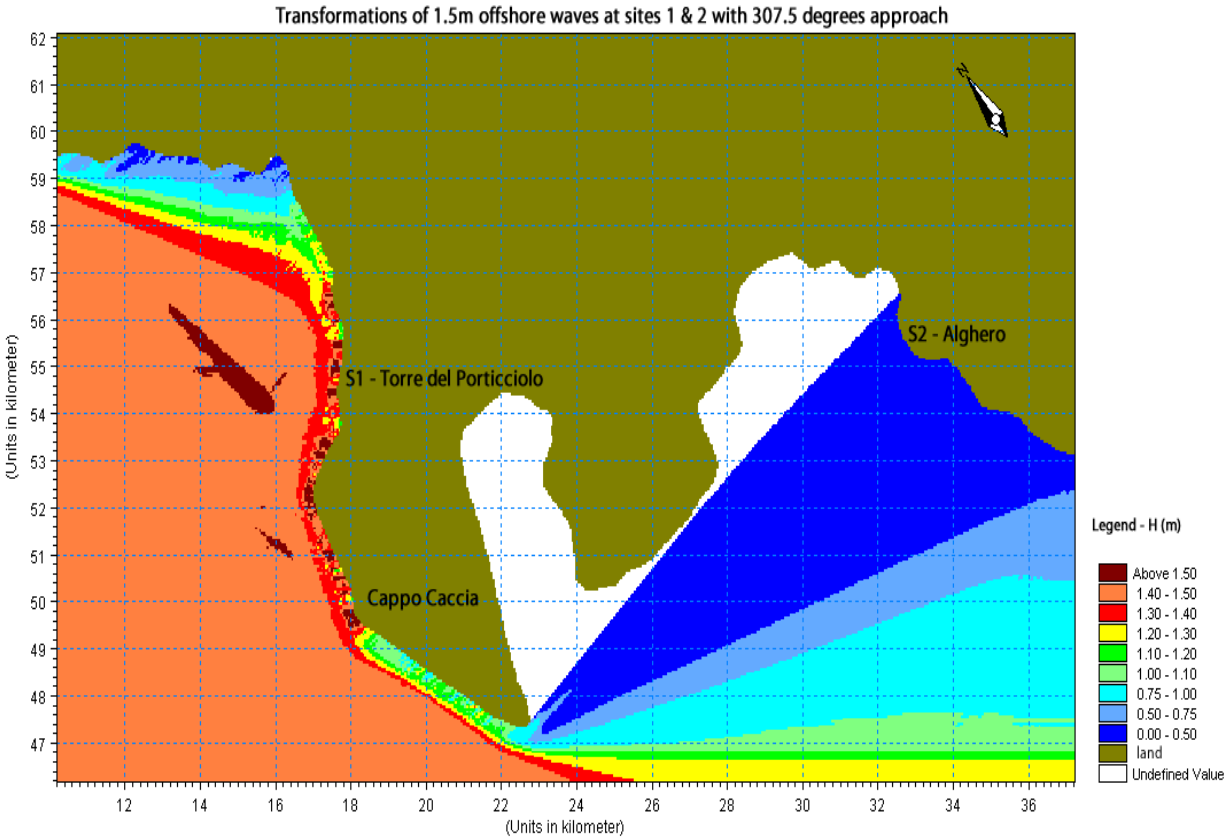

Figure 4.2 – Wave transformations at sites 1 and 2 (from the north-west)

Figure 4.3 concentrates on site 1. The selection area (shaded) is shown. There is some variation around the average height (1.4 m), with potential 'hotspots' existing where wave heights are above 1.5 m, and some less energetic areas where wave heights are closer to 1 m. Waves at site 1 reach an average height of 2.84 m on for an offshore wave of 6 m approaching from 307.5°.

Figure 4.4 shows sites 4 to 6. At site 5 wave heights are in the region of 0.5 m – 1.0 m (average 0.81 m). Waves reach a maximum height of 0.99 m at site 5 (from an offshore wave of 2.0 m). Shoreline waves at sites 4 and 6 are in the region of 1.19 m - 1.25 m.

Waves reach up to 2.26 m at site 6 and 2.16 m at site 4 for offshore waves of 6 m approaching from 307.5°.

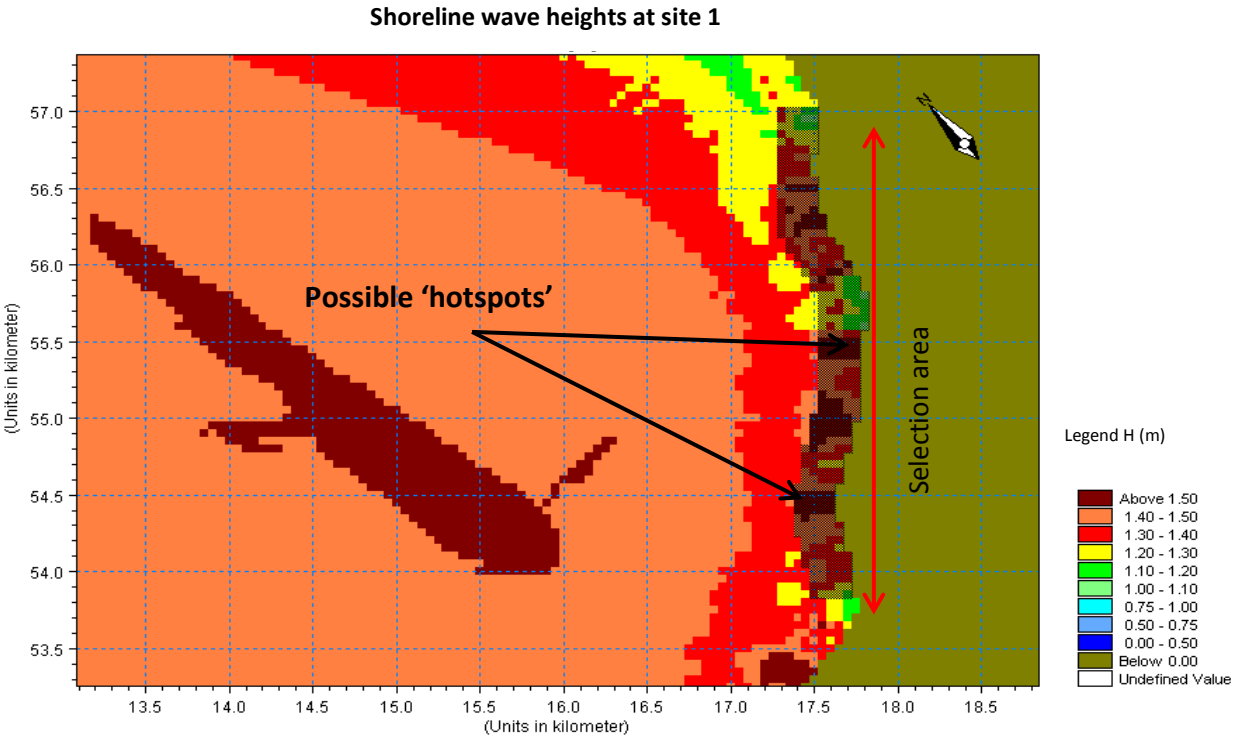

Figure 4.3 - Wave transformations at site 1 (from the north-west)

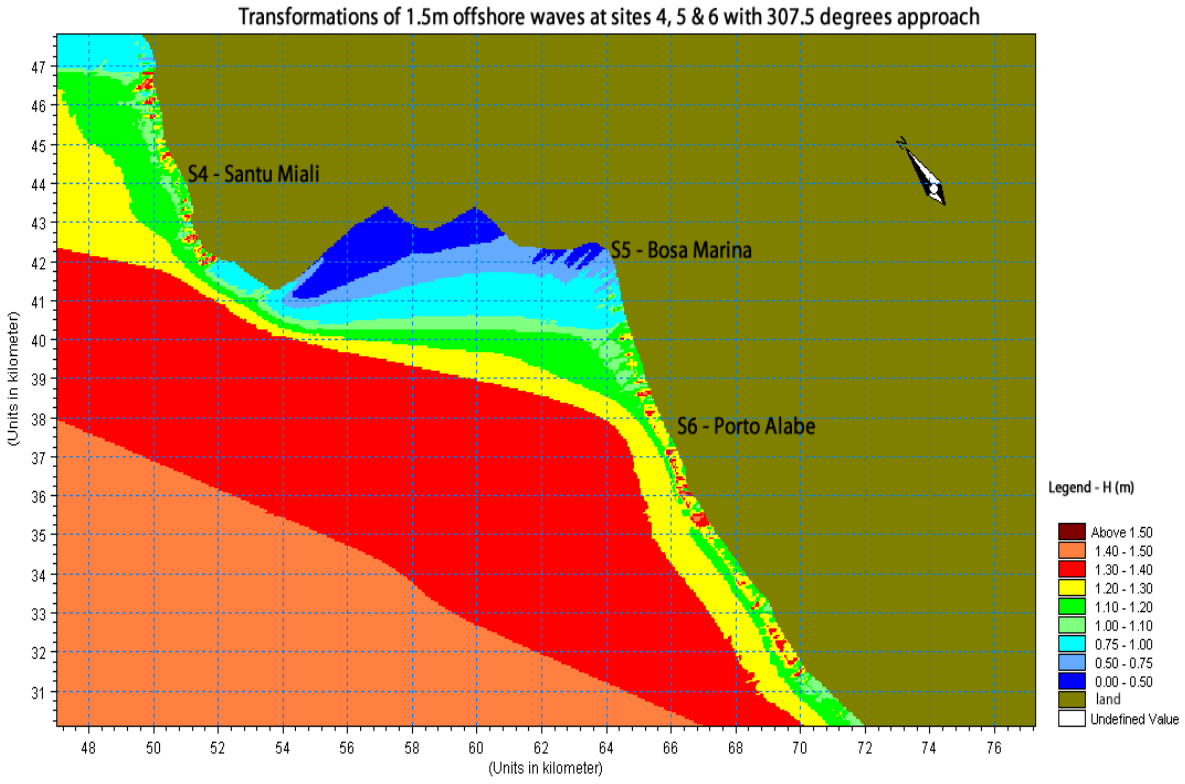

Figure 4.4– Wave transformations at sites 4 to 6 (from the north-west)

Figure 4.5 shows waves at site 1 and 2 originating from an offshore direction of 250°. At Alghero (S2), waves at the shoreline are in the region of 1.1m – 1.5 m. At site 1 waves are in the range of 0.5m – 1.2 m. Table 2 shows however that, as offshore wave heights and periods increase beyond 2 m and 6.2 s, then the shoreline wave height begins to fall at site 2 whereas at site 1 shoreline wave heights continue to increase as offshore wave heights increase, reaching 1.81 m from an offshore wave of 6 m. Waves at site 1 have an angle of attack of 10° when coming from the south-west.

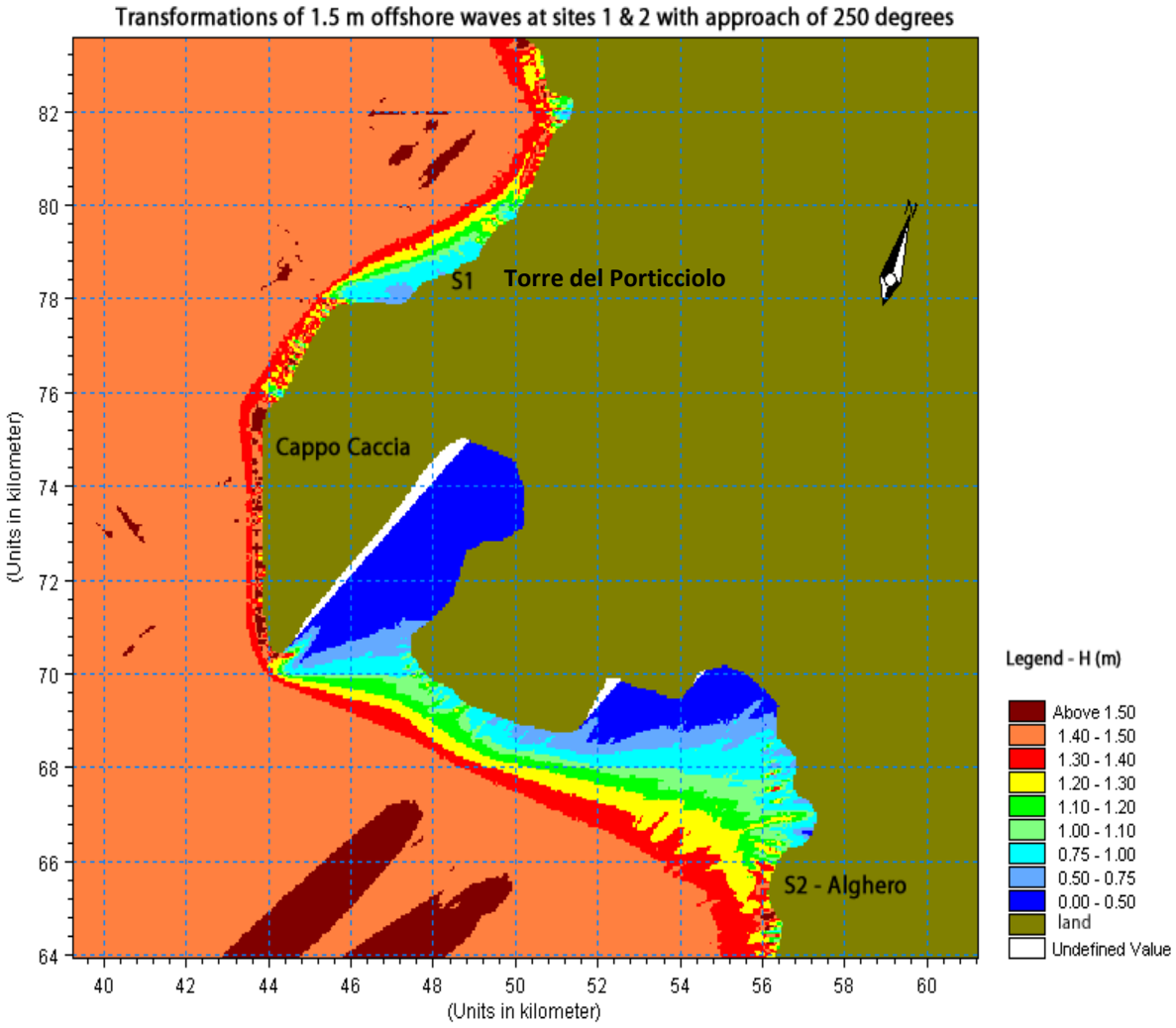

Figure 4.5 - Wave transformations at sites 1 and 2 (from the south-west)

Figure 4.6 shows waves at site 6 (Porto Alabe) approaching from the south-west. Shoreline wave heights have an average of 1.33 m resulting from an offshore wave of 1.5 m. Within the area shown there is some variation with waves reaching around 1.5 m in some locations whilst in others waves are lower at around 1 m. The highest waves recorded at site 6 for waves originating from the south-west were 1.77 m (for an offshore wave if 6 m).

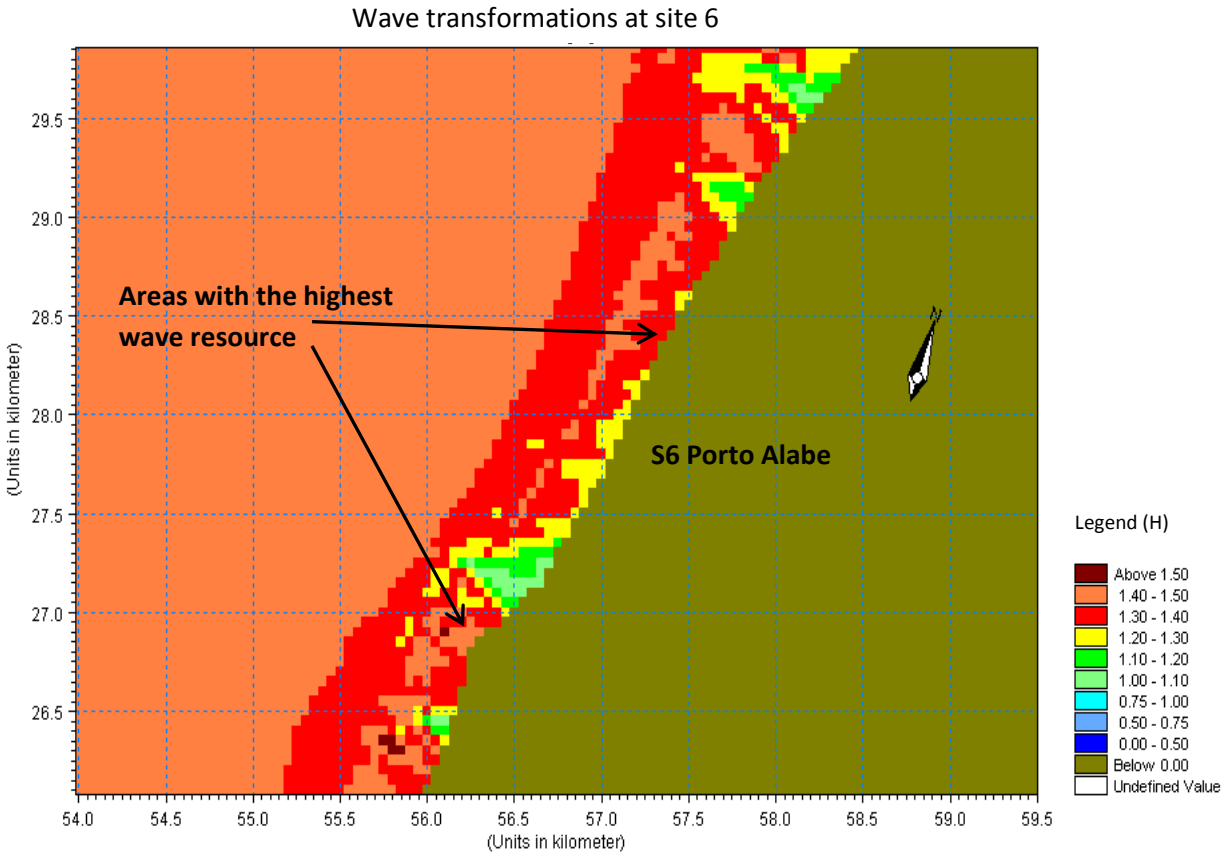

Figure 4.6 – Wave transformations at site 6 (from the south-west)

4.2 Discussion of wave simulations and shoreline wave heights

The results of the wave simulations indicate that some sites are more appropriate for the project than others. Figure 4.7 shows estimated average annual wave powers using the power equations (5) and (4) which were applied to each wave height. The results are shown as a range due to the large-bin sizes used for the initial assessment, and represent the sum of the maxima and minima of each bin multiplied by their frequency of occurrence. The results from the on-going study by Vicinanza (pers.comm.) are shown alongside.

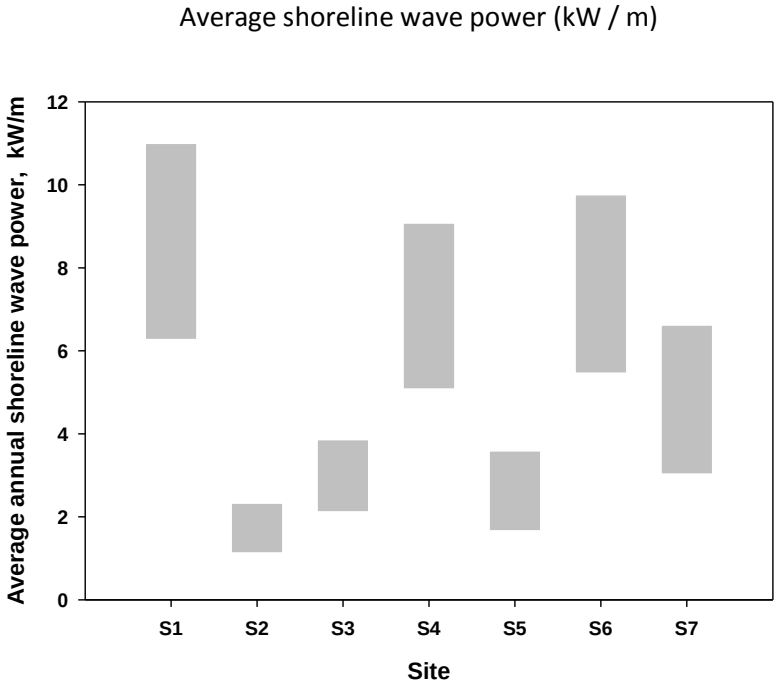

Site	Av. wave power at 20 m depth
S1	9.95 kW/m
S2	3.83 kW/m
S3	7.05 kW /m
S4	8.27 kW/m
S5	5.54 kW/m
S6	10.91 kW/m
S7	8.81 kW/m

Figure 4.7 - Average wave power at sites 1 to 7

In general the shoreline wave powers agree with the nearshore power levels in terms of the rankings of the different sites. Site 1 appears to be the most energetic site (2nd most energetic at 20 m depth) with an estimated average wave power of 6 – 11 kW / m and is therefore chosen for further analysis. Sites 2 and 5 are much less promising with the least energy. These two sites also have the least energy in the nearshore zone. At both sites there is an approximate reduction in the offshore energy of 70% to 80%, and a reduction in energy from the nearshore to shoreline of approximately 50% - 60%. Site 2, which was the site originally proposed, has very low wave heights for 72% of the year due to the 'shadowing' influence of Cappo Caccia headland, as well as due to it being situated within a bay, resulting in average power levels between 1 - 2 kW /m. Site 5 experiences

similar effects although to a lesser degree. Neither site 2 nor site 5 are considered appropriate for the project and are not discussed further.

Site 3 shows the importance of considering different wave directions. This site was the most energetic when considering waves approaching from the south-west, but during the rest of the year there seems to be little energy arriving at the coast, probably due again to the shadowing effect of the Cappo Caccia headland, and averaged across the year this area appears unenergetic. Sites 4 and 6 are both considerably more energetic than sites 2, 3 and 5 with average wave powers in the range of 5 – 9 kW / m. Both site 4 and 6 are interesting, with little discrepancy between shoreline wave heights originating from the north-west and the south-west. There is a higher discrepancy at site 1, where the highest waves in the region occur when approaching from the north-west but which is less energetic when waves approach from the south-west. Although site 1 appears to have a clear advantage in terms of available resource, this could translate into a higher installed capacity and so may not be the most cost effective site. Therefore site 6 (Porto Alabe), which has a slightly higher potential than site 4, will also be analysed further see if there is a benefit from a more consistent wave climate. If the analysis on site 6 is positive then it should be noted that site 4 may also be a possible site for the CSWEC. There is one other site that appears to have obvious potential. The Cappio Caccia headland appears to have a wave resource at least as high as site 1 (e.g. Figure 4.5), however this forms part of a marine conservation area and although Thorpe (1999) says the environmental impact of a shoreline device is generally low, this site is for the time being not considered.

It is noticeable that the highest shoreline waves recorded in the simulations were generally within the 1 m - 3 m range recommended by Müller (pers. comm.). Figure 4.8 shows the wave heights at site 1 where waves had an average height of 2.84 m resulting from 6 m offshore waves. This suggests that even in storm conditions the CSWEC could remain in operation (although this does not take into account storm surge).

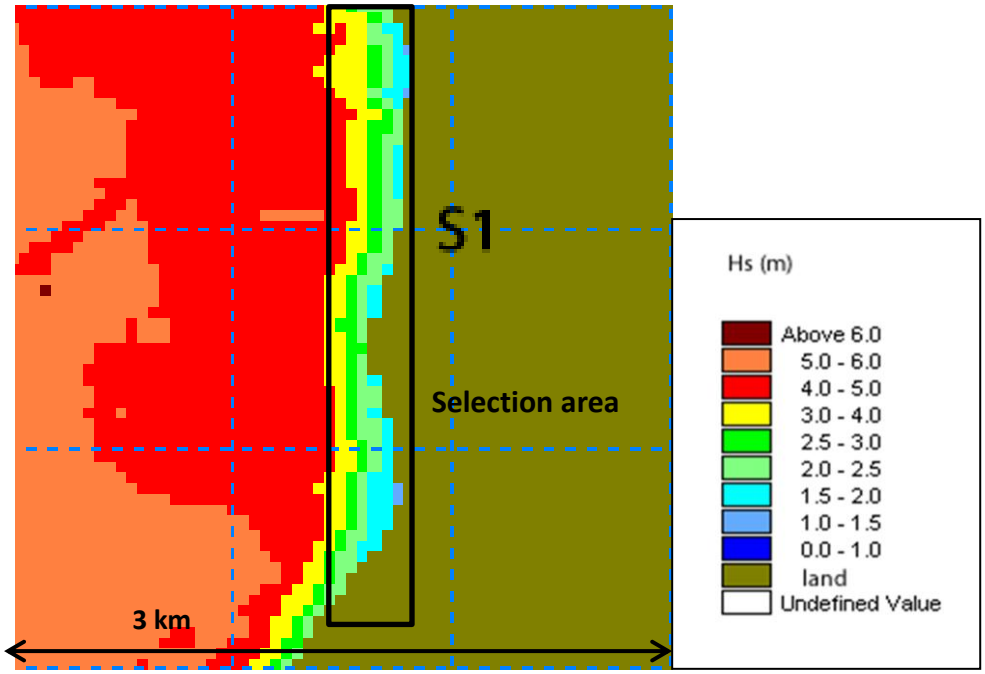

Figure 4.8 – Wave transformations of 6 m offshore waves at site 1

Waves breaking before the structure could also improve the operating window (i.e. lower waves and lower forces should limit exposure to high loadings). On the other hand, broken waves decrease in height and therefore the values in Figure 4.7 may be optimistic. Wave breaking has not been included for reasons discussed but warrants further investigation. In particular a better understanding of the bathymetry would give accurate foreshore slopes and shoreline water depth. If either of these are less than predicted, then increased wave breaking may occur. If either of the foreshore slope or water depth is greater, then less wave breaking is likely to occur. For steep beaches/foreshores, common in the Mediterranean, Huntley and Bowen (1975) predicted a breaker parameter of $\gamma = 1.2$, so it is plausible that the highest shoreline waves at site 1 (2.84 m) could arrive at the shoreline unbroken.

4.2.1 Further simulations at sites 1 and 6

Table 4.2 summarises the shoreline wave heights at sites 1 and 6 after all offshore wave heights were run. The full results are in Appendix A10 (all calculations are based on this). All waves produced values of ξ_{op} > 2, and are therefore non-breaking (on the structure). At both sites the waves approach at angle between 5° - 20°. Without observations to verify this, these figures appear plausible but need to be clarified if the project proceeds. Estimations of shoreline orientation made with Google Earth were generalised over the selection areas (1 to 3 km) and there is likely to be variation within each site, some favourable others unfavourable.

Table 4.2 – Summary of shoreline wave conditions: top) Site1; and, bottom) Site 6

H_{stoe} (m) at S1	Frequency of occurrence (%)	Period *T* (s)	Average shoreline wave-power at S1	% of Total power	Shoreline wave directions (shoreline orientation 295°)	
					% from 307° (n-west)	% from 285° (s-west)
< 0.7	50	3.9 – 5.1	7.14 kW/m	4	23	27
0.7 – 1.0	13	4.8 – 5.7		7	6	7
1.0 - 1.4	12	5.1 – 6.9		12	10	2
1.4 – 1.8	9	5.7 – 8.5		18	8	1
1.8 – 2.5	15	6.4 – 6.9		52	15	0
> 2.5	1	7.5 – 9.2		7	1	0

H_{stoe} (*m*) at S6	Frequency of occurrence (%)	Period *T* (*s*)	Average shoreline wave-power at S6	% of Total power	Shoreline wave direction (shoreline orientation 290°)	
					% 285° (from n-west)	% 270° (from s-west)
< 0.7	45	3.9 – 4.7	6.99 kW/m	4	32	13
0.7 – 1.0	15	4.8 – 5.2		9	10	5
1.0 - 1.4	15	5.2 – 6.0		18	9	6
1.4 – 1.8	18	5.2 – 9.2		42	14	4
1.8 – 2.5	7	7.5 – 9.2		27	7	0
> 2.5	na	na		Na		

The further analysis shows that both sites have in fact a similar average annual wave power. At site 1 the average shoreline power is 7.14 kW / m, representing a decrease of 20% compared with the offshore value (9.04 kW / m). Folley *et al.* (2007) suggest that waves dissipate approximately 10% of their energy between the offshore

and nearshore, so a further 10% loss at the shoreline seems plausible. If wave energy does increase to 9.95 kW / m in the nearshore, then the reduction between the nearshore and the shoreline is 28%. This is a relatively large reduction and could suggest that this study has underestimated the shoreline wave power. Alternatively it is not known how the study by Vicinanza (pers. comm.) was calibrated and *it* may have overestimated power levels. The energy at the shoreline at site 1 is however still greater than values reported at many of the offshore wave buoys around Italy by Vicinanza *et al*. (2009) and could still therefore constitute an energy 'hotspot' of sorts. Figure 4.3 showed that at site 1 'hotspots' may exist where wave heights are greater than the average levels outlined in Table 4.2, so reductions in energy will be less in these (very) specific areas. If the foreshore slope is steeper than assumed in this study (1:30 at sites 1 and 6) then this reduction may anyway prove to be less. 52% of the shoreline energy at site 1 is delivered by waves in the range of 1.8 m – 2.5 m coming from the north-west that occur 15% of the year. On the other hand over 50 % of the waves in the area are below 0.7 m and virtually useless for the CSWEC.

At site 6 there is a slightly lower average wave power at 6.99 kW / m. There are less calm periods below 0.7m (45%) at site 6 and a higher proportion of waves occur within the range of 0.7 m – 1.8 m (48% as opposed to only 34% at site 1). The highest proportion of power is delivered by waves between 1.4 m – 1.8 m (42%). The reduction in wave power from the 20 m depth to the shoreline is large (37%) possibly due again to a misrepresentation of the foreshore slope. On steep slopes the water depth can be considerable at a few meters from the shoreline (Pethick, 1984), which would reduce friction and increase wave energy. Also, wind was not included in the model set-up and yet site 6 is sufficiently far away from the wave buoy (at least 50 km) that waves might in reality continue to grow whilst in deep water. This is a possible error in the set-up and could have led to underestimations of the wave heights across the region.

Figure 4.9 shows the effects of a change in depth at site 6. There is a relatively high sensitivity to depth change. At -3 m the average power increases to 7.7 kW /m (a 10% increase) whilst at a 2 m depth wave power falls to 6.5 kW / m (7% decrease). Changes in foreshore slope would have been difficult to model, but a similar pattern should occur for reasons already explained. The results at a depth of 2.5 m are the ones carried forward in this study but it needs to be reiterated that a full bathymetric survey would be required for any site finally chosen.

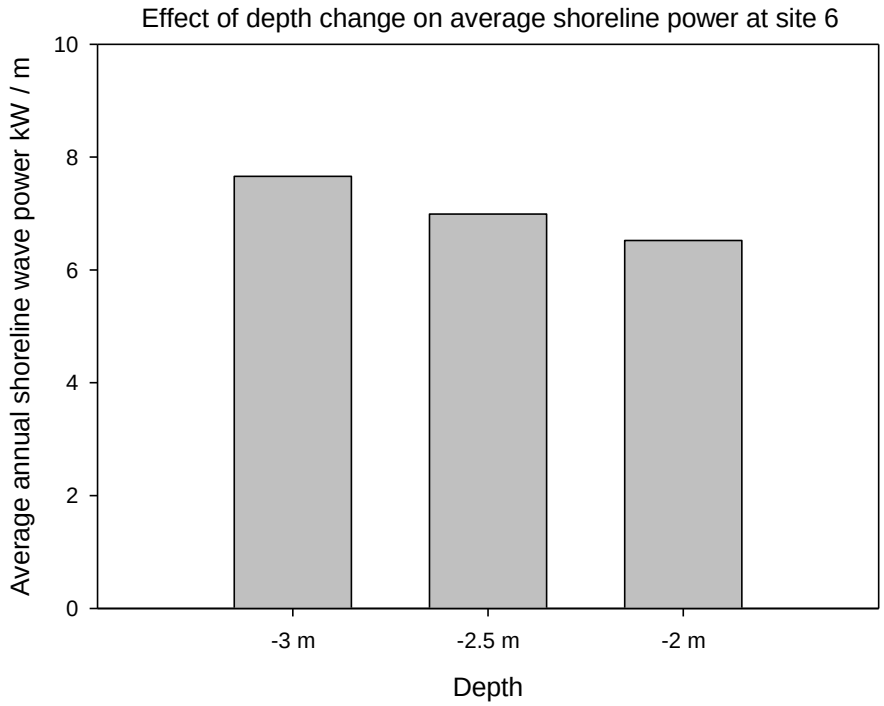

Figure 4.9 - Effect of depth change on shoreline wave power at site 6

4.3 Ramp Efficiencies at Sites 1 and 6

Figure 4.10 shows ramp efficiencies for typical wave heights at site 1, calculated using the VMJ model (Eq. (13)) and the 1:23 model, equations (6) and (7). Since the estimated foreshore slope is 1:30 so no reduction is required for shallow water. For a given freeboard the VMJ model predicts increasing efficiencies as the wave height increases. The maximum efficiency considering all waves was found to be 17%, obtained with a freeboard of 0.65 m. With a 1 m freeboard the overall efficiency falls to 15%. The 1:23 model has been adjusted for oblique waves and predicts higher efficiencies using 1 m and 1.5 m freeboards than the VMJ model, except for the 2.2 m wave. The maximum efficiency using the 1:23 model, considering all waves from both offshore directions and a 1 m freeboard, is 15 %.

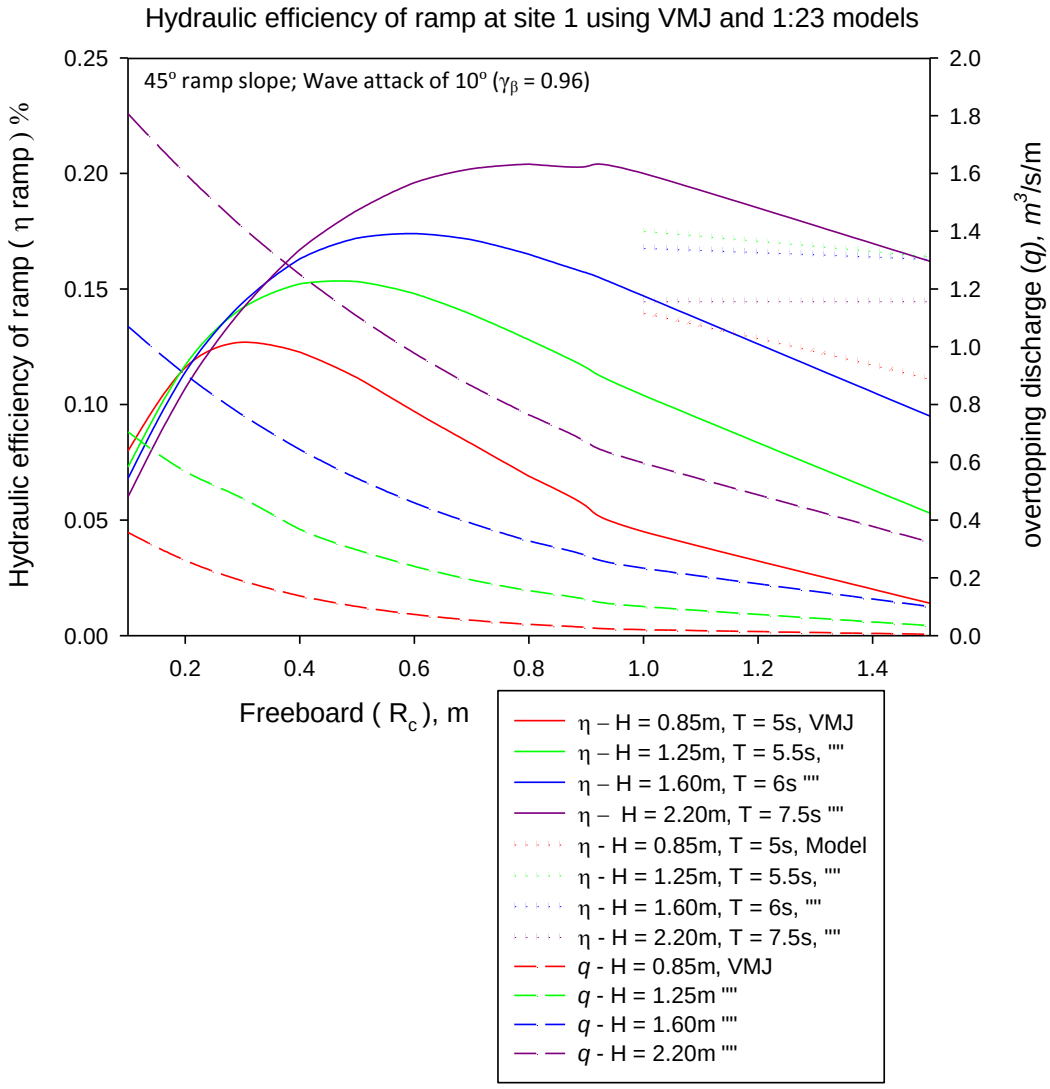

Figure 4.10 - Hydraulic efficiencies using VMJ and 1:23 models, site 1

Figures 4.11a shows ramp efficiencies at site 1 using the Kofoed model (Eq. (16)) which includes additional reductions for a 45° slope (λ_α = 0.9012) and for a low relative freeboard (variable). The efficiencies are similar to those obtained with the VMJ model, except that the maximum efficiency for the 2.2 m wave is lower (when λ_s = 0.82) at 18%. Overall efficiency with a 1 m freeboard is 13%.

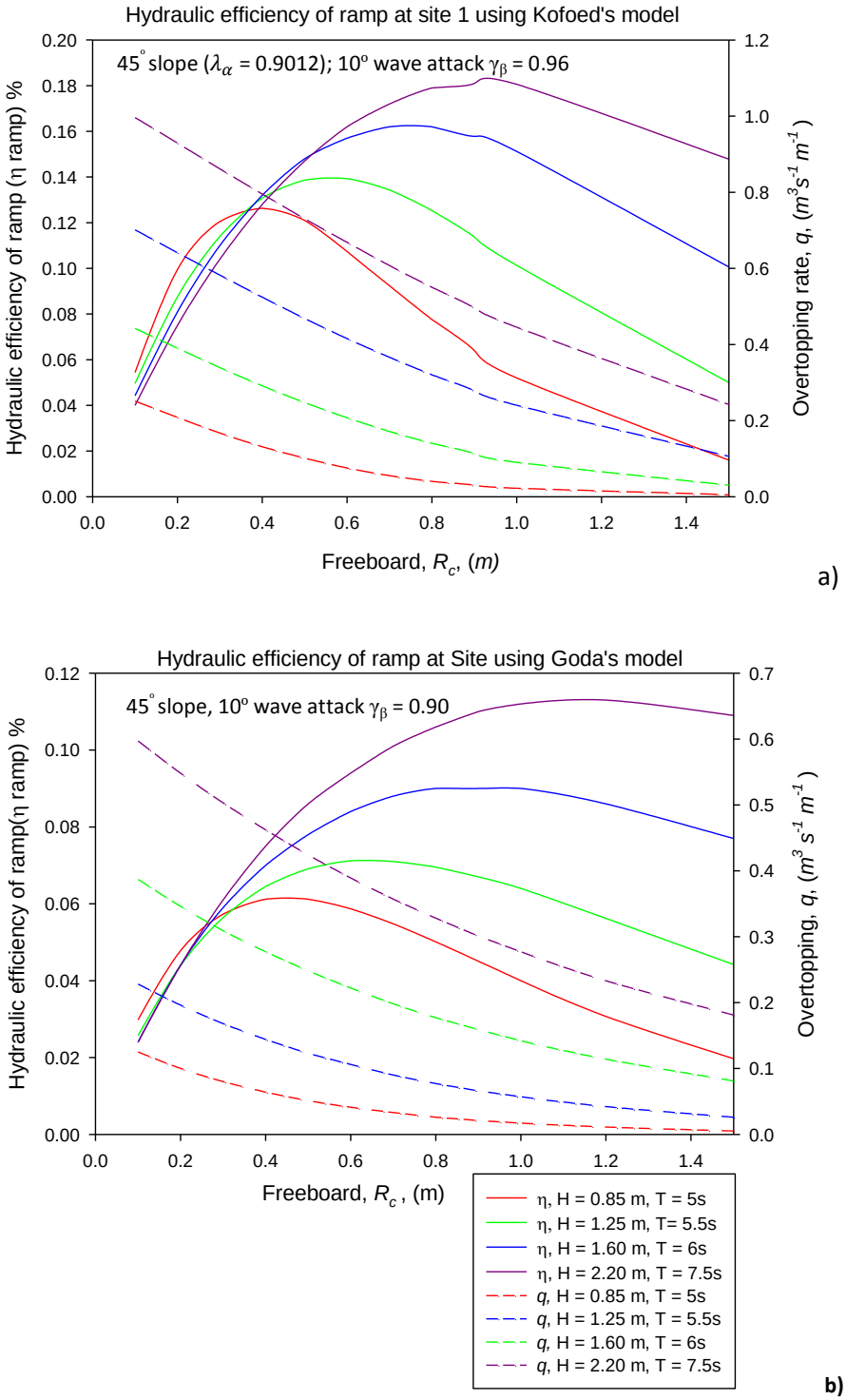

Figure 4.11 - Hydraulic efficiency of ramp using a) Kofoed's model; b) Goda's model at site 1

Figure 4.11b shows ramp efficiencies using Goda's model (Eq. (19)). Further reductions for ramp slope, water depth and foreshore slope which are all included within the main body of equation (19). There is also a greater reduction made for the angle of attack. The efficiencies for the selected waves range from 6% to 11% for a 1 m freeboard, with an overall efficiency of 8% for a 1 m freeboard.

Figure 4.12 shows the ramp efficiencies at site 6 for typical waves with an angle of attack of 5°. For a 1 m freeboard the VMJ model gives an overall efficiency of 14 % whilst for the same freeboard the 1:23 model gives an overall efficiency of 16%.

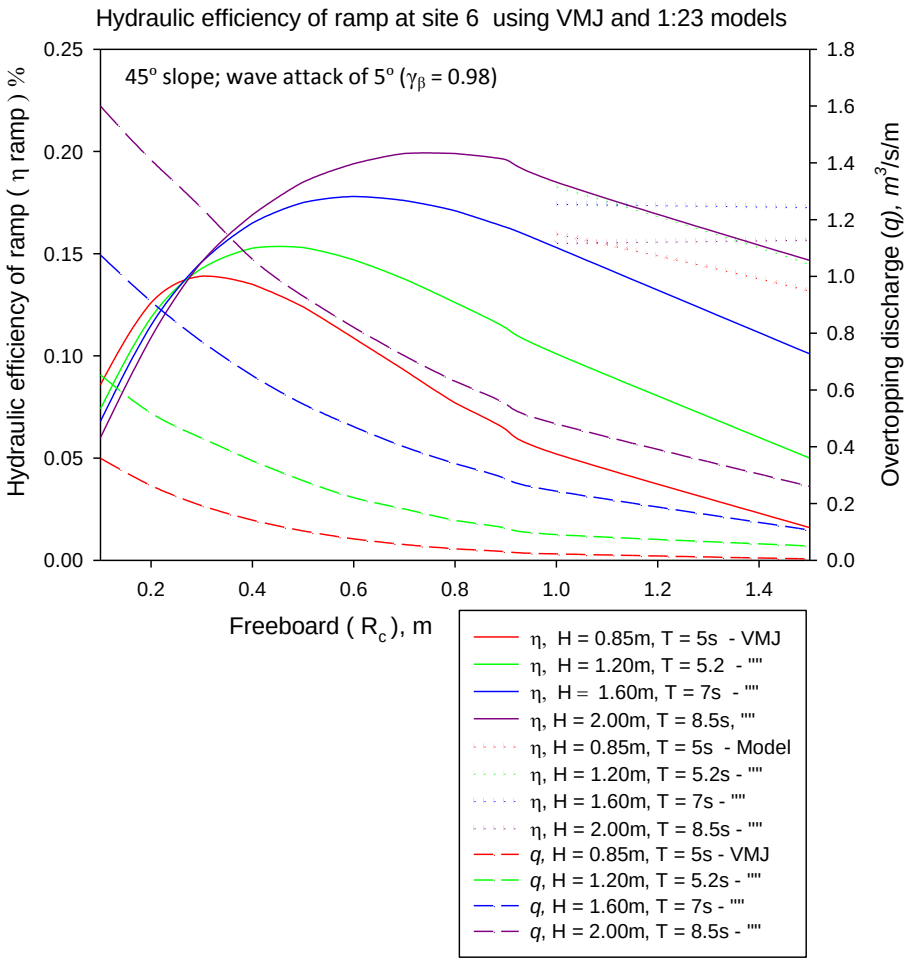

Figure 4.12 - Hydraulic efficiency using VMJ and 1:23 models at site 6

Ramp efficiencies at site 6 using the Kofoed and Goda models followed the same pattern as at site 1.

Figure 4.13 shows the flow-exceedance curve at site 1 (*q* is in l/s/m in this instance), using all waves. Table 4.3 shows the design flow and installed capacity. Since the hydraulic power is proportional to the overtopping rate the curve also represents the hydraulic power of the structure (Eq. (2)). For operational purposes only a 1 m freeboard is assumed for reasons already explained. Approximately 45% of the time, there is virtually no overtopping or hydraulic power. The VMJ model predicts a hydraulic power of 100 kW or above occurring 20% of the time with a maximum hydraulic power of 580 kW. The 1:23 model predicts that 100 kW will be available 25% of the time but gives a lower maximum power of 308 kW.

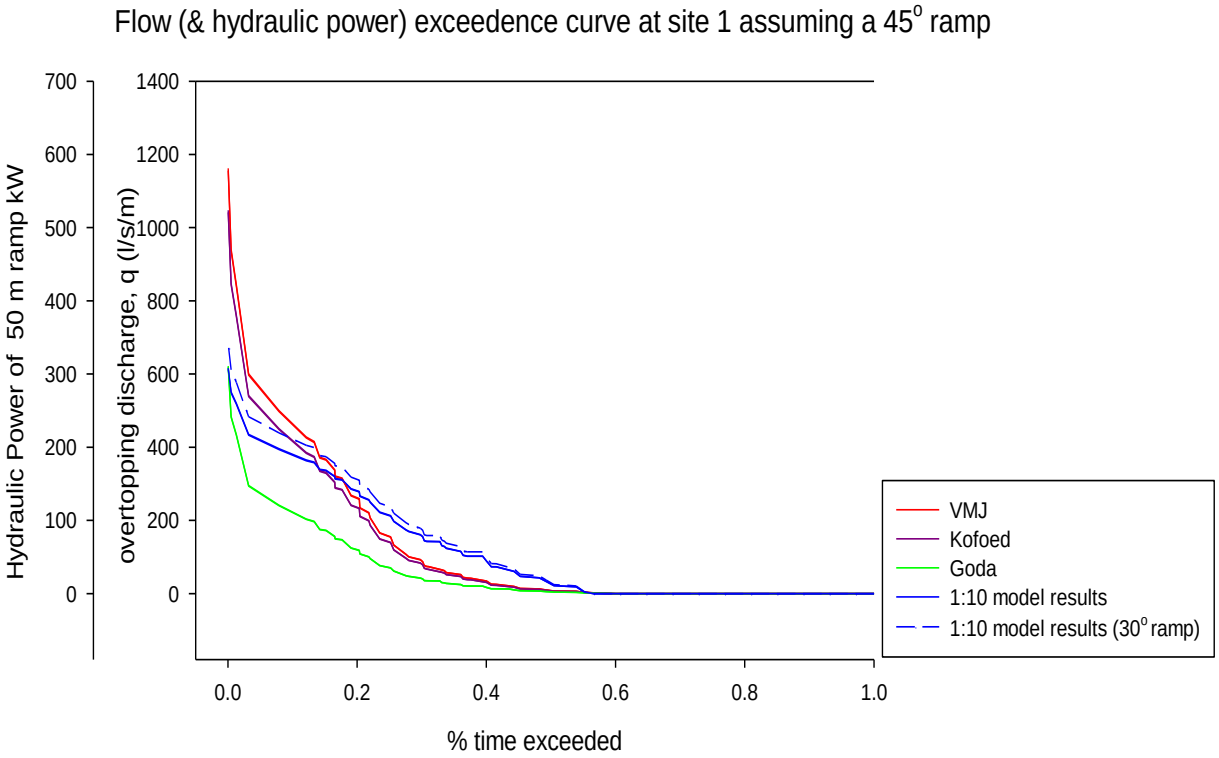

Figure 4.13 – Flow-exceedance curve at site 1

Table 4.3 – Design flow and installed capacity at site 1

Model	*qmax* (l/s/m)	*qdesign* (l/s/m)	Max hydraulic power (kW/50m)	Installed capacity (kW/m)
VMJ	1155	751	581	378
Kofoed	1042	677	523	340
Goda	619	402	311	202
1:23 45°	612	398	308	200
1:23 30°	-	-	342	222

Figure 4.14 shows the flow-exceedance curve for site 6. Table 4.4 shows the design flow and installed capacity. All models predict little or no power for 40% of the time when conditions are calm. The 1:23 model predicts that 50 kW will be exceeded 40 % of the time and 100 kW 25 % of the time. The VMJ model only exceeds 50 kW approximately 30% of the time and 100 kW 20% of the time. The Goda model predicts that 50 kW will be exceeded only 20% of the time. If a 30° ramp is introduced then the 1:23 model predicts higher hydraulic power levels, approximately 11% higher than for a 45° ramp. The 1:23 model predicts installed capacities of 151 kW and 168 kW for 45° and 30° ramps respectively. Kofoed's model predicts results within the range of the other models.

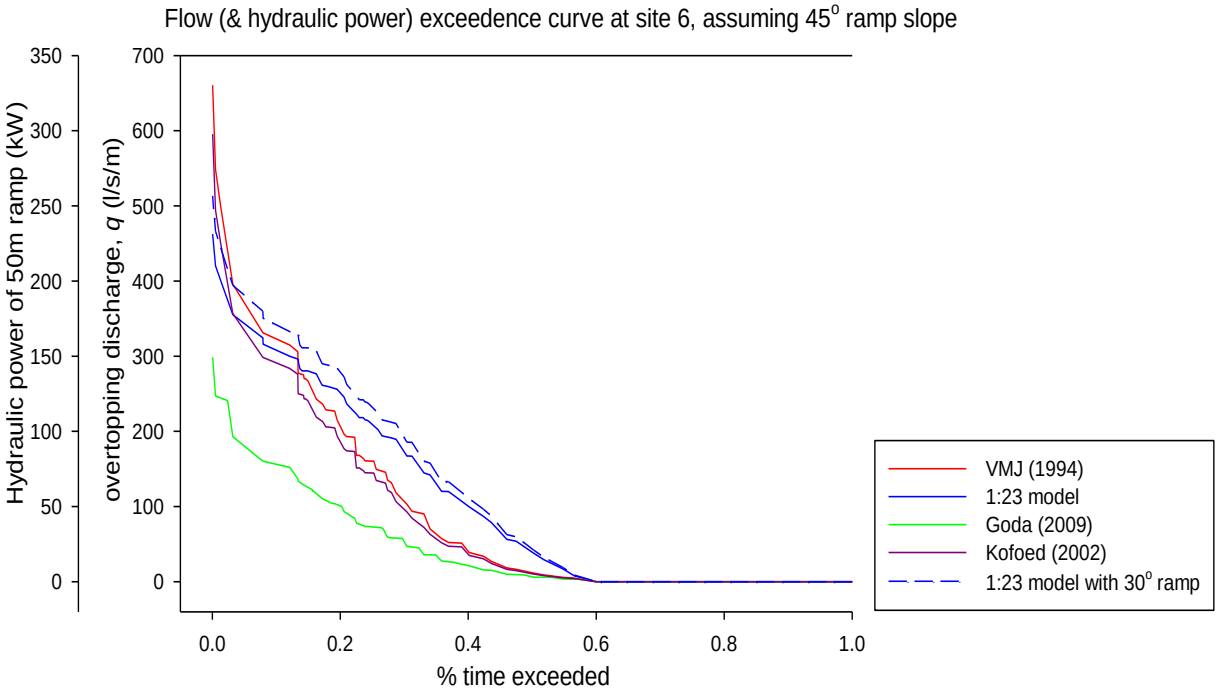

Figure 4.14 – Flow-exceedance curve at site 6

Table 4.4 - Design flow and installed capacity at site 6

Model	*qmax* (l/s/m)	*qdesign* (l/s/m)	Max hydraulic power (kW/50m)	Installed capacity (kW)
VMJ	661	429	332	216
Kofoed	598	387	299	195
Goda	298	194	150	98
1:23 45°	462	398	233	151
1:23 30°	-	-	258	168

4.4 Power Output at Sites 1 and 6

Figure 4.15 shows estimated annual electrical output at site 1. This was calculated by summing the power outputs for each wave height which were determined using the following equation:

$$P_{output} = P_{structure} * 24 * 365 * \eta_{wheel} * availability \quad (30)$$

where: η_{wheel} can be determined using Figure 2.7; 24 = hours in the day; and, 365 = the number of days in the year. Therefore:

$$P_{total\ annual\ ouput} = \sum_0^n P_{output} * frequency\ of\ occurrence \quad (31)$$

where: 0 = the lowest wave height; and, n = the highest wave at each site.

The VMJ model predicts an output of 356 MWh / y from an installed capacity of 368 kW. The 1:23 model predicts an output of 327 MWh / y from an installed capacity of 200 kW. The Goda model predicts a lower output of 162 MWh / y but from a similar installed capacity of 202 kW. These figures assume 100% availability.

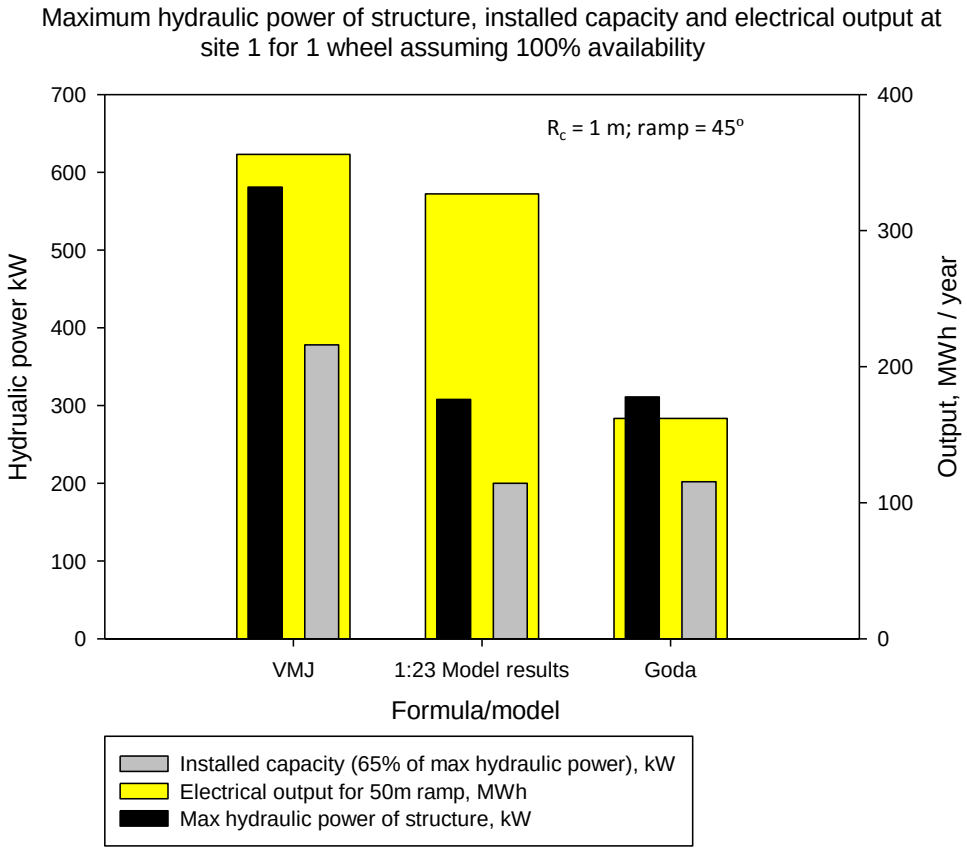

Figure 4.15 – Power output at site 1

Figure 4.16 shows the estimated power output at site 6. The VMJ model predicts an output of 260 MWh / y from an installed capacity of 216 kW. The 1:23 model predicts a higher output of 298 MWh / y from an installed capacity of 150 kW. The Goda model predicts a much lower output at 121 MWh / y for an installed capacity of 98 kW.

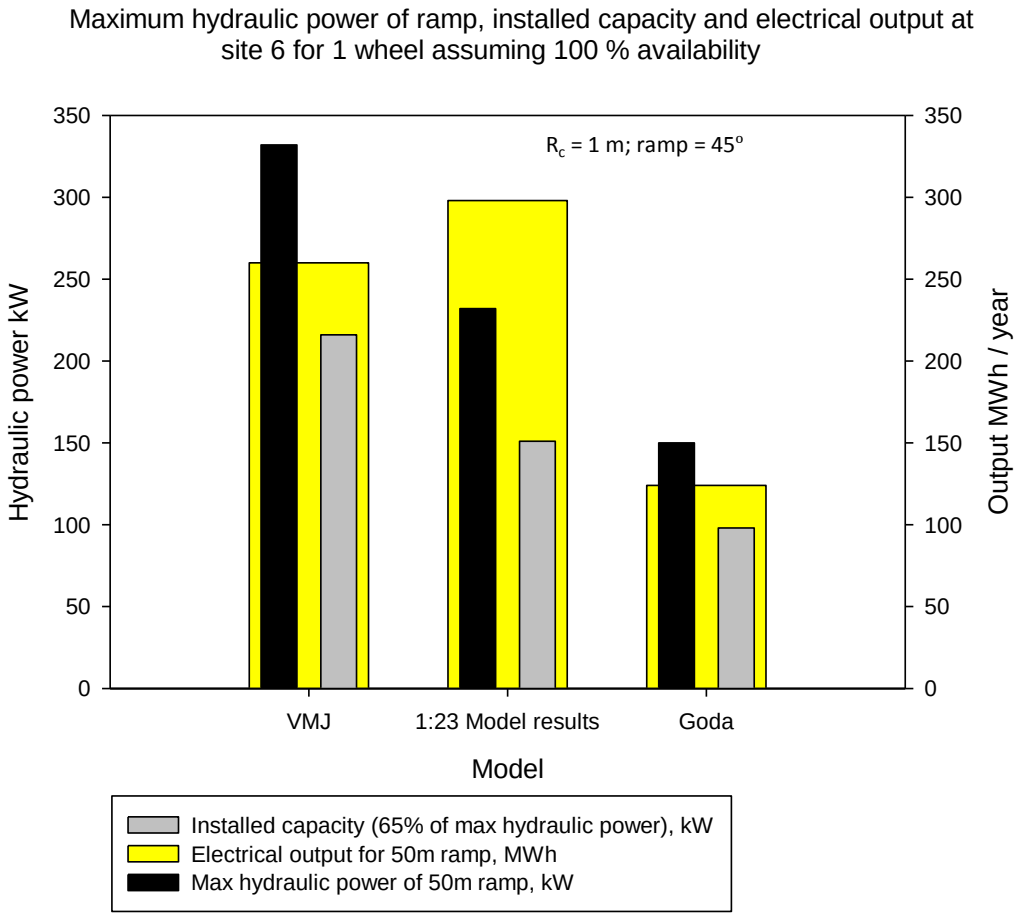

Figure 4.16 – Power output at site 6

Figure 4.17 shows additional output gained through use of more than one HPW at site 6. In each case the models predict there is essentially little or no additional output. Figure 4.18 shows the benefit to output from using more than one wheel, assuming 90 % availability when using 1 wheel, 95% availability when using 2 wheels and 100% availability when using 3 wheels . In this instance there is a noticeable change in the output. The 1:23 model produces an extra 32 MW h / y using 3 wheels, each rated at 50 kW, as opposed to using 1 wheel, rated at 150 kW.

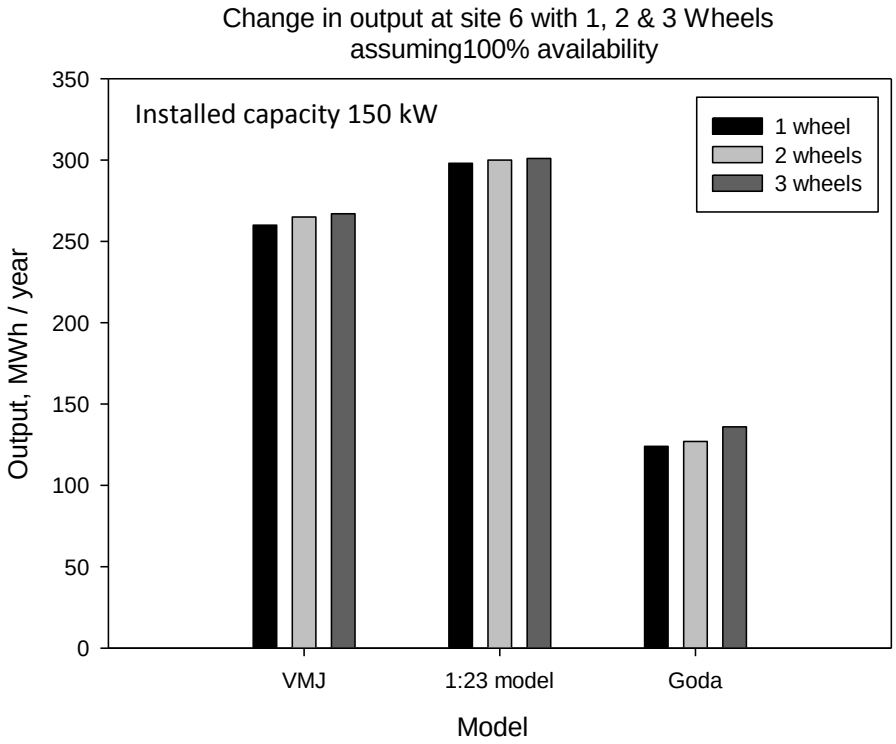

Figure 4.17 – Power output with 3 wheels and 100% availability

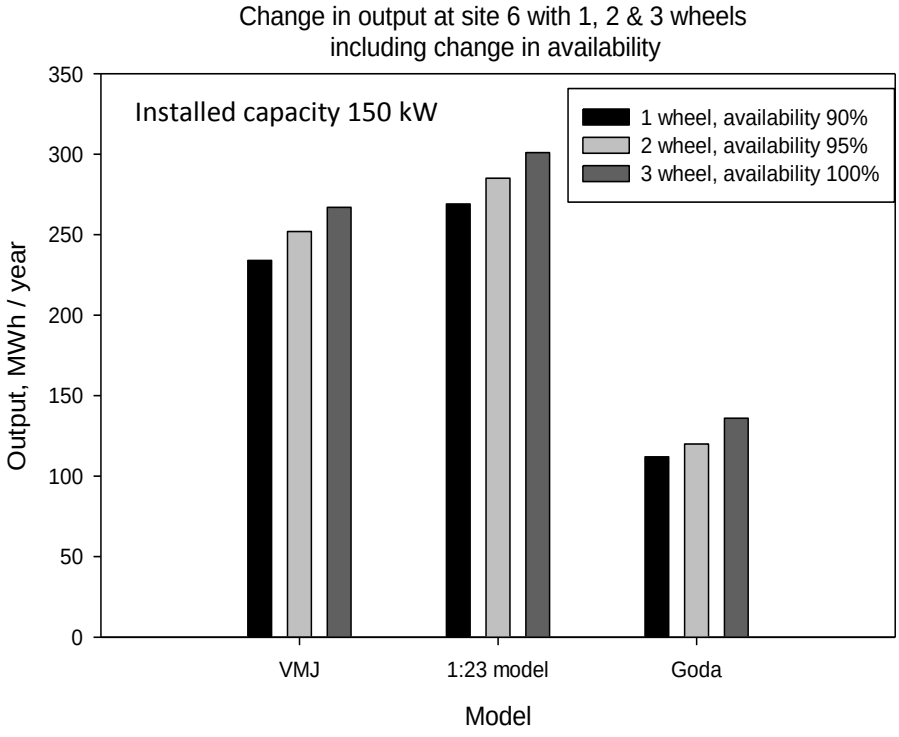

Figure 4.18 – Power output with 3 wheels and variable availability

Figure 4.19 shows the increase in costs when using more than 1 HPW at site 6. For the additional 32 MW h / y there is an increase in the cost of the HPWs of €336000 when switching from 1 to 3 HPWs.

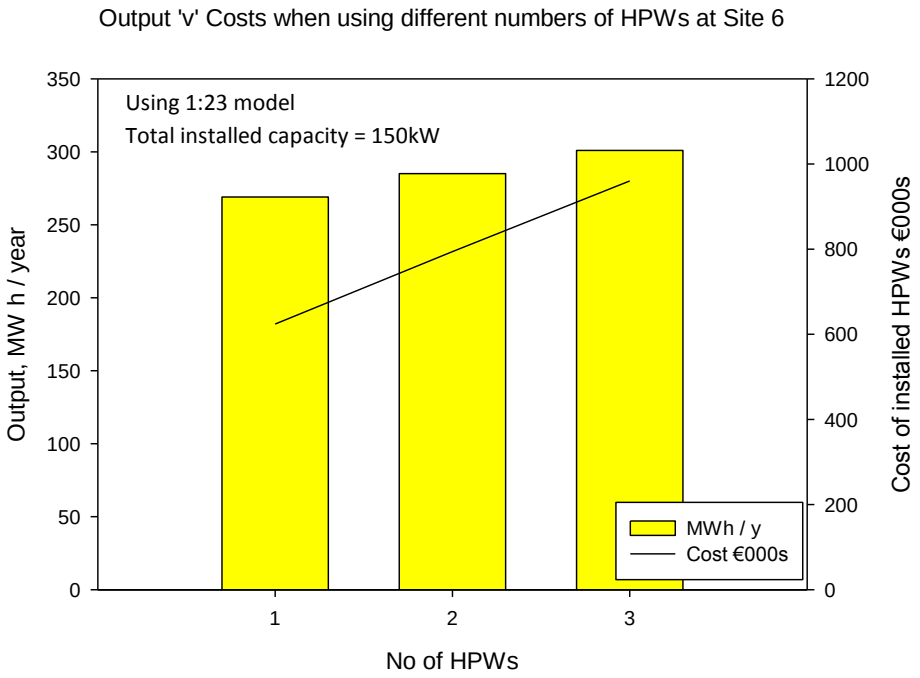

Figure 4.19 – Power output 'v' costs for 3 wheel option

4.5 COE and NPV and Sites 1 and 6

The COE and NPV are considered for a single (prototype) device and an array of devices, using the cash-flow models in Figures 3.4 and 3.5. The 1:23 model is used in this analysis, with a freeboard of 1 m and a ramp of 45^{o} assumed unless stated otherwise. The 3-wheel option, with 100% availability, is used since it gives the potential for a higher output. Cost details for Figures 4.20 to 4.22 are in Appendix A11.

Figure 4.20 shows the affect that changing CAPEX has on the COE and NPV, holding OPEX constant. No subsidy has been assumed here since it distorts the COE. At site 1 there is a COE of €0.13 / kWh. A 50 % reduction in CAPEX will result in a COE of €0.08 / kWh. At site 6 the COE is slightly higher at €0.135 / kWh, coming down to €0.08 / kWh if CAPEX is reduced by 50%. At both sites the NPV is negative even considering a reduction in CAPEX.

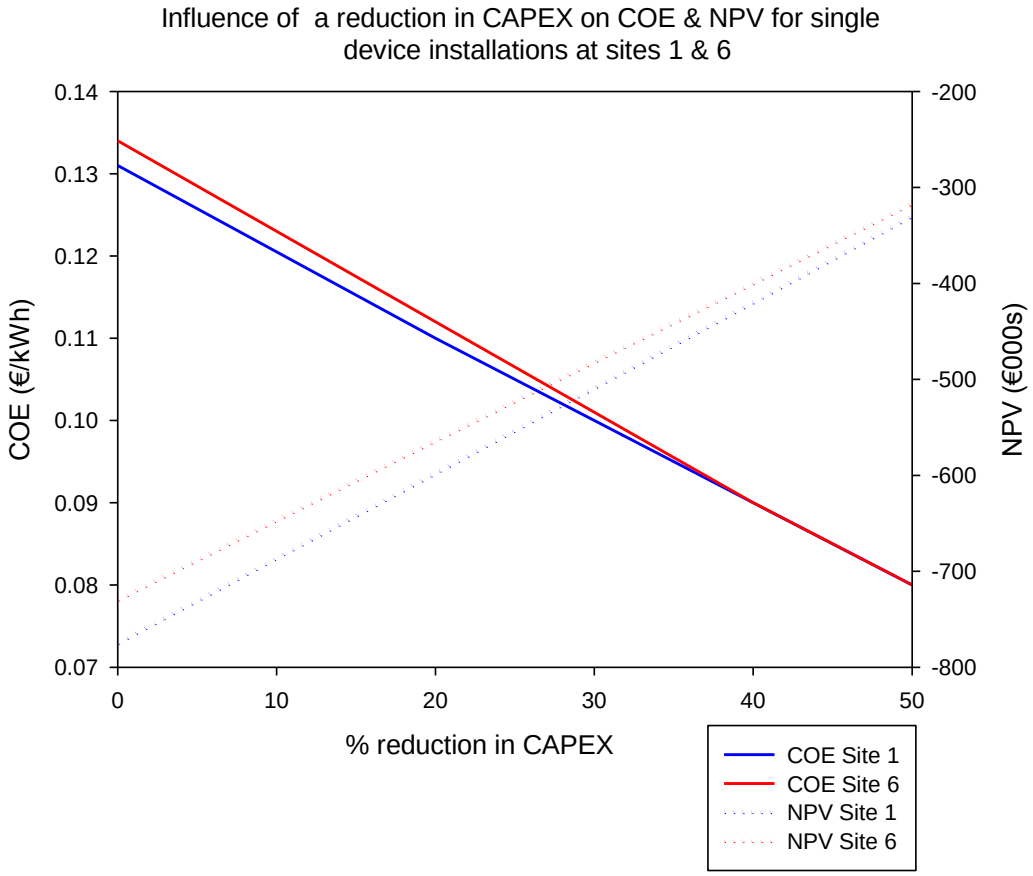

Figure 4.20 - Influence of CAPEX on COE & NPV

Figure 4.21 shows the effect that a change in OPEX has on the COE and NPV (CAPEX held constant). At both sites a reduction from 5% OPEX to 1% OPEX could bring the COE down by €0.02 / kWh.

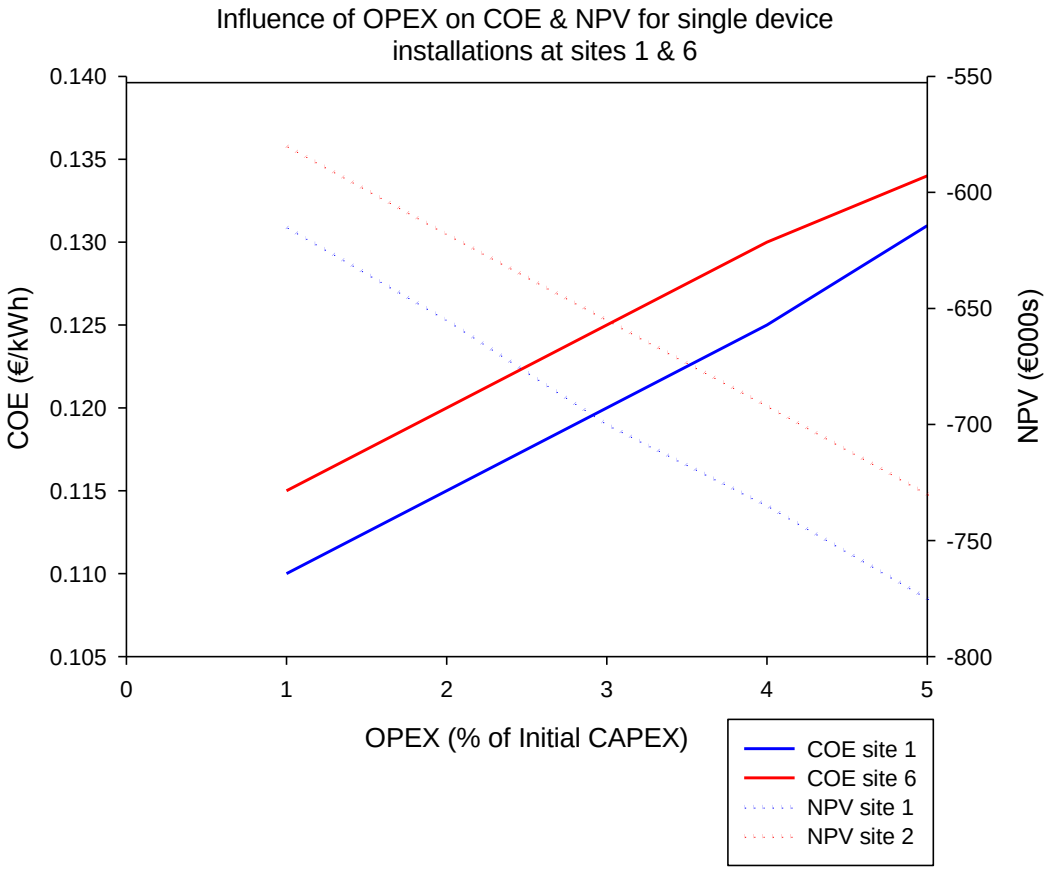

Figure 4.21 – Influence of OPEX on COE and NPV

Figure 4.22 shows the COE and NPV for an array of devices at site 1 with an installed capacity of 1MW. Table 4.5 describes the 4 scenarios. An 8% borrowing rate is used since it is assumed the project has passed the pilot stage successfully and the technology has proven itself. OPEX is assumed to have come down to 3% of CAPEX as a result of knowledge gained through the pilot stage. This is in the middle of the range of estimates in Table 2.2. The alternative HPW efficiency curve (max efficiency of 75%) for option 4 is in shown in Appendix 12. Without a subsidy none of the options return a positive NPV. If a subsidy is included, then option 4 returns a positive NPV of €225000. The COE resulting from the same option, not including subsidy, is €0.12 / kWh.

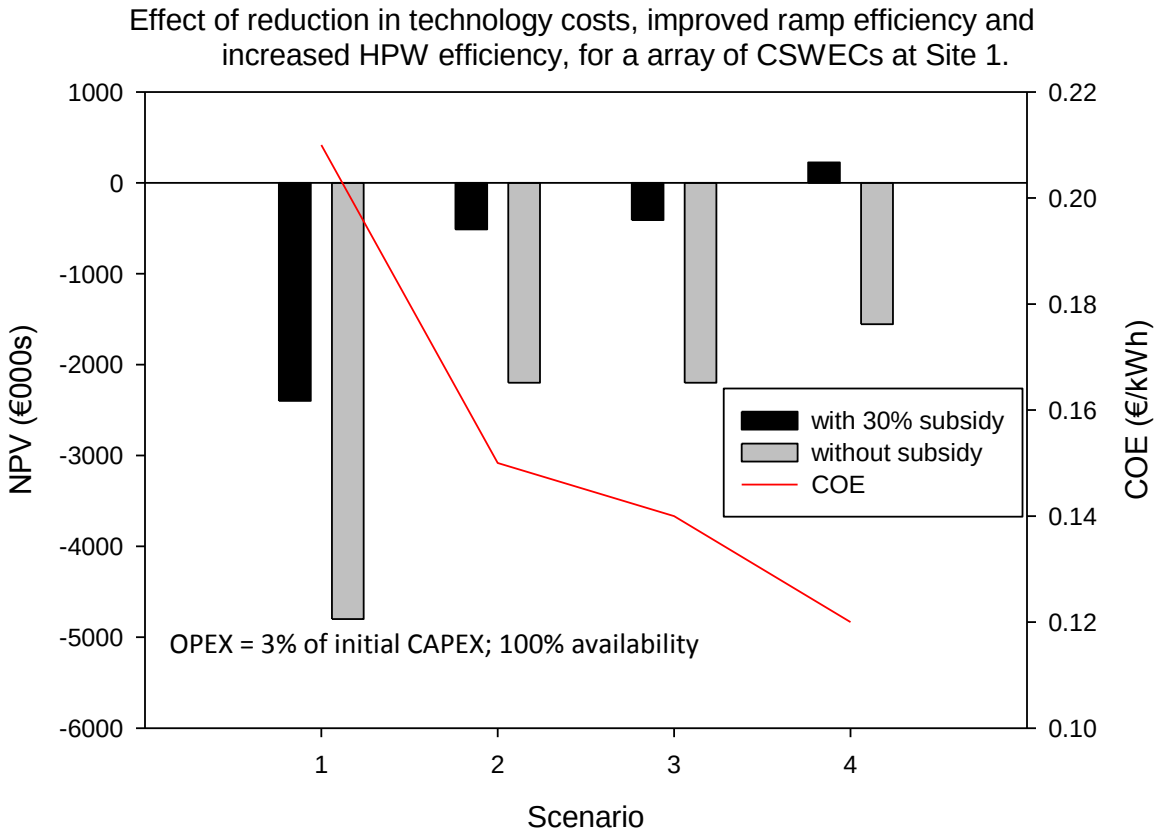

Figure 4.22 – COE and NPV for an array of devices

Table 4.5 – Options relating to Figure 4.22

OPTION	CAPEX	Ramp slope (°)	HPW max efficiency (%)
1	No reduction in cost of technology	45	65
2	30% reduction in “”	45	65
3	30% reduction in “”	30	65
4	30% reduction in “”	30	75

5 DISCUSSION

5.1 Ramp Efficiencies

The results show that when a 1 m freeboard is considered (for operational reasons), ramp efficiencies are within the range of 6% to 30% previously reported by Stagonas *et al*. (2010). There are, however, substantial differences between the results depending on the overtopping model used, to the extent that the choice of model could have a significant impact on the initial economic assessment of the project.

As shown in Figures 4.10 and 4.12, the 1:23 model predicts efficiencies ranging from 14% to 18% at both sites for waves ranging from 0.85 m - 2.2 m, with average overall efficiencies of 15% (site 1) and 16% (site 6), putting the overall efficiency in the middle of the 6% to 30% range. The VMJ model, which is well established and widely used across Europe (Reeve *et al*., 2008), gives average efficiencies of 15% and 14% respectively which is in good agreement with the 1:23 model. The Kofoed model predicts slightly lower efficiencies of 12% and 13% respectively, and the Goda model a lower still overall efficiency of 7% at both sites. In the case of the Goda model this is a predicted drop in efficiency of over 50% when compared to the 1:23 and VMJ models. Since established overtopping formulae such as the VMJ model are widely considered to underestimate overtopping rates in real-life situations (Pullen *et al*., 2007), it seems surprising that Goda's relatively new model should predict much lower efficiencies than the other formulae. It is not known whether Goda's formula has been widely used since its publication in 2009 and it might be wise to see how it performs in real-life situations before considering it for design purposes related to the CSWEC project (although it has been validated against CLASH datasets including small positive freeboards (Goda, 2009)). On the other hand, the model does include reduction factors for relative depth and foreshore slope that don't appear in the VMJ model (since the foreshore slope is less than 1:100 and so shallow water conditions are, rightly or wrongly, not considered), whilst the 1:23 model was based upon water conditions that were not depth limited, and with a foreshore slope of 1:10 (Birks, 2010), steeper than the 1:30 slopes assumed at sites 1 and 6 in this study. This suggests that it would be advisable for further model tests of the CSWEC to be carried out in shallower water depths and with gentler foreshore slopes to see how overtopping rates are affected, if at all.

Although the efficiencies are within the range reported by Stagonas *et al*. (2009), these could increase if the angles of wave attack were found to be less than reported in

this study. On the other hand Schüttrumpf *et al*. (2003) argue that for waves with angles of attack up to 20^{o} there is no discernible change in the rate of overtopping. Since the maximum angle of attack was 20^{o} (for waves coming from the south-west at site 6), then the coefficient γ_{β} could be set to 1 at both sites, and the overall efficiencies then rise from 15% to 16% at site 1 (using the VMJ and 1:23 models), and from 14% to 15 % (VMJ model) and 16% to 17% (1:23 model) at site 6. Although the changes are relatively small any efficiency increase should be considered important in an industry where different technologies are currently competing against each other to attract investment and funding. Contrastingly, Goda (2009a) predicts a greater reduction in overtopping for a given angle of attack (Figure 4.11b). Little is currently understood about the influence of oblique waves on overtopping (Pullen *et al*., 2007) and this in an area that should be modelled in the future.

It is suggested by Stagonas *et al*. (2010) that ramp efficiencies could be increased if greater wave heights are considered. As Figure 4.9 showed, wave power increased by 10% at site 6 when water depth was increased by 0.5 m (wave heights will increase too) and if steeper foreshore slopes are also found to exist then this could also increase wave heights at the shoreline (Pethick, 1984). Figure 4.3 also showed that possible 'hotspots' exist at site 1 although these would need to be investigated further. The VMJ, Kofoed and Goda models all show that greater efficiencies do occur for a 1 m freeboard with increased wave heights, although in the case of the Kofoed's and Goda's models these increases are less due to the reduction factors for small relative freeboards and relative toe depth that affect the highest waves rather than the smaller more moderate ones.

On the other hand Figures 4.10 and 4.12 both show that the 1:23 model predicts lower efficiencies for 2 m - 2.2 m waves (14%) than a 1.2 m wave (18%) or 1.6 m wave (17%), contrary to the trend shown by the other models. This is perhaps not surprising since equations (6) and (7) are linear expressions whilst wave power increases exponentially with wave height (Eq. (5)), meaning that after a certain point (in this case when $H_{stoe} \approx$ 1.75 m) the efficiency should decrease. (The 1.6 m to 2.2 m waves were in shallow water as well, so the wave period has no influence on the efficiency in this case). The drop-off in efficiency was previously shown in Figure 2.3. This could be seen as being consistent with and an extension of the Kofoed and Goda models since they both show reduced increases in efficiency for the highest waves when compared to the older VMJ model. There is also a gap in our understanding of overtopping rates for small positive freeboards (Reeve *et al*., 2008) and it is possible there could be a decrease in the

overtopping rates (and ramp efficiency) for larger waves. Another possible explanation is that the CSWEC experiments have so far not modelled enough large waves. Figures 2.3 and 2.4 show that relatively few waves above 1.50 m have been run compared with waves between 1 m – 1.50 m, and even fewer above 2 m. Since overtopping is stochastic (Pullen *et al*., 2007) it may be that the overtopping values recorded for waves above 1.50 m were at the lower end of might be considered representative results. After all, Figure 2.4 shows a 1.06 m wave producing a wide range of hydraulic powers for a 50 m structure, from 50 – 90 kW. Further experiments may yield an exponential relationship between wave height and hydraulic power (and therefore between wave height and overtopping rates) in which case efficiency should rise with increased wave heights, in a similar fashion to the other models. This could conceivably lead to efficiencies within the 20% - 25% range, similar to the range reported by Kofoed (2006) for the Wave Dragon, especially as VMJ model already predicts 20% efficiency for a 2.2 m wave (Figure 4.10) and was also found to predict 23% efficiency for a 2.84 m wave.

The 1:23 model predicts higher efficiencies for more moderate waves (e.g. 1.2 m – 1.8 m), ranging from 16% to 18%. Figures 4.13 and 4.14 show the implications of this. At both sites the 1:23 model predicts higher overtopping rates (and subsequently higher levels of hydraulic power) than the other models for approximately 40% of the year. This increase in overtopping appears plausible since models such as the VMJ model are widely accepted to underestimate overtopping by a factor of 1 to 3 when compared to real-life situations (Pullen *et al*., 2007). By this logic, and because small-scale models are thought to underestimate overtopping (De Rouck *et al*., 2003), it may be possible to conclude that the 1:23 model also under-predicts overtopping, in which case the ramp would become more efficient at capturing power from the more moderate waves in the range of 1 m – 1.8 m, that occur for 21% and 33% of the time at sites 1 and 6 respectively. Further experiments, preferably at a larger scale, are needed to confirm whether these relatively high efficiencies for low wave heights really do occur. The Sardinian coast is also subject to frequent and strong mistral winds (Furberg *et al*., 2002) which should also increase overtopping (Besley, 1999). Furthermore a 30^{o} ramp theoretically increases overtopping rates by 11% (e.g. Figure 4.12), and if all the possibilities for increased efficiency are explored, which could include the reflectors and convex-elliptic ramp used by the Wave Dragon, then the efficiencies of 30% to 40% claimed by the SSG could be within the capability of the CSWEC.

5.2 Power Output

If the 1:23 model is correct then this is potentially important for the economic performance of CSWEC project. Figures 4.15 and 4.16 show there is approximately the same power output as when using the VMJ model, and far more power than when using the Goda model. At site 1 the output is 10% below the VMJ model, whilst the output is 5% higher at site 6, despite the fact that at each site the 1:23 model predicts a requirement of a lower installed capacity than the VMJ model (and the same installed capacity as the Goda model). As noted this is because the 1:23 model predicts the more efficient use of more moderate, frequent waves. In this respect, even if further modelling of the CSWEC reveals an exponential relationship between the wave height and overtopping rate with subsequent higher efficiencies for larger waves, it might be that a decision could be made not to design for the higher waves because the device already works efficiently and effectively for lower waves. This fits into the argument of Cruz (2008), which is that a WEC should be designed for the more moderate and frequent waves rather than for more extreme conditions. From an economic point of view this can make sense, since higher installed capacity results in higher CAPEX. Operationally this may also make sense. This study has not looked at survivability, but there may be times when storms force the device to shut. Shoreline wave heights have generally been shown to be within the 1 m to 3 m range advised by Müller (pers. comm.), suggesting no closures, but simulations did not include storm surge. If a 0.5 m increase in depth is used as a proxy for a storm surge then at site 1, where waves already reach 2.84 m, waves could be expected to exceed the recommended range. If the highest wave conditions are being designed for then this creates a problem since plant closures could mean that the power from those waves cannot actually be harvested.

There is relatively little difference between the output at each site using the 1:23 model, within the range of 300-330 MWh /y for installed capacities of 150 – 200 kW and equating to wave-to-wire efficiencies of 9% to 10%. This would provide electricity for 60-70 homes using an EU average of 4.7 MWh / year. This output is close to that reported by Margheritini *et al*. (2009) for the SSG pilot device, which was 320 MWh / y from an installed capacity of 163 kW, with wave-to-wire efficiencies of 10% to 26%. The figures for the CSWEC do however assume 100% availability (i.e. no plant closure), which may be optimistic. On the other hand Margheritini *et al*. (2009) say there is an objective of 96% availability for the SSG. This is in a region (Kvitsoy, Norway) that experiences a more energetic wave climate (an average of 17 kW /m) which may force more closures, whilst

Stagonas *et al*. (2010) have commented that the SSG is a complex device, suggesting the device have higher maintenance needs. It is also not known what tidal regime there is on Kvitsoy. Therefore 100% availability might not be impossible for the CSWEC. Firstly it will not be affected by tides if deployed in the Mediterranean (although even a small tide may slightly alter ramp efficiencies since they are sensitive to changes in freeboard). Secondly as already noted it is a simple device and local manufacture should ensure quick delivery of spares if needed. Furthermore, since neither sites 1 nor 6 appear particularly remote (Vicinanza, pers. comm.) then operational issues should be dealt with quickly. It should be noted that Margheritini *et al*. (2009) do also include reservoir efficiencies (35% to 80% due to changing reservoir levels) and if allowances were made for this it is expected the output of the CSWEC would decrease. A pump system could potentially overcome this issue however there could also be issues with losses due to evaporation.

Availability should increase through use of multiple wheels since they offer a back-up if one of the wheels fails. Figure 4.18 shows that the use of multiple wheels could result in an increase in output in the region of 32 MWh / y, enough to supply around 7 households annually. Whilst this may not sound a lot, Italian energy companies are under obligation to increase their share of renewable output by 0.75 % per annum (EREC, 2009), a figure which is likely to increase in 2012 (*ibid*.) and so a multiple wheel option may be attractive to them. For an array of 5 devices this increase in output becomes 160 MWh / y and for 10 devices 320 MWh / y, which begins to look more significant. On the other hand, the use of more wheels would result in higher costs (Figure 4.19) which may affect the economics of the project since initial costs are discounted at a lower rate than revenue streams later in the project. Therefore the choice to increase output needs to be considered against increased costs. Such a decision is likely to depend on what the specific objectives of the project are. In a country where there have been regular power blackouts over the last decade (IEA, 2010) and which has recently rejected nuclear power, the option of maximising output might conceivably be considered the more desirable option.

5.3 COE and NPV

Using the 1:23 model, the estimated COE of the project appears to be attractive and competitive with other wave energy devices. Figure 4.20 shows that for the pilot plant stage the COEs at both sites are around €0.13 / kWh, using a disadvantageous borrowing rate of 15%, as recommended for immature technology (Davey *et al.,* 2009), and an OPEX value of 5% of initial costs which is at the higher end of the current estimates in Table 2.2. The estimated COE falls within the lower end of the range of values quoted by Allan *et al*. (2011) and Raventos *et al*. (2010) and tends to agree with those that argue that shoreline devices can be a cost-effective way of exploiting wave energy (e.g. Folley *et al*., 2007). It is also very close to the estimated COE of €0.12 / kWh for the SSG device (Margheritini *et al*., 2009). Since the two devices are relatively similar then some degree of confidence can perhaps be attached to this initial estimate. To back this up the HPW costs have a high confidence whilst the ramp costs have been verified by two different sources. The outflow system cost has also been assumed to be at the high end of the estimates by Müller (€100000). As discussed it is possible also that wave heights have been underestimated and in certain locations within each site there are visible 'hotspots' where the wave resource may be higher (e.g. Figure 4.3). Overtopping rates are also likely to be 1 to 3 times higher in reality (Pullen *et al.,* 2007). These factors could counteract the possibly optimistic assumption of 100% availability and the fact that the reservoir efficiency has not yet been accounted for.

The choice of overtopping model will impact upon the COE. Using the VMJ model (for a single device installation), the COE was found to rise to €0.17 / kWh at site 1 and to €0.14 / kWh site 6. As discussed, the output using the VMJ model is similar to the 1:23 model predictions at both sites, but installed capacity is much higher. At site 1 the installed capacity and therefore the costs of the wheels are approximately doubled if the VMJ model is used. These figures are still however within the estimates made by Allan *et al*. (2011) and in fact are lower than the £0.18 / kWh given as the central estimate for wave energy in that study (euros and sterling being similar in value currently). The VMJ model COEs are useful to consider then as they show that even with much higher capital costs for the same output, the project could still deliver a COE within current industry expectations.

Figures 4.20 and 4.21 both show the importance of making cost improvements. Reductions in CAPEX bring the COE of the project down to €0.11 / kWh for a 20% reduction and to €0.08 / kWh for a 50% reduction, therefore putting the device close to

being competitive with offshore wind, which has an estimated COE of £0.08 / kWh (Allan *et al*., 2011). The same effect occurs when reducing OPEX, which should be achievable as lessons are learnt through operational experience. If OPEX is reduced to 3% and 1% of CAPEX then COE can be lowered by €0.01 / kWh and €0.02 / kWh respectively. Therefore a reduction in both CAPEX and OPEX could see the CSWEC become more competitive.

The NPV of the scheme is negative for a single device installation at both sites, in the order of -€700000 to -€800000 with a borrowing rate of 15% (Figure 19). A 30% reduction in CAPEX (which is more or less synonymous with a 30% subsidy) would still return a negative NPV at both sited of around -€500000, based on initial investments in the region of €1.7 - 1.8 million. Even a 50% reduction in CAPEX (which could be approximately equated to a 30% subsidy plus an EU loan) returns a negative NPV of -€300000. As an investment it may not therefore appear attractive. However for the pilot stage it is questionable whether a negative NPV should be considered that important and Calloway (2007) says that most developers at pilot stage are not even thinking of making a profit. Raventos *et al*. (2010) say that initial WEC installations are always associated with high costs that will require significant funding to overcome. The reductions in CAPEX and OPEX that are likely to come with operational experience do show though that the NPV can improve substantially which should attract investors looking for promising technology for the future (Davey *et al*., 2009) rather for short-term profit. This could include the Italian and/or Sardinian governments, both of whom have renewable energy targets to meet of 20% and 30% respectively, as well as energy companies that have their own renewable obligations. Therefore the COE is arguably a more important factor to consider for the pilot project. Furthermore if the project proves its worth in the pilot stage then the borrowing rate should reduce, which will help to improve the NPV on subsequent multi-device installations.

The COE and NPV for a 1MW array at site 1 (5 times greater than the 200 kW single installation at the same site), will depend very much on lessons learnt and the technological improvements that can be made during the pilot stage. Without any improvement in the costs of the technology then the scheme looks less competitive (Figure 4.22, option 1). The COE rises to above €0.20 / kWh, although actually this is again still towards the lower end of current industry estimates (e.g. Raventos *et al*., 2010). This is despite a lower borrowing rate of 8%. Raventos *et al*. (2010) have previously commented on how lower borrowing rates can result in higher COEs and lower NPVs. Large capital costs are discounted less at the start of the project than they would be with

a higher borrowing rate (the benefit being that the revenue is now discounted less later on). In the array installation cash-flow analysis the whole project was also brought forward by two years relative to the pilot project. If cost reductions in technology are included then the benefits of a lower borrowing rate are apparent and the COE can be seen to fall sharply to €0.15 / kWh, and continues to fall again if increased ramp efficiency is included (using a 30^{o} ramp – which involves slightly higher capital costs since installed capacity goes up). If an increase in the HPW's maximum efficiency from 65% to 75% is included (Figure 4.22, option 4) then a COE of €0.12 / kWh is achievable, which is similar to the pilot project and which would make the scheme very competitive under current estimates. A positive NPV is also returned. The output for option 4, at 2.1 GWh / y is similar to that predicted for a 500 m installation of the SSG. Assuming the same scenario (option 4), an installation of 840 kW (5 times the single installation) at site 6 also returns a similar COE of €0.11 / kWh with a NPV of €560000 (slightly higher than site 1), with an output of 1.91 GWh / y.

The reduction in CAPEX moving from the pilot stage to full-scale production is assumed as being 30% (Gross, 2004; Ernst & Young, 2010), that is the costs of the HPWs and ramp are assumed to decrease 30% per unit. This may actually be conservative. Gross (2004) says that figure of 30% is based on production doubling. The array of CSWECs at site (installed capacity 1MW) represents a five-fold increase in production so arguably the costs could come down more and the COE could improve further. This should help to improve the NPV which currently only returns a positive return for the most beneficial option (option 4). This includes a 30% government subsidy but no EU funding. Since most wave energy projects appear to have some form of European funding (e.g. the SSG, Margheritini *et al*., 2009), then if this is factored in then the project could achieve a higher return and it is possible that even options 2 and 3 could return a positive NPV in such a case. Option 1 would still most likely return a large negative NPV but this likely to be an unrealistic option. Actually, options 2 & 3 have relatively small negative NPVs (approximately -€500000). Therefore, even without EU funding, they might still be attractive to energy companies who have obligations to fulfil and who risk financial penalties if they fail to meet them (EREC, 2009).

Options 2 and 3 (Figure 4.22) also illustrate a point made earlier, in that increased efficiency in the ramp may not pay economic dividends since increased efficiency will likely result in increased installed capacity. There is relatively little difference in the NPV between options 2 and 3 (although the COE does fall by €0.01 / kWh). On the other hand

option 4, which includes the higher HPW efficiency, makes a more efficient use of the available hydraulic power resulting in a positive NPV and a further drop in the COE of €0.02 / kWh. This suggests that, along with reductions in costs that should occur with time, improvements in the efficiency of the HPW are arguably the most important area to focus on during the CSWEC's on-going development if a positive NPV is the project's goals. On the other hand, reducing the COE to levels that will make the CSWEC competitive with other WEC technology, as well as other energy sources, will require on-going improvements in the efficiency of both the ramp and the HPWs.

6 CONCLUSIONS

An investigation has been carried out into the economic feasibility of a proposed CSWEC pilot plant in north-west Sardinia. Based upon wave conditions along two different stretches of the coast, the results suggest the CSWEC could be competitive with other wave energy converters. At €0.13 / kWh the COE is at the lower end of current industry estimates and similar to that of another overtopping-type device - the SSG. Reductions in costs, coupled with improvements in the ramp and converter efficiencies could see this figure come down further to between €0.08 - 0.12 / kWh. This will be of interest to investors looking for promising technology as well as the Italian government and energy companies trying to increase their share of renewables. It should also be of interest to the Sardinian government since like on many islands electricity prices there are prohibitively high (Vicinanza, pers. comm).

Since this analysis has been carried out at an early stage in the CSWEC's development the figures should be treated with some degree of caution, whilst there are grounds for scepticism. Firstly, it was not possible to obtain accurate bathymetric data for the shoreline areas. As has been shown to be the case with the LIMPET (Boake *et al*,. 2002) a failure to correctly represent bathymetry can lead to reduced performance so there is some uncertainty attached to the estimated COE. In addition to this, reservoir efficiencies have been ignored. These are estimated at 35% - 80% for the SSG (Margheritini et al., 2009) and could significantly impact upon performance. An optimistic 100% availability has also been assumed whilst costs will only truly be known once engineers carry out a detailed design of the installation.

On the other hand there are reasons to be optimistic. This study tends to agree with previous work done by Vicinanza (pers. comm.), in that the Torre del Porticciolo and Porto Alabe regions both appear to have a relatively high wave resource (an average annual shoreline wave power of 7 kW / m each), and within these areas there are possible 'hotspots'. There *are* large reductions in the average annual wave power between the nearshore and the shoreline (30% to 40%) however this *may* suggest that wave heights in this study have been underestimated. Furthermore, in the Mediterranean, foreshore slopes are often steep and if steeper than have been assumed here then wave heights may again be larger than reported.

There should also be scope for efficiencies to improve. The 1:23 empirical model produced results that showed lower efficiencies for large waves (+1.75 m) than more

moderate waves (1.2 m – 1.6 m), which was contrary to the more established overtopping models. This is likely to be due to the fact that few large waves appear to have been modelled yet in tests on the CSWEC and so the 1:23 empirical model may be 'incomplete'. Higher efficiencies for larger waves, if realised, could reasonably be expected to push overall hydraulic efficiency close to and above 20%. In addition it is likely that efficiencies will also rise for the more moderate waves since small-scale models are widely thought to underestimate overtopping (De Rouck *et al*., 2003).

6.1 Recommendations

The following action is recommended:

- Further modelling, preferably at a larger scale than already done, should be carried out to increase the understanding of the ramp's efficiency. In particular, larger waves in the region of 1.5 m – 3 m should be modelled since these conditions occur relatively often in north-west Sardinia. The effects of oblique waves, shallow water and gentle foreshore slopes should be included within this work.
- At the same time tests should be carried out on the ramp geometry to assess the optimum slope and shape of the ramp. Of particular importance is to assess whether potential gains in efficiency are wiped out by increased costs.
- Development is already going on to improve the HPW's efficiency.
- An assessment of the reservoir's efficiency ought to be made, especially since there are likely to be losses through evaporation for an installation in the Mediterranean.
- Efforts should be made to acquire accurate and reliable bathymetric data for the Torre del Porticciolo and Porte Alabe regions. If possible, direct wave measurements should also be made so that further numerical modelling can be better calibrated. This could allow for a clearer picture to emerge as to whether these site themselves contain any 'hotspots'.
- The economic impacts of any gains/losses in efficiency and decreases/increases in costs should be considered on a continual basis during the CSWEC's development.

(TOTAL WORDS -19800)

REFERENCES

Allan G, M Gilmartin, P McGregor and K Swales. 2010. Levelised costs of Wave and Tidal energy in the UK: Cost competitiveness and the importance of "banded" Renewables Obligation Certificates. Energy Policy 39 (1), pp. 21-39.

Allsop W, T Bruce, J Pearson and P Besley. 2005. Wave overtopping at vertical and steep seawalls. Proceedings of the Institute of Civil Engineers. Maritime Engineering 158, pp. 103-114.

Beels C, P Troch, JP Kofoed, P Frigaard, J Vindahl, C Kromann, PHeyman, M Donovan, J De Rouck and G De Backer. 2011. A methodology for production and cost assessment of a farm of wave energy converters. Renewable Energy 36 (12), pp. 3402-3416.

Belmont MR. 2010. Increases in the average power output of wave energy converters using quiescent period predictive control. Renewable Energy 35, pp. 2812-2820.

Besley P. 1999. Overtopping of seawalls – design and assessment manual. Bristol Env. Agency, in assoc. with HR Wallingford. Report W178, HR Wallingford, pp. 1-37.

Birks J. 2010. Composite Seawalls for Energy Generation. 3rd year Thesis, Department of Civil Engineering and the Environment, University of Southampton, UK.

Boake CB, TJ Whittaker, M Folley and H Ellen. 2002. Overview and Initial Operational Experience of the LIMPET Wave Energy Plant. Proceedings of the 12th International and Polar Engineering Conference, Kitakyushu, Japan, 2002.

Bruce T, J Pearson and W Allsop. 2003. Violent Wave Overtopping: Extension of Prediction Method to Broken Waves. Proceedings of Coastal Structures 2003. ASCE. Conf. Proc. 147 (41).

Calloway E. 2007. To Catch a Wave. Nature 450, pp. 156-159.

Carbon Trust. 2006. Future Marine Energy: Capital, maintenance and operating costs.

Clement A, P McCullen, A Falcao, A Fiorentino, F Gardner, K Hammarlund, G Lemonis, T Lewis, K Nielsen, S Petroncini, M Teresa Pontes, P Schild, BO Sjostrom, HC Sorensen and T Thorpe. 2002. Wave energy in Europe: current status and perspectives. Renewable and Sustainable Energy Reviews 6, pp. 405-431.

Cruz J (Ed.). 2008. Green Energy and Technology: Ocean Wave Energy. Current Status and Future Perspectives. Springer, Berlin.

Dalton GJ, R Alcorn and T Lewis. 2010a. Case study feasibility analysis of the Pelamis wave energy convertor in Ireland, Portugal and North America. Renewable Energy 35, pp. 443–455.

Dalton GJ, R Alcorn and T Lewis. 2010b. Operational expenditure costs for wave energy projects: O/M, insurance and site rent. 3rd International Conference on Ocean Energy, Bilbao, Spain, 2010.

Davey T, GP Harrison and T Stallard. 2009. Procedures for Economic Evaluation. EQUIMAR Deliverable D7.2.1.

De Rouck J, B Van de Walle, J Geeraerts, P Troch, L Van Damme, A Kortenhaus and J Medina. 2003. Full Scale Wave Overtopping Measurements. Proceedings of Coastal Structures 2003. ASCE Conf. Proc. 147 (41).

Douglass SL. 1986. Review and Comparison of Methods for Estimating Irregular Wave Overtopping Rates. Rep. CERC-86-12, U.S Army Corps of Engineers.

EREC (European Renewable Energy Council). 2009. Renewable Energy Policy Review: Italy. Available online at www.erec.org

Ernst & Young. 2010. Cost of and financial support for wave, tidal stream and tidal range generation in the UK. A report for the Department of Energy and Climate Change and the Scottish Governement.

Eurostat. European Commission. http://epp.eurostat.ec.europa.eu/portal/page/portal/eurostat/home/

Folley M, TJT Whitaker and A Henry. 2007. The effect of water depth on the performance of a small surging wave energy converter. Ocean Engineering 34, pp. 1265-1274.

Furberg M, DG Steyn and M Baldi. 2002. The Climatology of Sea Breezes on Sardinia. International Journal of Climatology 22, pp. 917-32.

Galvin CJ. 1972. Wave breaking in shallow water. In Meyer R (ed.). Waves on beaches, pp. 413-455, Academic Press, London.

Goda Y. 2000. Random Seas and Design of Maritime Structures. Advanced Series on Ocean Engineering, Vol. 15. World Scientific Publishing Co. Singapore.

Goda Y. 2009a. Derivation of unified wave overtopping formulas for seawalls with smooth, impermeable surfaces based on selected CLASH datasets. Coastal Engineering 56, pp. 385-399.

Goda Y. 2009b. A performance test of nearshore wave height prediction with CLASH datasets. Coastal Engineering 56, pp. 220-229.

Grantham KN. 1953. Wave Run-Up on sloping structures. Transactions of the American Geophysical Union 34 (5), pp. 720-724.

Gross R. 2004. Technologies and innovation for system change in the UK: status, prospects and system requirements of some leading renewable energy options. Energy Policy 32, pp. 1905–1919.

Hedges TS and MT Reis. 1998. Random wave overtopping of simple sea walls: a new regression model. Proceedings of the Institute of Civil Engineers. Water, Maritime & Energy 130 (1), pp. 1-10.

Hedges TS and MT Reis. 2008. A Comparison of Empirical, Semiempirical, and Numerical Wave Overtopping Models. Journal of Coastal Research 24 (2B), pp. 250-262.

Hospers G. 2003. Localization in Europe's Periphery: Tourism Development in Sardinia. European Planning Studies 11 (6), pp. 629-645.

Huntley D and A Bowen. 1975. Comparison of hydrodynamics of steep and shallow beaches. In Hails J and A Carr (ed.). Nearshore sediment dynamics and sedimentation. Wiley, London, UK.

IEA (International Energy Agency). 2010. Oil & Gas Security. Emergency Response of IEA Countries. Italy. Available online at www.iea.org

Kofoed JP. 2002. Wave Overtopping of Marine Structures – Utilization of Wave Energy. PhD Thesis. Hydraulics & Coastal Engineering Laboratory, Department of Civil Engineering, Aalborg University.

Kofoed JP and A Nielsen. 1997. The wave dragon – an evaluation of a wave energy converter. MSc Thesis, Aalborg University. Graduate report in Civil Engineering.

Kofoed JP, P Frigaard, E Friis-Madsen and HC Sørensen.2006. Prototype testing of the wave energy converter wave dragon. Renewable Energy 31 (2), pp. 181-189.

Kramer M and P Frigaard. 2002. Efficient Wave Energy Amplification with Wave Reflectors. Proceedings of the 12th International Offshore and Polar Engineering Conference, Kitakyushu, Japan, 2002.

Margheritini L, D Vicinanza and P Frigaard. 2009. SSG wave energy converter: Design, reliability and hydraulic performance of an innovative overtopping device. Renewable Energy 34, pp. 1371-1380

Masselink G and MG Hughes. 2003. Introduction to Coastal Processes and Geomorphology. Hodder Arnold, London.

Mori M, Y Yamamot and K Kimura. 2008. Wave force and stability of upright section of high mound composite seawall. Proc. ICCE 2008, Vol.4, pp. 3164-3172.

Oumeraci H, H Schuttrumpf and M Bleck. 1999. OPTICREST Task 3.5 and 5 – Wave Overtopping at Seadikes, Comparison of Physical Model Tests and Numerical Computations. MAS3-CT97-0116, Dept. of Hydromechanics and Coastal Engineering, Technical University of Braunschweig, Germany.

Owen MW. 1980. Design of Sea Walls Allowing for Wave Overtopping. Rep. EX 924, HR Wallingford, UK.

Pethick J. 1984. An Introduction to Coastal Geomorphology. Arnold, London, UK.

Polinder H and M Scuotto. 2005. Wave energy converters and their impact on power systems. Proceedings of the International conference on future power systems, Amsterdam, Holland, 2005.

Pullen T, NWH Allsop, T Bruce, A Kortenhaus, H Schüttrumpf and JW Van der Meer. 2007. Eurotop: Wave Overtopping of Sea Defences and Related Structures: Assessment Manual, EA/ENW/KFKI, p. 201.

Raventos A, A Sarmento, F Neumann and N Matos. 2010. Projected Deployment and Coast of Wave Energy in Europe. Proceedings of 3rd International Conference on Ocean Energy, Bilbao, Spain, 2010.

Reeve DE, A Soliman and PZ Lin. 2008. Numerical study of combined overflow and wave overtopping over a smooth impermeable seawall. Coastal Engineering 55, pp. 155-166.

Schüttrumpf H, U Barthel, N Ohle, J Moller and KF Daemrich. 2003. Run-up of oblique waves on slope structures. COPEDEC VI Conf. Colombo, Sri Lanka.

Senior J, P Wiemann and G Müller. 2008. The rotary hydraulic pressure machine for very low head hydropower sites. Hidroenergia 2008. Session 5B.

Senior J, N Saenger and G Müller. 2010. New hydropower converters for very low-head differences. Journal of Hydraulic Research 48 (6), pp. 703-714.

Stagonas D, G Müller, N Maravelakis, D Magagna and D Warbrick. 2010. Composite seawalls for wave energy conversion: 2D experimental results. Proceedings of 3rd International Conference on Ocean Energy, Bilbao, Spain, 2010.

Stallard T, GP Harrison, P Ricci and JL Villate. 2009. Economic Assessment of Marine Energy Schemes. Proceedings of the 8th European Wave and Tidal Energy Conference, Uppsala, Sweden, 2009.

Tedd J and JP Kofoed. 2009. Measurements of overtopping flow times series on the Wave Dragon, wave energy converter. Renewable Energy 34, pp. 711-717.

Thorpe TW. 1999. A Brief Review of Wave Energy. ETSU Report Number R – 120 for the DTI, May 1999.

Van der Meer JW and JPFM Janssen. 1994. Wave run-up and wave overtopping at dikes and revetments. Delft Hydraulics, publication no.485.

Vengopal V, T Davey, F Girard, H Smith, G Smith, L Cavaleri, L Bertotti and J Lawrence. 2010. Application of Numerical Models. EQUIMAR. Deliverable D2.3.

Vicinanza D and P Frigaard. 2008. Wave pressure acting on a seawave slot-cone generator. Coastal Engineering 55, pp. 553-568.

Vicinanza D, L Cappietti and P Contestabile. 2009. Assessment of Wave Energy around Italy. Proceedings of the 8th European Wave and Tidal Energy Conference, Uppsala, Sweden, 2009.

Weber J, R Costello, F Mouwen, J Ringwood and G Thomas. 2010. Techno-economic WEC system optimisation – Methodology applied to Wavebob system definition. Proceedings of 3rd International Conference on Ocean Energy, Bilbao, Spain, 2010.

Electronic sources:

www.idromare.it	IDROMARE
www.epp.eurostat.ec.europa.eu	Eurostat. European Commission.
www.nauticalchartsonline.com	Nautical Charts Online
www.refer.eu.com	Responsible energy for European regions
www.wavegen.co.uk	Wavegen
www.sidimare.it.net	SidiMare

.

APPENDIX A1 Explanation of significant wave height

In overtopping theory a distinction is made between the significant offshore wave height, H_s, and the significant wave height at the toe of the structure, $H_{s,toe}$. According to Pullen *et al*. (2007) and to the authors whose formulae are used in this study (Van der Meer & Jannsen, 1994; Kofoed, 2002; and, Goda, 2009a), the significant wave height at the toe of the structure ($H_{s,toe}$) is required for calculating overtopping discharge. Pullen *et al.* (2007) define $H_{s,toe}$ as the spectral wave height at the structure toe, $H_{mo,toe}$. The spectral wave height (H_{mo}) was returned by the wave buoy near to Alghero, Sardinia and so it was possible to estimate $H_{mo,toe}$ with the use of the numerical model MIKE 21. In this study therefore $H_s = H_{mo}$ and $H_{s,toe} = H_{m,toe}$. In addition to this, an empirical method (Goda, 2009b) was used to derive shoreline wave heights at a set point with which to calibrate the numerical model. This method returns the significant wave height, $H_{1/3,toe}$, which is defined as the statistical average of the highest third of the waves. In deep water, $H_{mo} \approx H_{1/3}$, however in shallow water there is a difference between the two, to the order of 10 -15% (Pullen et *al*., 2007). On the other hand Goda (2009b) said that there is uncertainty as to the relationship between H_{mo} and $H_{1/3}$ and ignored any differences between the two in shallow water. In respect of this *and* for the sake of simplicity, this study adopts a similar position and it is assumed that $H_{s,toe}$, $H_{mo,toe}$ and $H_{1/3,toe}$ are equal and are referred to only as $H_{s,toe}$ (also assumed as the shoreline wave height).

APPENDIX A2 Missing data from the Alghero wave buoy

Table A2 - Missing data from Alghero wave buoy

Year	% of missing records
1989	July-Dec only
1990	4
1991	5
1992	5
1993	5
1994	8
1995	1
1996	4
1997	2
1998	4
1999	1
2000	3
2001	21
2002	20
2003	20
2004	31
2005	55
2006	49
2007	4
2008	Jan-April only

APPENDIX A3 Full list of offshore wave heights run with MIKE 21

Table A3 - Wave characteristics at Alghero wave buoy

Wave height (H_s), m		Wave Period (T), s	Wavelength (L_0), m	Frequency (%)	% of bin size coming from:	
(Range)	Value used				307.5°	250°
(0-0.70)	0.25	3.9-4.4	23.7	27.3	72	28
(0.5-0.69)	0.60	4.7	30.2	12.8		
(0.7-0.79)	0.75	4.7	34.5	5.3	65	35
(0.8-0.89)	.85	4.8	36.0	4.5		
(0.9-0.99)	.95	5	39.0	4.2		
(1-1.09)	1.05	5.1	40.6	3.7		
(1.1-1.19)	1.15	5.2	42.2	3.4		
(1.2-1.29)	1.25	5.4	45.5	3.1		
(1.3-1.39)	1.35	5.5	47.2	2.8		
(1.4-1.49)	1.45	5.6	49.0	2.7	70	30
(1.5-1.59)	1.55	5.7	50.7	2.4		
(1.6-1.69)	1.65	5.9	54.3	2.1		
(1.7-1.79)	1.75	6	56.2	2.0		
(1.8-1.89)	1.85	6.2	60.0	1.6		
(1.9-1.99)	1.95	6.2	60.0	1.8		
(2-2.09)	2.05	6.4	64.0	1.7		
(2.1-2.19)	2.15	6.4	64.0	1.6		
(2.2-2.29)	2.25	6.6	68.0	1.4		
(2.3-2.39)	2.35	6.6	68.0	1.2		
(2.4-2.49)	2.45	6.9	74.3	1.1	91	9
(2.5-3)	2.75	6.9	74.3	4.7		
(3-3.99)	3.5	7.5	87.8	5.2		
(4-4.99)	4.5	8.5	112.8	2.1		
(5-5.99)	5.5	8.5	112.8	0.9		
(6+)	6	9.2	132.1	0.5		
				100	72	28

APPENDIX A3 (continued)

The deep-water wavelength was calculated using the following equation:

$$L_0 = \frac{gT^2}{2\pi} \quad \text{(A1)}$$

Wave tables were then used to establish the wavelength L at the shoreline. This was used to calculate the wave number k using the following equation:

$$k = \frac{2\pi}{L} \quad \text{(A2)}$$

k is then used to calculate the group velocity C_g (or C_n) where:

$$g = \frac{1}{2}\left[1 + \frac{2kh}{\sinh(2kh)}\right] \quad \text{(A3)}$$

In shallow water g = 0.5 (Masselink and Hughes, 2003)

APPENDIX A4 Wave rose for period Jan 1990 to Dec 2000

The wave rose shown below was downloaded from www.idromare.it.

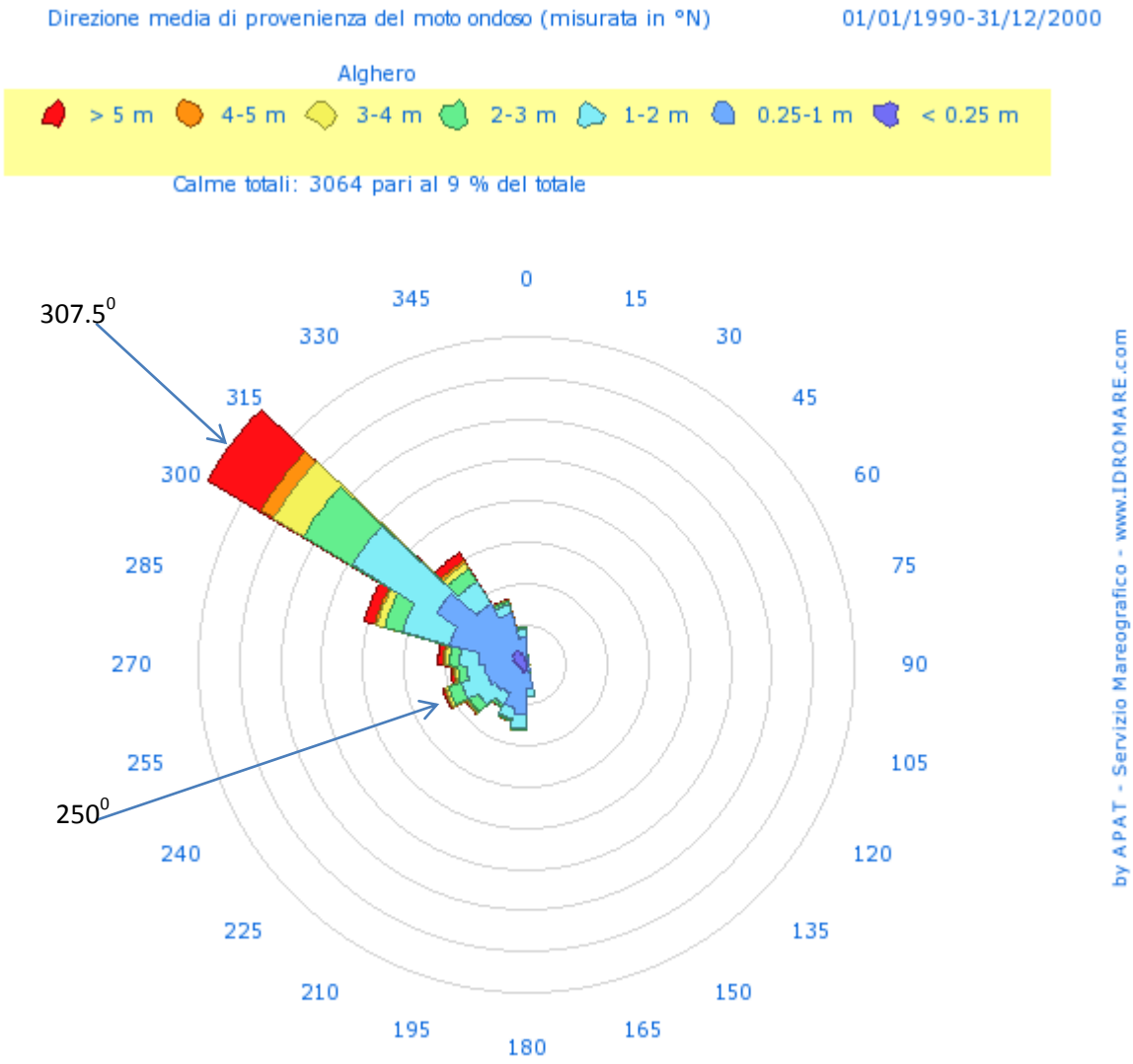

Figure A3 - Wave rose for Alghero wave buoy from Jan 1990 – Dec 2000

APPENDIX A5 Average monthly wave power at Alghero wave buoy

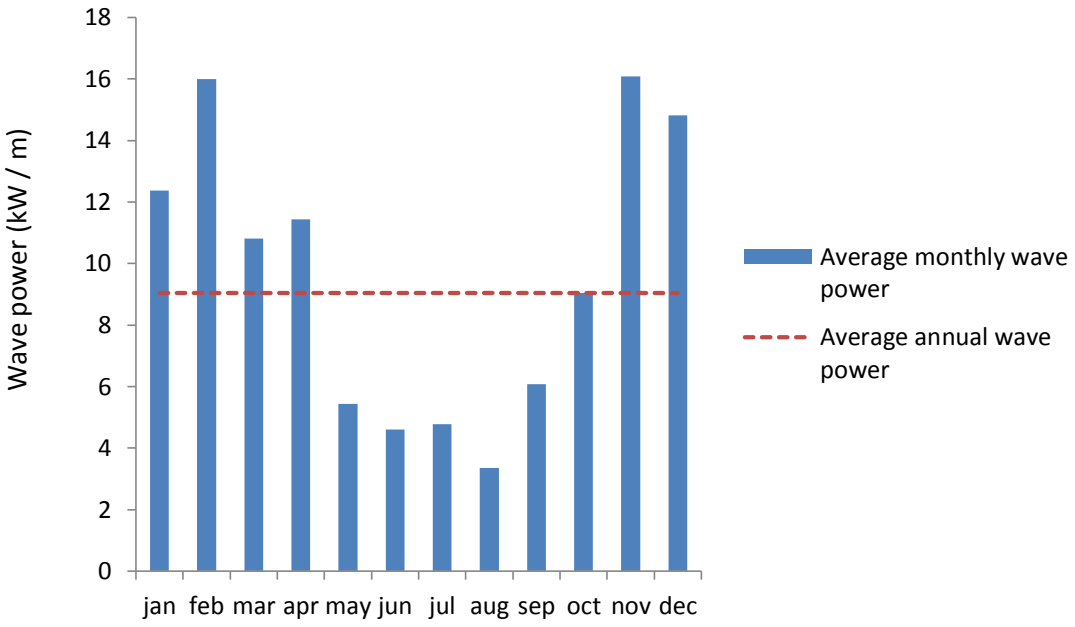

Figure A4 - Average monthly and annual offshore wave power at the Alghero wave buoy

APPENDIX A6 Raster image used for creating bathmetry contours

The origin (bottom left-hand corner) has coordinates: 7°12’0”E; 39°24’0”N. The top right corner has coordinates: 8°36’0””E; 41°24’0””N.

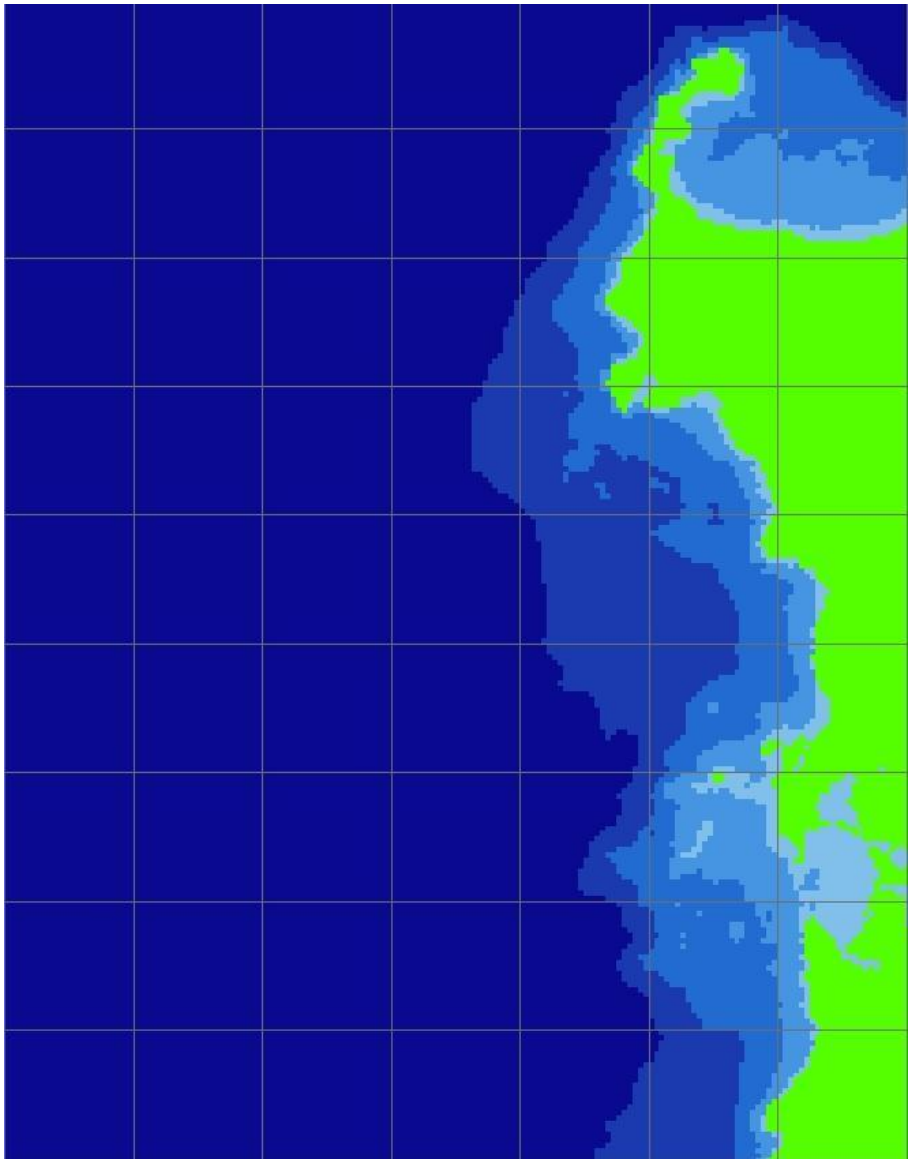

Figure A5 - Raster image use to create bathymetry (GEBCO)

APPENDIX A7 Interpolated bathymetry for waves approaching from 250°

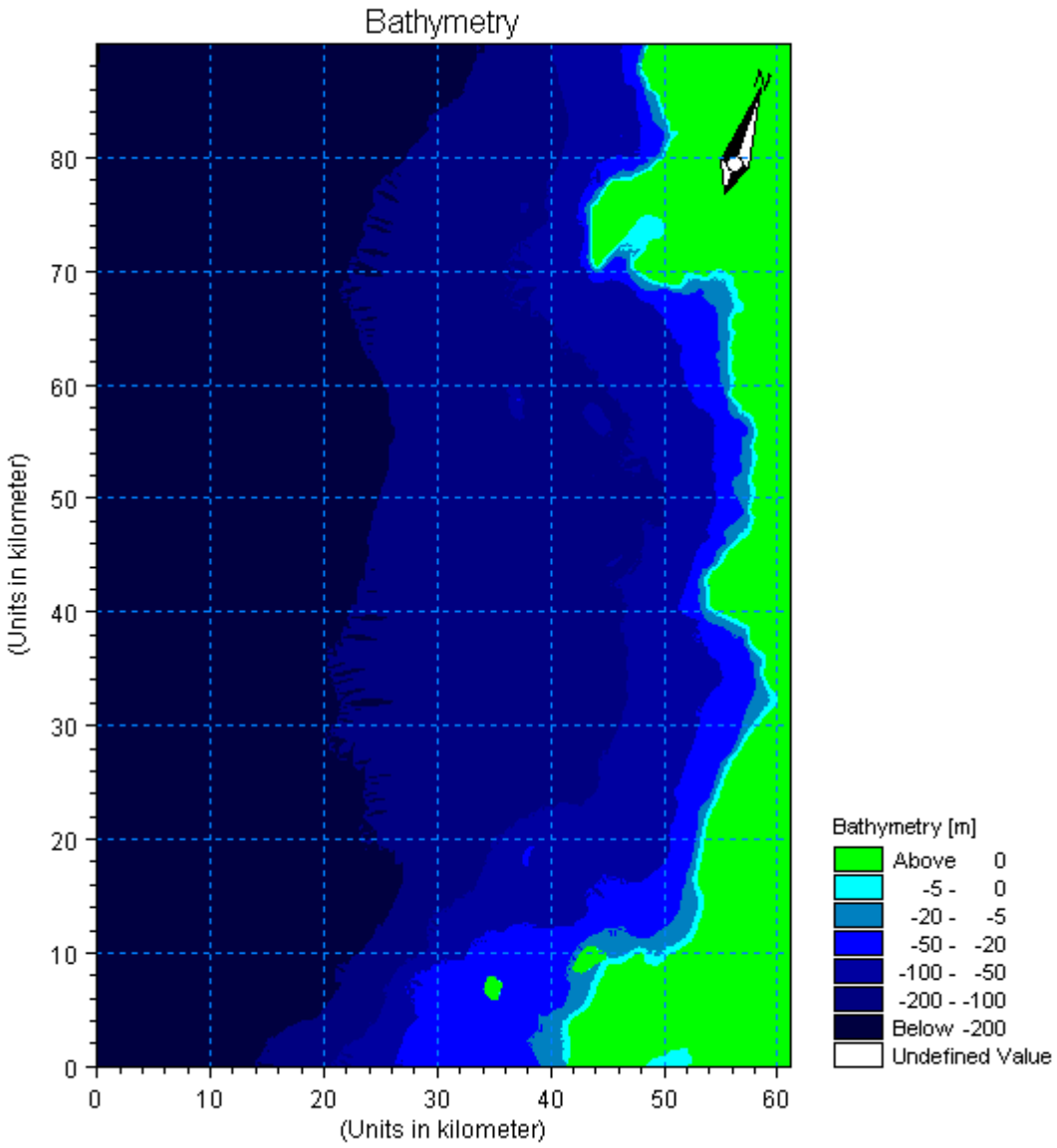

Figure A6 - Bathymetry for waves approaching from 250°

APPENDIX A8 Details of 'selection' areas used for calculating wave heights

Table A8 - Selection area coordinates (approx.)

Site	Approx. coordinates of centre of 'selection' area
1	8°10'0.10"E, 40°39'17.432"N
2	8°18'12.258"E, 40°33'38.729"N
3	8°19'40.872"E, 40°30'28.421"N
4	8°22'42.43"E, 40°23'11.320"N
5	8°28'39.681"E, 40°16'56.320"N
6	8°27'49.381"E, 40°15'19.81"N
7	8°28'57.804"E, 40°6'9.984"N

APPENDIX A9 Goda's (2009) method for calculating shoreline wave heights

Figure A9.1 shows the area where the model was calibrated. This area was chosen since it has parallel contours to the shoreline which is required for calculating the refraction coefficient using Goda's (2000) method.

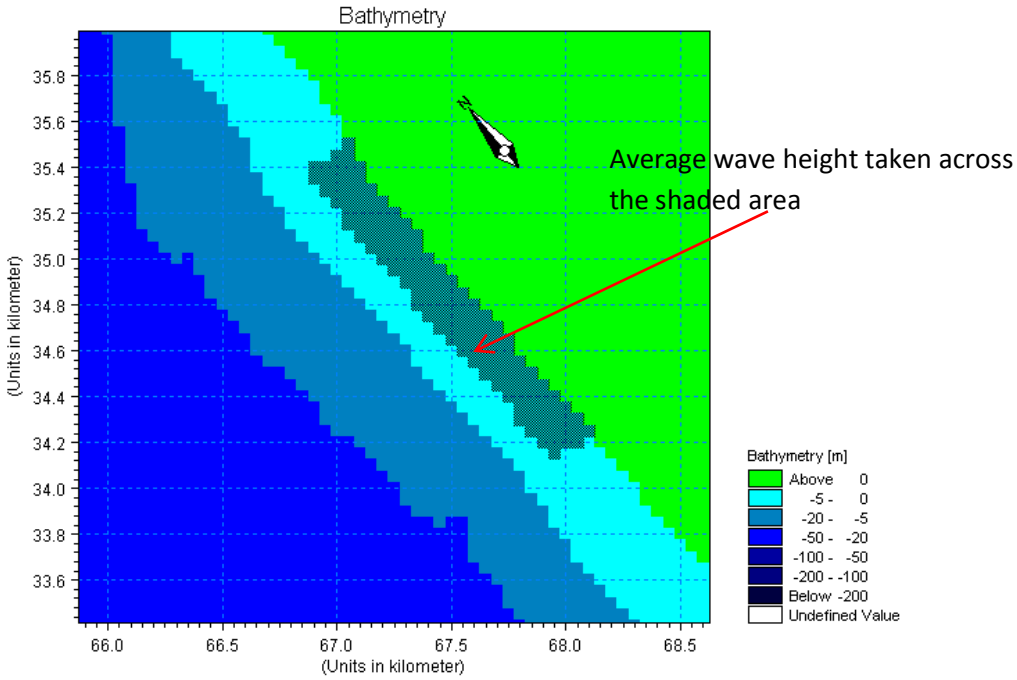

Figure A9.1 - Calibration area

Goda (2009b) uses the following method to calculate wave height at the shoreline:

$$H_{1/3} = \{\min(\beta_0 H'_0 + \beta_1 h_m), \beta_{max} H'_0, K_s H'_0\} : h/L_0 < 0.2 : \quad \text{(A9.1)}$$

where:

$$\beta_0 = 0.028(\frac{H'_0}{L_0})^{-0.38}\exp(20tan^{1.5}\theta) \quad \text{(A9.2)}$$

$$\beta_1 = 0.52\exp(4.2tan\theta) \quad \text{(A9.3)}$$

$$\beta_{max} = max\left\{0.92, 0.32\left(\frac{H'_0}{L_0}\right)^{-0.29}\exp(2.4tan\theta)\right\} \quad \text{(A9.4)}$$

where: θ = the foreshore slope; L_0 = the deepwater wavelength; h = the water depth; and, H'_0 = the equivalent deepwater significant wave height.

The equivalent deepwater wave height can be estimated using the following methods that account for refraction and diffraction (Goda, 2000).

For refraction the offshore angle of wave approach (α_p) is used to calculate the coefficient K_r . Figure A9.2 is then used to estimate K_r. The curve for $S_{max} = 25$ was used as it is recommended for swell conditions (Goda, 2000).

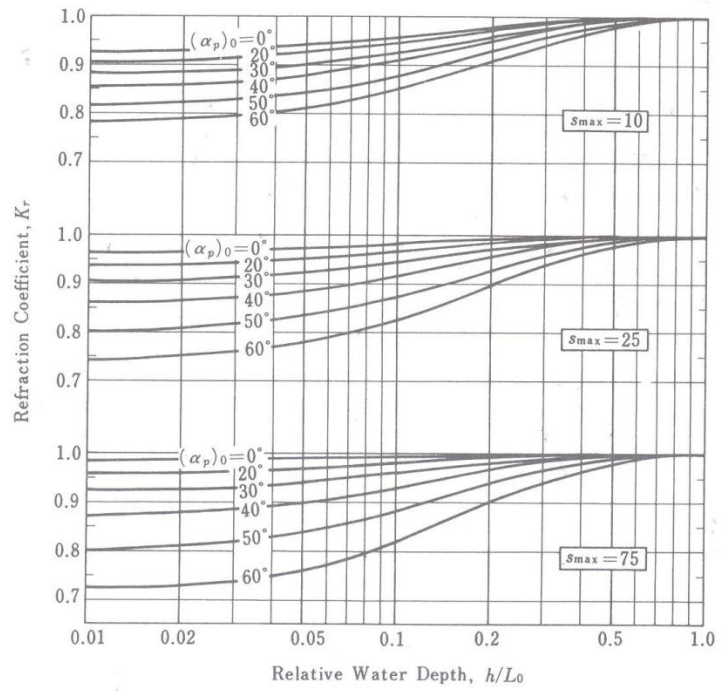

Figure A9.2 - Refraction diagram (Goda, 2000)

For diffraction the following methodology is used. Firstly the angle between the wave approach and the nearest obstructing headland is required (e.g. Figure A9.3). This was estimated using Google Earth. Figure A9.4 is then used, again taking the curve representing $S_{max} = 25$. The diffraction coefficient $K_d$is obtained using the following equation:

$$K_d = \sqrt{(PE(\theta)} \qquad \text{(A9.5)}$$

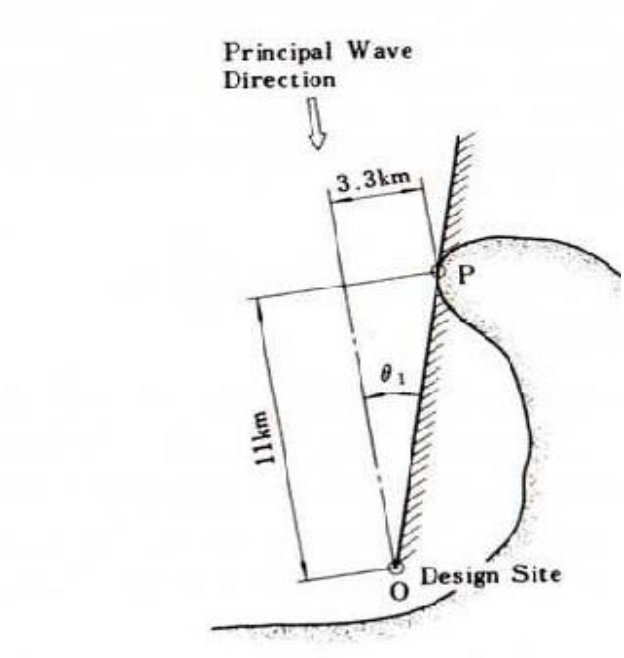

Figure A9.3 - Diffraction diagram (Goda, 2000)

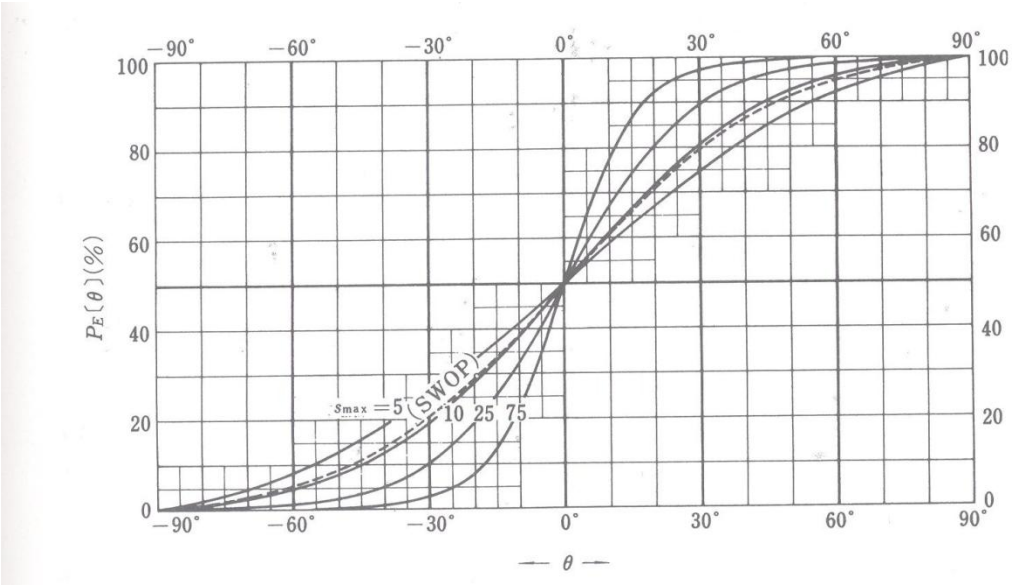

Figure A9.4 - Diffraction diagram (Goda, 2000)

Table A9.1 shows the calculated values for K_d and K_r and the results of the calibration.

Table A9.1- Calibration detail

	Wave direction 307.5° ($K_d = 0.91$)			**Wave direction 250°** ($K_d = 0.99$)		
Offshore H_s	**Goda (2000)** H_{stoe}	**MIKE21** H_{stoe}	K_r	**Goda (2000)** H_{stoe}	**MIKE21** H_{stoe}	K_r
1	0.84	0.85	0.9	0.95	0.98	0.96
1.5	1.29	1.30	0.9	1.41	1.41	0.96
2	1.65	1.66	0.89	1.67	1.69	0.96
2.5	1.70	1.70	0.89	1.75	1.74	0.95
3	1.75	1.76	0.88	1.78	1.77	0.94
3.5	1.78	1.79	0.88	1.83	1.83	0.94
4	1.83	1.81	0.87	1.87	1.89	0.94
4.5	1.87	1.87	0.86	1.92	1.93	0.93
5	1.9	1.89	0.86	1.95	1.96	0.93
6	1.99	1.99	0.86	2.05	2.06	0.93

APPENDIX A10 – Shoreline wave characteristics at sites 1 and 6

Table A10.1 - Detailed list of shoreline wave heights at site 6

Hso (m)	$Hstoe$ (m)	T (s)	Direction (^{o})	Frequency of occurrence
0.5	0.25	3.9	-	0.400
0.75	0.63	4.7	307.5	0.034
	0.68	4.7	250	0.018
0.85	0.71	4.8	307.5	0.030
	0.77	4.8	250	0.016
0.95	0.80	5	307.5	0.027
	0.85	5	250	0.014
1.05	0.89	5.1	307.5	0.024
	0.97	5.1	250	0.013
1.15	0.97	5.2	307.5	0.022
	1.07	5.2	250	0.012
1.25	1.04	5.4	307.5	0.020
	1.10	5.4	250	0.011
1.35	1.12	5.5	307.5	0.018
	1.20	5.5	250	0.010
1.45	1.21	5.6	307.5	0.019
	1.28	5.6	250	0.008
1.55	1.29	5.7	307.5	0.017
	1.37	5.0	250	0.007
1.65	1.38	5.9	307.5	0.015
	1.47	5.9	250	0.006
1.75	1.41	6.0	307.5	0.014
	1.38	6.0	250	0.006
1.85	1.49	6.2	307.5	0.013
	1.45	6.2	250	0.004
1.95	1.57	6.2	307.5	0.014
	1.54	6.2	250	0.004
2.05	1.65	6.4	307.5	0.014
	1.61	6.4	250	0.004
2.15	1.74	6.4	307.5	0.012
	1.70	6.4	250	0.004
2.25	1.54	6.6	307.5	0.011
	1.41	6.6	250	0.003
2.35	1.60	6.6	307.5	0.010
	1.46	6.6	250	0.003
2.45	1.67	6.9	307.5	0.009
	1.53	6.9	250	0.002

2.75	1.77	6.9	307.5	0.042
	1.47	6.9	250	0.004
3.5	1.88	7.5	307.5	0.047
	1.63	7.5	250	0.005
4.5	2.04	8.5	307.5	0.019
	1.70	8.5	250	0.002
5	2.11	8.5	307.5	0.008
	1.71	8.5	250	0.001
6	2.26	9.2	307.5	0.005
	1.77	9.2	250	0.000
0.75				

.

Table A10.2 - Detailed list of shoreline wave heights at site 1

Hso (m)	$Hstoe$ (m)	T (s)	Direction (^{o})	Frequency of occurrence
0.5	0.25	3.9	-	0.400
0.75	0.69	4.7	307.5	0.034
	0.49	4.7	250	0.018
0.85	0.79	4.8	307.5	0.030
	0.56	4.8	250	0.016
0.95	0.89	5	307.5	0.027
	0.62	5	250	0.014
1.05	1.00	5.1	307.5	0.024
	0.68	5.1	250	0.013
1.15	1.08	5.2	307.5	0.022
	0.74	5.2	250	0.012
1.25	1.15	5.4	307.5	0.020
	0.78	5.4	250	0.011
1.35	1.25	5.5	307.5	0.018
	0.85	5.5	250	0.010
1.45	1.35	5.6	307.5	0.019
	0.90	5.6	250	0.008
1.55	1.44	5.7	307.5	0.017
	0.96	5.0	250	0.007
1.65	1.54	5.9	307.5	0.015
	1.02	5.9	250	0.006
1.75	1.60	6.0	307.5	0.014
	1.01	6.0	250	0.006
1.85	1.67	6.2	307.5	0.013
	1.06	6.2	250	0.004
1.95	1.76	6.2	307.5	0.014
	1.12	6.2	250	0.004

2.05	1.85	6.4	307.5	0.014
	1.17	6.4	250	0.004
2.15	1.95	6.4	307.5	0.012
	1.23	6.4	250	0.004
2.25	1.77	6.6	307.5	0.011
	1.11	6.6	250	0.003
2.35	1.86	6.6	307.5	0.010
	1.16	6.6	250	0.003
2.45	1.93	6.9	307.5	0.009
	1.21	6.9	250	0.002
2.75	2.06	6.9	307.5	0.042
	1.28	6.9	250	0.004
3.5	1.00	7.5	307.5	0.047
	1.42	7.5	250	0.005
4.5	2.50	8.5	307.5	0.019
	1.58	8.5	250	0.002
5	2.61	8.5	307.5	0.008
	1.66	8.5	250	0.001
6	2.84	9.2	307.5	0.005
	1.81	9.2	250	0.000
TOTAL				1

APPENDIX A11 Cost details

Table A11.1 – Installation of single device at site 1 - 200kW installed capacity

T

Units	Costs (€s)	TOTAL (€s)	OPEX @ 5% of I. CAPEX
eHPWs	= (67 * 5000 * 3) + (3*20000)	= 1065000	
Structure + ramp	= 1 * 330000	= 330000	
A Transmission	= 1 * 20000	= 20000	
12 Outflow	= 1 * 100000	= 100000	
. TOTAL INSTALLATION		=1515000	
1 Management etc.		= 245000	
_TOTAL INITIAL CAPEX		= 1760000	= 88000
Decommissioning		= 468000	
TOTAL CAPEX		= 2073000	

Table A11.2 - Installation of a single device at site 6 - 150kW installed capacity

Units	Costs (€s)	TOTAL (€s)	OPEX @ 5% of I. CAPEX
HPWs	= (50 * 6000 * 3) + (3*20000)	= 960000	
Structure + ramp	= 1 * 330000	= 330000	
Transmission	= 1 * 20000	= 20000	
Outflow	= 1 * 100000	= 100000	
TOTAL INSTALLATION		=1410000	
Management etc.		= 228000	
TOTAL INITIAL CAPEX		= 1638000	= 82000
Decommissioning		= 435000	
TOTAL CAPEX		= 2073000	

Table A11.3 - Installation of an array at site 1 - 1MW, 45° ramp, 3 wheels per unit per unit

Units	Costs (€s)	TOTAL (€s)	@ 70% (cost reductions)	OPEX @ 3% of I. CAPEX
HPWs	= (67 * 5000 * 15) + (15*20000)	= 5325000		
Structure + ramp	= 5 * 330000	= 1650000		
Transmission	= 5 * 20000	= 100000		
Outflow	= 5 * 100000	= 500000		
TOTAL INSTALLATION		=7575000		
Management etc.		= 1050000		
TOTAL INITIAL CAPEX		= 8625000	6037500	= 181000
Decommissioning		= 959000		
TOTAL CAPEX		= 9590000		

Table A11.4 - Installation of an array at site 1 - IMW, 30° ramp, 3 wheels per unit

Units	Costs (€s)	TOTAL (€s)	@ 70% (cost reductions)	OPEX @ 3% of I. CAPEX
HPWs	= (74 * 5000 * 15) + (15*20000)	= 5850000		
Structure + ramp	= 5 * 330000	= 1650000		
Transmission	= 5 * 20000	= 100000		
Outflow	= 5 * 100000	= 500000		
TOTAL INSTALLATION		=8100000		
Management etc.		= 1128000		
TOTAL INITIAL CAPEX		= 9230000	6460000	= 194000
Decommissioning		= 1025000		
TOTAL CAPEX		= 10780000		

Table A11.5 – Installation of an array at site 6 – 0.86MW, 30° ramp, 3 wheels unit

Units	Costs (€s)	TOTAL	@ 70% (cost reductions)	OPEX @ 3% of I. CAPEX
HPWs	= (56 * 5000 * 15) + (15*20000)	= 4200000		
Structure + ramp	= 5 * 330000	= 1650000		
Transmission	= 5 * 20000	= 100000		
Outflow	= 5 * 100000	= 500000		
TOTAL INSTALLATION		=6750000		
Management etc.		= 940000		
TOTAL INITIAL CAPEX		= 7690000	5380000	= 161000
Decommissioning		= 854000		
TOTAL CAPEX		= 10780000		

APPENDIX A12 HPW efficiency curve at max. 75%

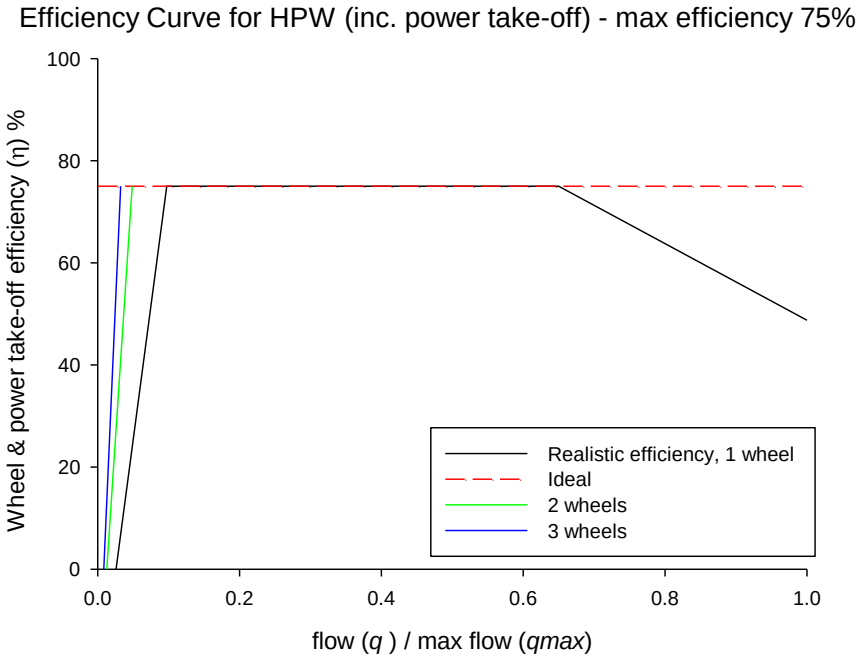

Figure 12.1 – HPW efficiency curve